HYDRODYNAMIC STUDY OF A DOWNWARDS CONCURRENT BUBBLE COLUMN

Mario Marchese Mecklenburg

A thesis submitted to the
Faculty of Graduate Studies and Research
in partial fulfilment of the requirements for
the degree of
Master of Engineering

Dept. of Mining and Metallurgical Engineering
McGill University
Montreal, Canada

To my wife Bárbara
and my son Francisco Javier,
the reasons for this work.

The decision is only yours, you have
to choose from a wide variety of alternatives,
and your choice,
while giving you many satisfactions,
will make you grow as a person....

(Anonym)

ABSTRACT

Downwards concurrent bubble columns of various forms have been used in mineral processing since the early years of this century. The limited aeration and consequently poor recoveries of the early versions suggested little promise. In the mid '80s in Australia the development of a more refined device (the Jameson cell) reintroduced the technology to the mineral industry.

The hydrodynamics of the downwards concurrent flotation column (CDFC) of the Jameson design has been studied. The effect of operating variables on the gas holdup in two- and three-phase mixtures was measured. To measure gas holdup, the isolating technique (as an independent direct check), conductivity and pressure techniques were employed. Gas fractions between 10 and 65 % were achieved. These high holdups are a consequence of bubbles being forced downwards against their buoyancy. The high gas fraction may account for the fast flotation claimed for this cell.

The conductivity technique using Maxwell's equation gave a maximum error of 6%, in both two- and three-phase systems (considering the water-solids mixture as one phase).

The pressure technique required two measurements (one inside at the top and the other outside, aligned with the discharge). A pressure balance -including a term for the deceleration of the liquid jet- was used to estimate gas holdup. The method was successful in two- and three-phase systems, suggesting potential for its application in industry.

The drift flux model was applied to try to correlate the data. Both two- and three-phase systems showed consistent trends. The model was used to estimate bubble size. In the Richardson and Zaki equation the m factor was in the range 2.9 to 3.1. A dimensionless drift flux was defined assuming $m=3$ which fitted the data. For three-phase systems, however, the results predicted a trend in bubble size that seemed opposite to observation.

RÉSUMÉ

Des colonnes de flotation concurrantes de divers formes furent utilisées par la industrie miniére depuis le début du siecle. Ce procédé peu prometteur á l'epoque due á sa faible capacité de récuperer le minerai, ácause de l'aereation limitée dans les colonnes. Au milieu des annes '80 en Australie, le developpement d'appareil plus sophistique (p.ex. la cellule de Jameson) donna un nuveau souffle á cette technologie dans le domaine minier.

Les aspects hydrodynamiques de la cellule da Jameson furent étudiés plus en détails. L'effet des variables opérantes, sur la fraction gaseuse du melange binaire et ternaire a été mesurées. La fraction gaseuse fût mesurée de façon indirecte: conductivite et pression. Dans les conditions étudies la fraction gaseuse observée varia de 10 á65%. Cette forte fraction gaseuse est due aux mouvements descendants des bulles dans la colonne. Conséquement, une bonne récupération du minerai fût obtenue.

A l'aide du modéle de Maxwell l'erreur associée à l'évaluation de la fraction gaseuse n'excéde pas 6%.

L'évaluation de la fraction gaseuse realisée á l'aide de mesure de pression necessite deux mesures: la premiere ál'interieur et en tête de la colonne, la seconde a l'exterieur et au bas de celle-ci. Une balance de pression tenant compte du sciesaillement du liquide descendant dans la colonne fût utilisée pour évaluer la fraction gaseuse. Cette méthode s'applique aussi ádes melanges binaire et ternaire. Ainsi cette derniére trouvera peut-être des applications industrielles.

"The drift flux model" fut utilisépour correler les données et eváluer la taille des bulles pour les systemes binaire et ternaire. Cependant dans le cas du systeme ternaire (gas, solide, eau) les résultats calculés (la taille des bulles) sont en opposition avec les observations expérimentales.

RESUMEN

Columnas descendentes de Burbujeo en co-corriente de varios tipos han sido utilizadas en el beneficio de minerales desde principios de este siglo. La limitada aireación y consecuentemente la baja recuperación de las primeras unidades en funcionamiento mostraron ser poco promisorias. En la década de los ochenta, en Australia, el desarrollo de una celda mejorada (la celda Jameson) reintrodujo el uso de esta tecnología en la industria minera.

Las características hidrodinámicas de una columna del tipo Jameson fueron estudiadas en este trabajo. Se midió el efecto de las variables de operación en la fracción de gas en el tubo de descenso para dos y tres fases. Para medir la fracción de gas se utilizó la técnica de aislamiento (como método independiente) como también conductividad y presión. Fracciones de gas entre 10 y 65% fueron medidas como consecuencia del movimiento de las burbujas contra su natural tendencia a ascender. La alta fracción de gas explicaría la alta cinética de flotación que se ha dicho es una caraterística importante de este equipo.

La técnica de conductividad, utilizando el modelo de Maxwell, dió un error máximo de un 6% para dos y tres fases (se considera la mezcla agua-sólidos como una fase).

La técnica de presión requirió de dos mediciones (una en el tope del tubo de descenso y otra en el compartimiento de separación a nivel con la descarga del tubo). Un balance de presión -incluyendo el término debido a la desaceleración del jet- se utilizó para estimar la fracción de gas. El método resultó exitoso en dos y tres fases y muestra un gran potencial de aplicación en la industria.

Se utilizó el modelo de drift flux para intentar correlacionar los datos experimentales. En dos y tres fases los resultados mostraron tendencias consistentes. El factor m del modelo de Richardson and Zaki mostró variación en el rango 2.9 a 3.1. Se definió un término adimensional de drift flux, asumiendo $m=3$, para ajustar los datos experimentales. Para tres fases, sin embargo, los resultados predicen una tendencia para el diámetro de burbuja opuesto a lo observado.

ACKNOWLEDGEMENTS

This work would not be completed without recognizing the essential contributions of many people whose names do not appear on the title page. First of all, I am indebted to ·

My wife, Bárbara, for her support and encouragement during these fifteen months of work, and for giving me the most wonderful thing in this world: our son Francisco Javier.

My supervisor, Prof. J.A. Finch, for his constant enthusiasm, advice and helpful discussions, and finally for his patience throughout the preparation of this thesis.

My friend, Dr. Alejandro Uribe-Salas, for his reception, fruitful discussions and especially for his comradeship.

As well, I gratefully acknowledge the friendship and help of Dr. S.R. Rao, M Leroux and all my colleagues at McGill Mineral Processing group, which fortunately form a long list. The help of Mr. M. Knoepfel in building the experimental apparatus is also acknowledged.

TABLE OF CONTENTS

CHAPTER V EXPERIMENTAL RESULTS, DISCUSSION AND CONCLUSIONS

LIST OF FIGURES

LIST OF TABLES

LIST OF APPENDICES

INTRODUCTION

Increased competition for mineral products in recent years has created the need to lower production costs through the use of more efficient processes. Mineral processing for example has seen a growing interest in novel devices which promise increased efficiency: flotation columns are in this category.

Column flotation have been successfully applied worldwide over the last ten years (although were developed in the early '60s (Boutin and Tremblay, 1960)). More recently, derivative devices have been developed. One example is the Jameson cell, where a slurry jet is injected to create a downwards concurrent bubble column. Chapter 1 of this thesis reviews the use of liquid jets to aspirate and entrain gases as the dispersed phase. Some of these devices were used in mineral processing in the early years of this century.

One feature of these devices is the absence of equipment needed to blow gas into the system: the use of plunging jets naturally aspirates and entrains gas into a liquid. Although, multi-phase downwards concurrent columns as such have not been widely studied, they are analogous to flow of multi-phase mixtures in pipes, for which there is a substantial body of work. Chapter 2 summarizes the theory involved in two-phase flow in pipes, making special reference to the case being studied here.

The use of various instrumental techniques, to measure process variables on-line in flotation has attracted the attention of many researchers in recent years. Gas holdup in multi-phase flow is a typical example of a process variable for which reliable on-line measurements are needed. Chapter 3 presents the theory involved in the use of conductivity to measure the gas holdup.

As the aim of this thesis is to measure the effect of operating parameters on the gas holdup, the experimental equipment used for the laboratory work, described in Chapter 4, includes details on all the pertinent instrumentation.

The experimental work included a study of the effect of variables on the gas holdup, as well as a study of the application of the conductivity technique for gas holdup estimation. A technique based on pressure measurements was developed, to estimate gas holdup. Chapter 5 presents the experimental results carried out using water-air and water-solids-air mixtures.

CHAPTER I

A REVIEW OF GAS ENTRAINMENT DEVICES

1.- Introduction

The need for more efficient and economical processes to separate and concentrate minerals forms part of the reason for the surge of interest in flotation columns, and other innovative flotation devices in the last ten years. These examples of devices include: the Outokumpu High Grade cell (Ulan et al., 1991), Pneumatic Flotation (Brzezina and Sablik, 1991), the Leeds cell (Hall, 1991), and the Jameson cell (Kennedy, 1990; Brewis, 1991).

The Jameson cell is probably the most innovative of the new devices, being simple in design and combining the ability to produce high gas fractions in a turbulent environment in one section with quiescent conditions in another section to allow bubbles to disengage from the pulp and produce a froth.

The high gas fraction in the Jameson cell is produced by a plunging slurry jet aspirating and entraining gas. In this section devices that use this principle of aeration are reviewed. Some of them have been used in mineral processing.

1.1.-The Hydraulic Compressor

The entrainment of gas by a liquid flowing into an inclined or vertical pipe has long been recognized and utilized to provide compression of the gas. One of the oldest devices using this principle is the Taylor Hydraulic Compressor, which was first erected by the Taylor Hydraulic Air Compressing Co. of Montreal in 1896 (Peele, 1941).

In the Hydraulic Compressor, water is allowed to flow down a vertical shaft which is opened to the air at the top. Air is entrained and carried down the shaft by the flowing water to a large settling chamber at the bottom of the shaft where the sudden decrease in velocity causes the air to separate from the water. The amount of compression obtained depends on the height of the water column, defined by the difference between the inlet to the shaft and the water level in the settling chamber.

Examples of applications of this device are a 36,000 scfm unit at the Victoria Copper Mine, Michigan, USA; and a 40,000 scfm unit installed near Cobalt, Ontario, Canada, installed in 1906, where air was compressed from atmospheric pressure up to

120 psi (Chase, 1971).

1.2.-The Cascade Machine

The concept of the cascade machine was doubtless suggested by the frequently observed formation of froth wherever a stream carrying flotation reagents dropped to a lower level.

Among the earliest flotation machines using this principle of a falling stream plunging into a pool to entrain air were those reported by Seale and Shelshear in 1914 at Broken Hill, Australia (Truscott, 1923), and another described in 1915 at the Ray Consolidated Copper Co. in Australia (Fairchild, 1917). Clifford Wilfley, from Ouray, Colorado, USA, claimed he was the inventor of the device but had not patented it (Wilfley, 1917(a)).

The idea behind the cascade machine was to develop an economical and efficient machine, suitable for a small mill whose ore reserves did not justify an expensive plant.

In the design described by Seale and Shelshear (Figure 1.1), the pools were contained in individual boxes, or cells, with the pulp level kept constant, and each box discharging pulp by gravity to the next box directly below. A series of rectangular boxes was arranged in a tier, step fashion, on an inclined supporting frame, in such a manner that spigots at the bottom of each cell discharged pulp over an inclined feed apron which caused the stream to spread and plunge into the pool below, across the full width of the cell.

The froth formed covered the surface of the cell and discharged from the front, which was lower than the three other sides.

In order to keep the pulp level constant, and take care of irregularities in the feed (e.g. %solids, grade, rate), an open slot was provided at the front lip under the froth baffle, and a small amount of pulp was allowed to run over the lip through the slot and down the front side of the cell, joining the flow from the spigots below. In practice, the spigots, which were preferably regular discharge gates, were regulated by hand to keep a thin layer of pulp overflowing.

Water falling 3 or 4 feet over a weir entrains sufficient air to form a froth. The difficulty of spreading the stream evenly over the apron width is one reason why this

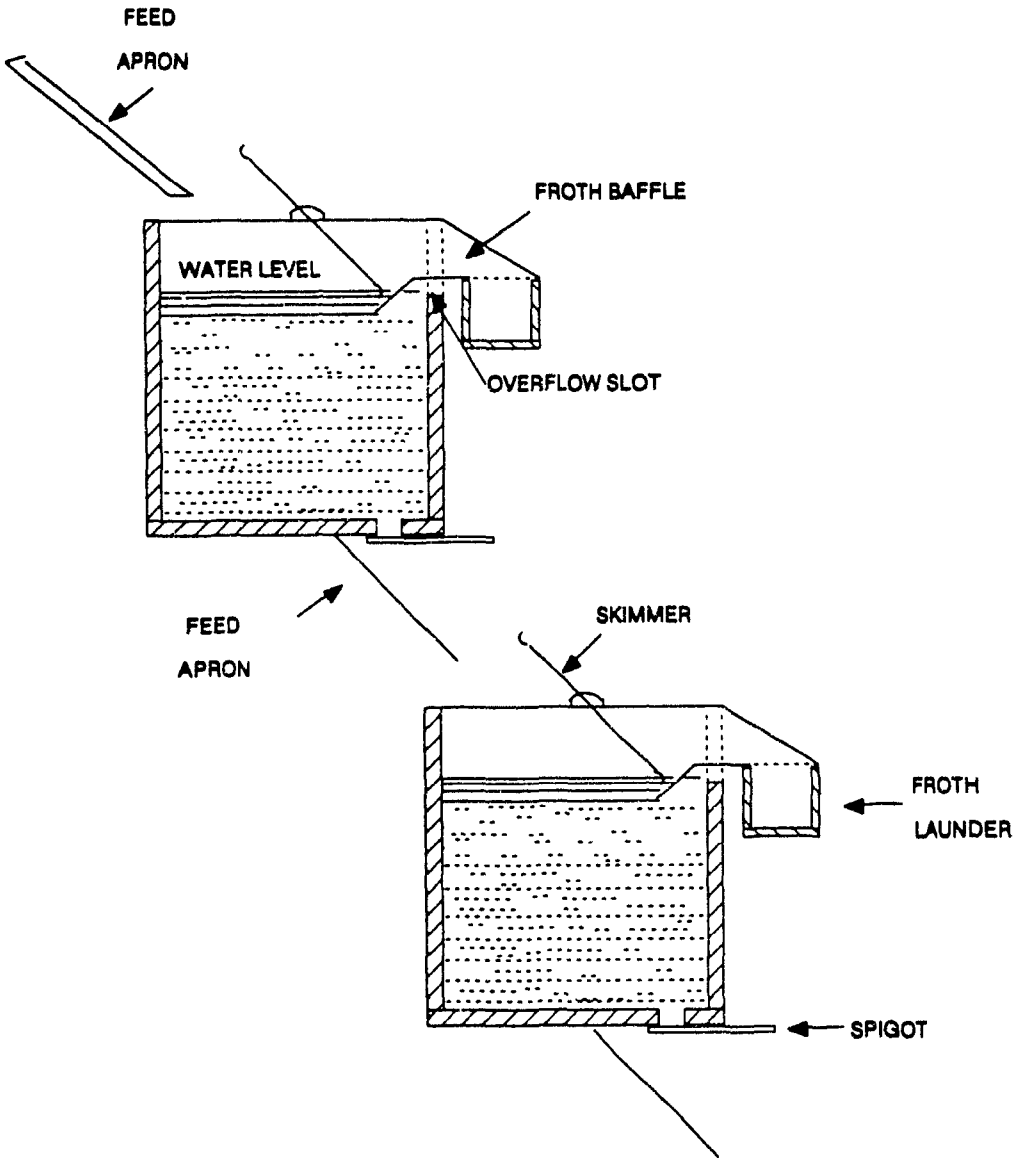

Figure 1.1 The Cascade Machine as described by Seale and Shelshear in 1914 (Truscott, 1923)

arrangement was not widely used.

A more efficient way of entraining air is to form water jets from nozzles (Harvey, 1918). One arrangement using nozzles (Figure 1.2) consisted of a number of frothing boxes in series, placed one below the other. The pulp after plunging into the first box which yielded some mineral recovery, discharges from the bottom across an air gap to the next box, where a second froth product forms, and so on. Figure 1.3 shows a schematic of one design of cascade machine, where the distance between the bottom of successive boxes was about 4½ or 5 ft, of which about 3 ft was occupied by the drop, and the remainder by the depth of the box itself. Along the length of the cell are three nozzles to allow the pulp to flow to the cell below. Normally nine cells were placed in series, with intermediate elevation of pulp between the fourth and fifth cells, with a treatment capacity of 100 tpd per each series of cells (Harvey, 1918).

As cascade machines were presented as simple and easy to build flotation machines, it was common to find home-made units with some particular features, some of these different cascade machines are described in detail in Appendix B.

The main reasons for the eventual abandonment of the cascade machine were its low aeration rate and consequently low capacity.

Compared with the violent agitation of mechanical machines and the abundant air-supply of the pneumatic machines, the aeration effected by these simple machines is both mild and limited with the result that, even granted an adequate previous mixing, the froth is both "evanescent and meagre" (Truscott, 1923). Bubbles were relatively large and the disturbance of the pulp body slight (Fairchild, 1917), and there was a rapid rise of these bubbles through the pulp which does not promote good loading of the bubble surface (Taggart, 1921). The capacity per unit of volume was low and the height required made for expensive installations. The control of aeration was also difficult and unsatisfactory (Taggart, 1927).

In practice, therefore, cascade machines were little used in mills due to low recoveries, except with ores that floated easily.

The principle of the cascade machine was not completely abandoned, however; using the arrangement shown in Figure 1.4 it is now applied in the recovery of copper

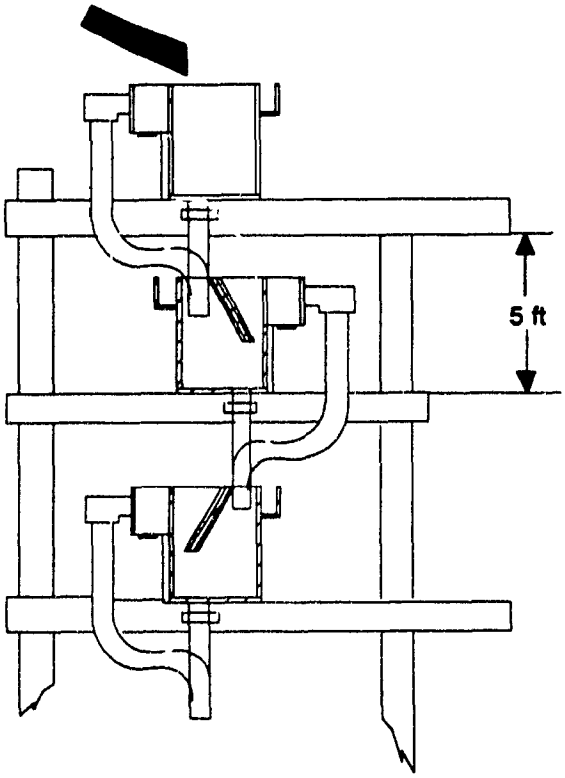

Figure 1.2 The cascade machine with nozzles (Harvey, 1918)

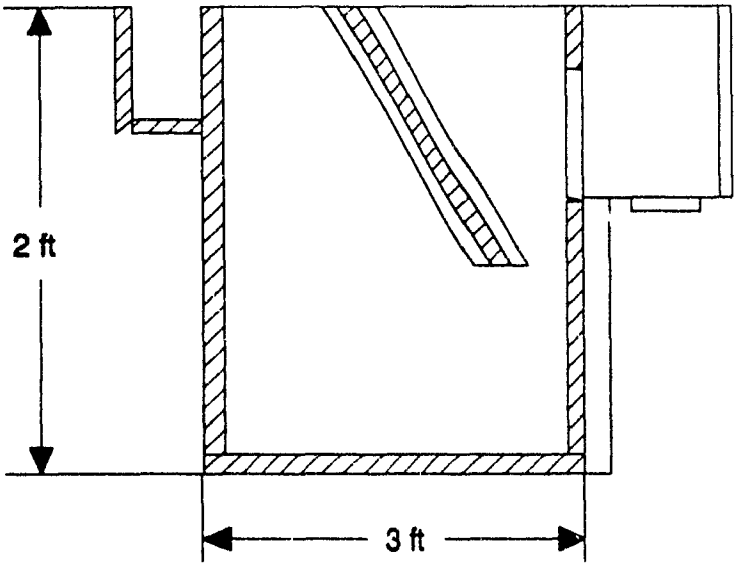

Figure 1.3 Schematic diagram of the Cascade Machine (Harvey, 1918)

from the tailings channel at the Chuquicamata, El Salvador, Andina and El Teniente copper mines in Chile (Marchese, 1991). The tailings stream is forced through several short pipes and the resultant jet hits the surface of the channel below entraining air and forming a froth. The height between each set of aerators or pipes is provided by the inclination of the terrain. The operation recovers about 400 tpd of copper concentrates from the tailings in the case of the Chuquicamata Mine.

1.3.-The Jet Pump

The existence and application of jet pumps has been reported since 1922 (Hoefer,1922), and also in a number of German and Russian papers.

The jet pump (Figure 1.5) is basically a device for inducing pumping of one fluid by means of a high velocity jet of the same or another fluid (Folsom,1948). The principal phenomenon involved is the transfer of some momentum from the high velocity fluid jet to the second fluid. The nozzle converts the potential energy of the drive fluid into kinetic energy and the resulting high speed jet entrains the second fluid by means of the mixing process; the combined fluids flow into a diffuser and pass out of the pump, with the result that all the fluids leaving the mixing region have about the same velocity.

In addition to energy transfer from the jetting fluid to the second fluid, the transfer of mass and heat, or chemical reactions can take place; therefore the jet pump combine the functions of a flow transfer machine and reactor (Hongqi, 1983). The action is simple and no moving parts are required.

1.3.1 Mechanism of pumping action. As a jet of fluid penetrates a stagnant or slowly moving fluid, the two flows progress and the mixed stream spreads. The undisturbed high-velocity core progressively decreases in diameter until it disappears. Confined by parallel throat walls, the second fluid enters a region of decreasing area, that area being the annulus between the nozzle and the throat wall (Cunningham,1957). At the throat exit the mixture stream has spread until it touches the wall of the throat. Then all of the secondary fluid has been mixed with the primary jet.

1.3.2. Classification. Jet pumps are known by various names, which are usually associated with the application. Among such names are injector, ejector, eductor, and water-jet heat exchanger. The steam injector, for example, is a jet pump designed to

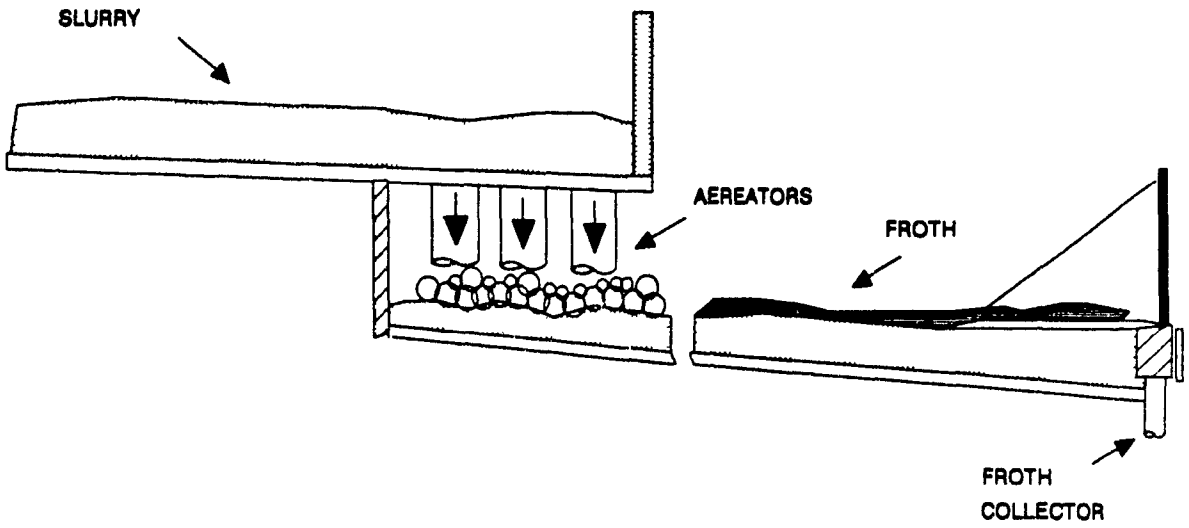

Figure 1.4 Cascade Machine Type in the Chuquicamata Concentrator, Chile.

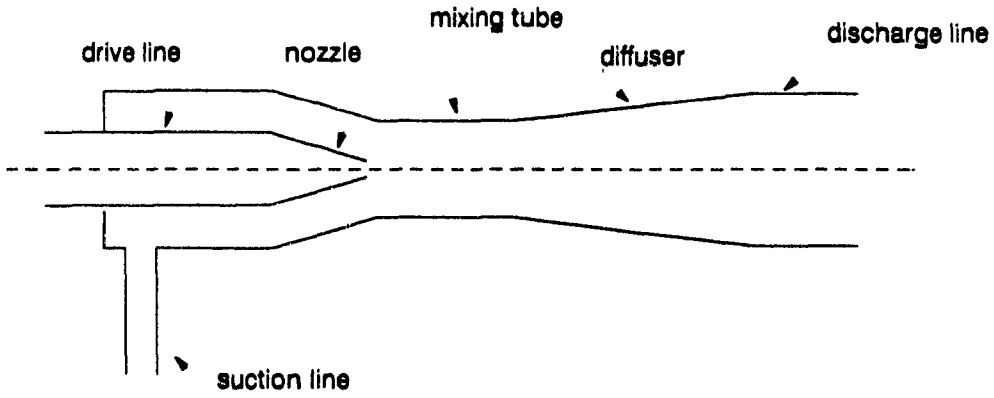

Figure 1.5 Schematic diagram of a simple jet pump indicating its parts (Folsom,1948)

supply feed water to a steam boiler, the driving fluid being a portion of the steam generated by the boiler. The water-jet ejector, on the other hand, is designed to draw leakage air and other non-condensable gases from the exhaust of a steam turbine plant.

When operating as an eductor, the driving fluid, e.g. water, is used to entrain additional water so as to obtain a greater mass flow, but at a lower pressure than that of the driving fluid.

The water-jet heat exchanger is essentially the same as a steam-jet injector, the name "heat exchanger" means that the pump supplies heat to the feed water.

There are four basic forms of jet pump: gas-gas, liquid-liquid, gas-liquid and liquid-gas, the first mentioned fluid in each case corresponding to the one used as the driving fluid. Jet pumps may also be classified in accordance with the fluid components and fluid phases. For example, a steam-jet water injector is a two-phase, one component jet pump, since steam and water are two different phases of the same fluid. A water-jet air ejector, on the other hand, is a two-component, two-phase jet pump (Bonnington, 1976).

1.3.3. Applications Jet pumps are applied to many pumping problems due to their low investment cost, simplicity of operation and ability to mix thoroughly two fluids. Among the instances where jet pumping techniques may be utilized are: solid materials handling, water and oil well pumping, pump priming, gas fuel installations, ventilation, distillation, generator cooling and cryogenic pumping (Bonnington, 1976).

In the handling of solids by hydraulic means, the jet pump is of particular value. The pumps that supply the high pressure driving water to the nozzle are only required to handle a clean liquid, so that the wear and, therefore, frequent replacements normally associated with hydraulic transport are confined to the cheap and easily maintained mixing assembly.

Results show that high concentrations of solids can be pumped economically with jet pump type of equipment (BHRA Fluid Engineering, 1968). The jet pump is installed on the discharge of the centrifugal pump and high pressure water is delivered from the centrifugal pump to the jet nozzle where the entrainment of solids with a relatively small amount of water takes place. On entering the mixing tube, the solids are mixed with the

jet water and are boosted into the discharge pipe. With this arrangement, the solid material passes through pipes only and does not come into contact with any moving parts. Large particles can be transported in this manner.

Also, the jet pump has applications where the use of centrifugal pumps is not possible, such as: priming devices, to create a siphon without the necessity of using foot valves (Figure 1.6); as a tail-water suppressor in hydroelectric dams, e.g. when high levels of water are required downstream of a dam, a jet pump can be incorporated in the design to increase the effective head for power production (Figure 1.7); as a deep-well pumping system, when a liquid has to be raised from a well (Figure 1.8).

1.4.- Other devices

Using the same principle of a jet issuing from a nozzle at high speeds to aspirate a second fluid, some devices have been used to create vacuum in a closed vessel by aspirating gas from the interior.

1.4.1. The laboratory water-jet pump. Several different principles are involved in the various pumps and devices used to produce low pressures, by means of aspiration or by condensation, to eliminate the gas from inside vessels (Spinks, 1966).

The principle of the water jet pump, used mainly in the laboratory, consists of water supplied from a fast-running tap, which is fed through a tube (A, Figure 1.9) into the nozzle. The water stream, coming out from the nozzle at high velocity from the converging jet (B), is surrounded by a cone to prevent splashing and the possibility of backflow into the vessel where the low pressure is being produced, and also the cone guides the water stream downwards, directly to the exit (C). A side tube (D) is connected to the vessel to be evacuated, and air in the region of (B) is trapped by the high speed jet and forced out into the atmosphere thus decreasing the pressure.

The minimum pressure that can be attained by using these water jet pumps is that due to the water vapour, which is about 10 mmHg under normal conditions. These pumps do not pump very quickly and are normally used for filtration and distillation work in the laboratory, where a high speed is not required.

1.4.2. The steam ejector. Another example of a gas-gas jet pump is represented by the steam ejector. Since the effectiveness of these ejectors in evacuating large volumes, to

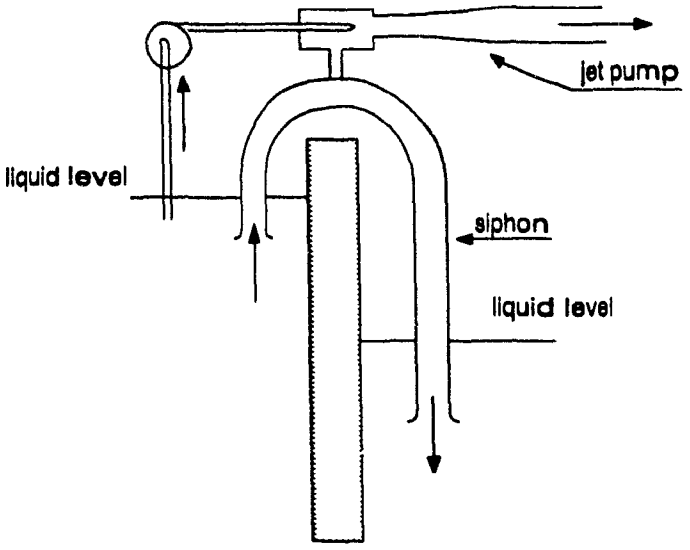

Figure 1.6 A jet pump used as a priming device eliminating the use of foot valves.

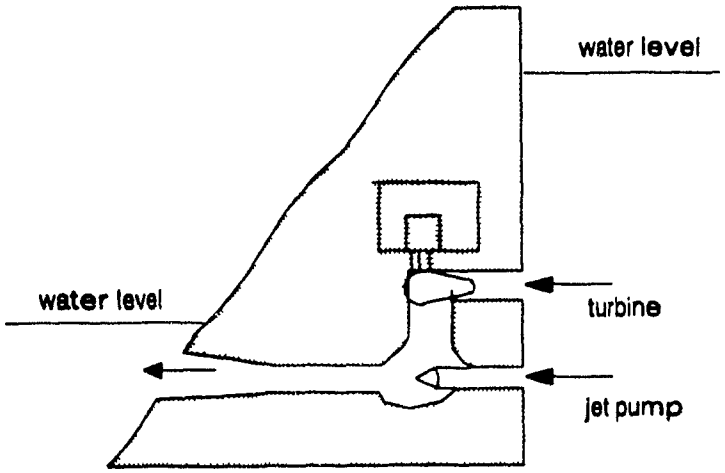

Figure 1.7 Jet pump used as a tail-water suppressor hydroelectric dams.

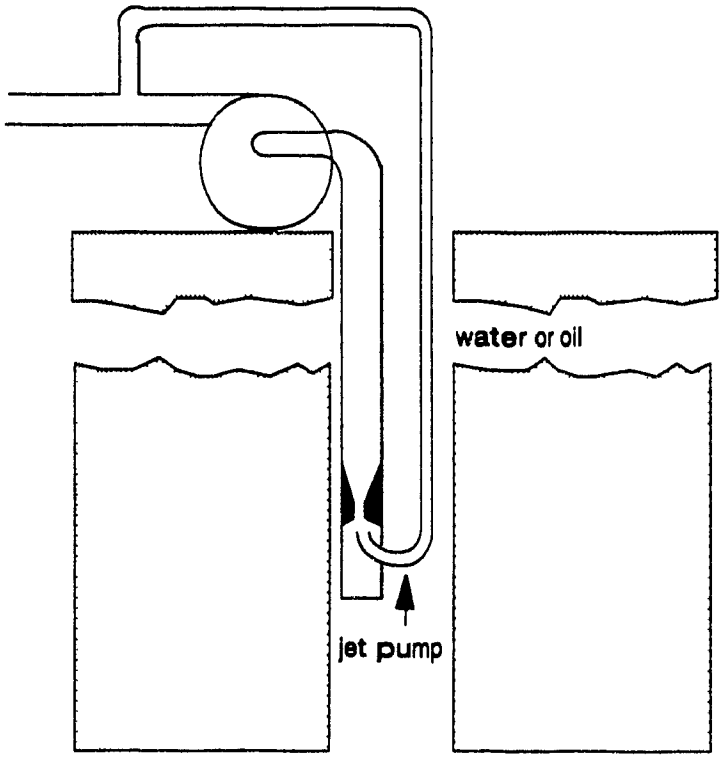

Figure 1.8 Jet pump used for deep-well pumping to raise liquids

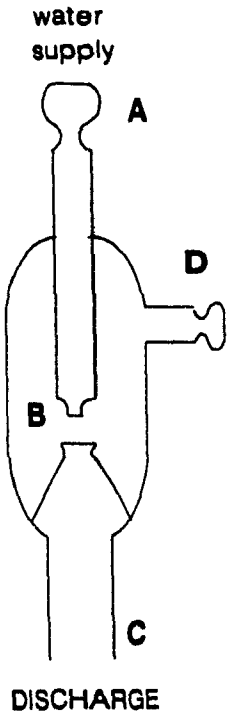

Figure 1.9 Water jet pump to produce vacuum for laboratory use (Spinks, 1966)

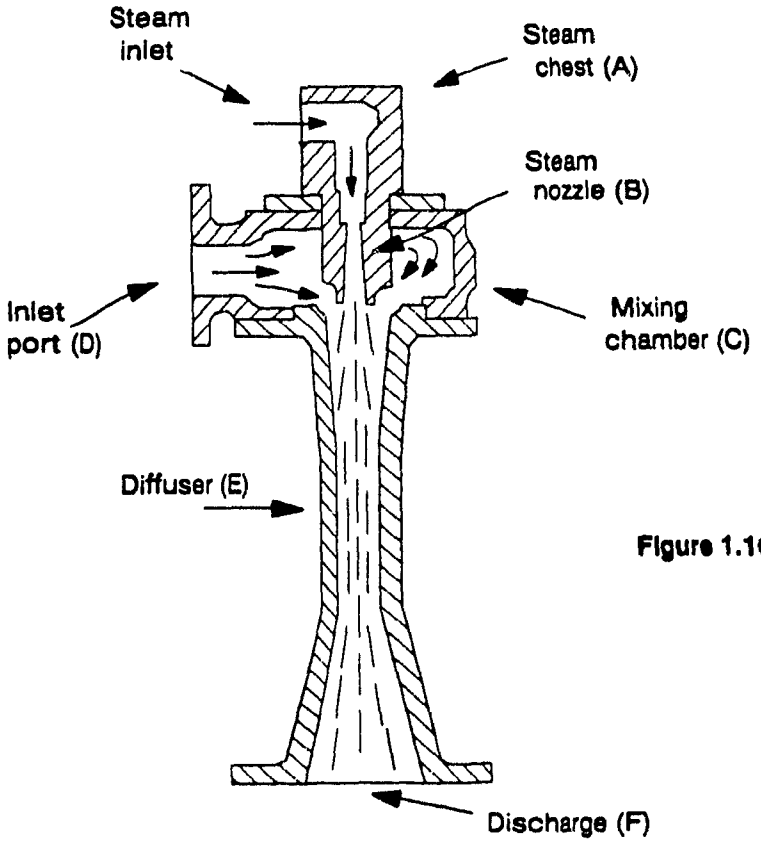

Figure 1.10 Cross section of typical steam ejector

pressures of the order of about 1 mmHg, has been demonstrated (LeBlanc, 1962), steam ejectors have been used successfully in a variety of rough vacuum applications. A typical steam ejector is shown in Figure 1.10, and consists of: (A) a steam chest in which the pressure and temperature are maintained at the proper values; (B) the nozzle through which the steam flows to form a jet; (C) the mixing chamber through which the steam jet passes and entrains gas admitted to the chamber through (D) the inlet port; and (E) the diffuser through which the jet carries the entrained gas to (F) the discharge (Van Atta, 1965). Under normal operating conditions the pressure in the mixing chamber is very low as compared with that in the steam chest and at the discharge port so that the steam expands when passing through the nozzle and then is compressed when passing through the diffuser. Since the cross-sectional area of the steam chest is large as compared with that of the nozzle, the directed or drift velocity in the steam chest is small as compared with that through the nozzle. The random energy of thermal motion of the steam is therefore converted in passing through the nozzle into directed kinetic energy with the formation of a supersonic jet (Mote, 1981).

1.4.3. Diffusion pumps. The term *diffusion pump* is normally applied to jet pumps which utilize the vapour of liquids of comparatively low vapour pressure at room temperature and which provide base pressures significantly lower than those easily attainable with oil-sealed mechanical vacuum pumps.

Typical diffusion-pump jet assemblies consist of three or four annular nozzles, as shown in Figure 1.11, or three annular nozzles and an ejector type of nozzle located in the discharge port. The downwardly directed vapour stream from each annular nozzle entrains gas molecules incident from above and gives them momentum downward toward the discharge port. Each annular jet is capable of maintaining performance against a specific pressure, which is relatively low for the first jet, where the radial clearance is large and relatively high for the final jet, where the radial clearance is small. In a pump of optimum design, the forepressure limits for the successive jets are in regular progression (Van Atta, 1965).

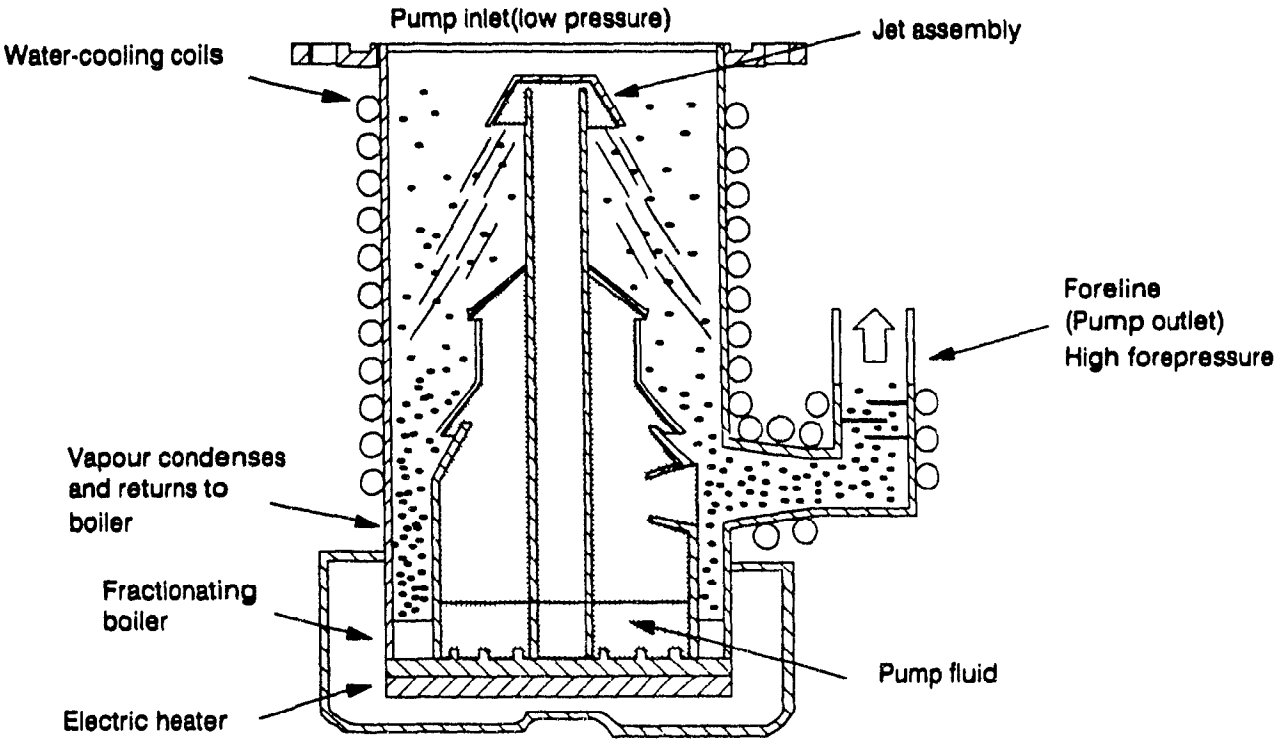

Figure 1.11 Cross section of typical diffusion-pump indicating its parts (Van Atta, 1965)

1.5.- The Jameson Cell

In recent years there has been a considerable increase in the use and application of flotation columns in the minerals industry driven by the never-ending search for more economic and efficient methods of mineral concentration.

The Jameson cell has been described as a high intensity flotation column (Jameson, 1988; Jameson and Manlapig, 1991), and represents a new approach to flotation. Devised by Professor Graeme Jameson of the Department of Chemical and Materials Engineering, University of New Castle, New South Wales, Australia, in 1986, it was conceived as an alternative to the flotation column. Similar devices, although not for flotation, have recently been described in publications from Japan (see Section 1.8).

The main features of the Jameson cell are shown in Figure 1.12. Figure 1.13 compares the Jameson cell dimensions with those of a conventional column.

1.5.1. Basic description. The slurry or suspension is introduced through a nozzle into the first chamber, called *the downcomer*. The plunging jet thus created entrains air producing fine bubbles through shear stresses (Bevilaqua, 1977), in a similar way as in jet-pumps, giving a high gas-slurry area of contact and high particle collection rates. The gas-slurry mixture moves downwards and discharges into a second chamber, called here the *separation compartment*, where the particle-laden bubbles disengage from the slurry, rise up the annular gap between the downcomer and the separation compartment walls to form a froth bed. Nonhydrophobic particles which enter the froth (referred to as entrainment recovery) are usually removed by adding wash water (as done in column flotation). The water-washed float product discharges over the chamber lip as usual.

To illustrate some of the features of the cell, consider that at the start-up there is no liquid in the downcomer. The gas valve is closed, so that no air is admitted into the downcomer and the flow of feed slurry to the downcomer is started. At this stage, the jet is plunging directly into the liquid near the bottom of the downcomer entraining air and forming bubbles. Because of the net downwards motion of the liquid, small bubbles are carried out of the bottom of the downcomer and, if no air is admitted, after a period of time most of the air originally in the downcomer will have been carried out, with the consequence that the liquid is drawn up filling the downcomer, to the level of the of the

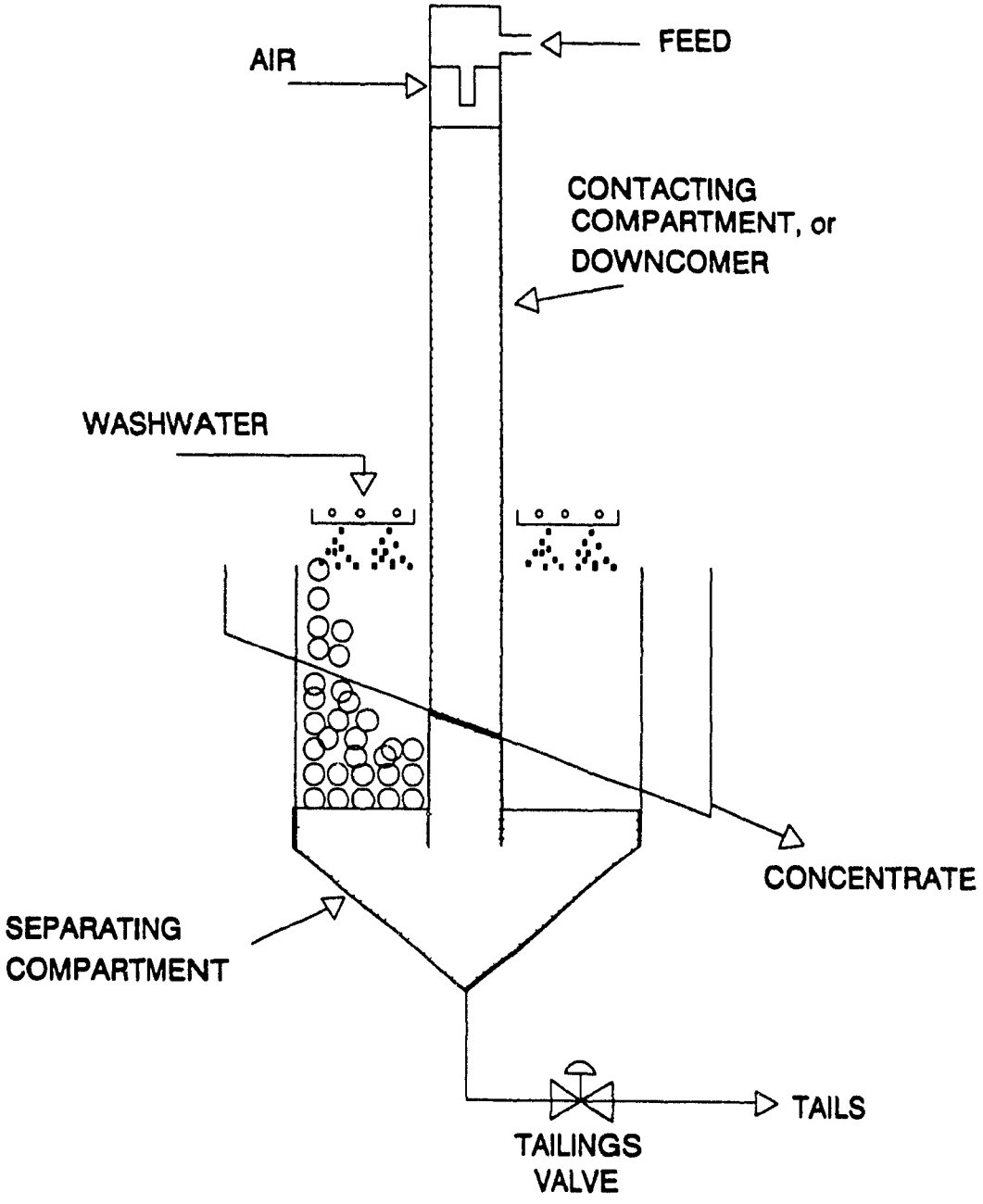

Figure 1.12 Schematic diagram of the Jameson cell

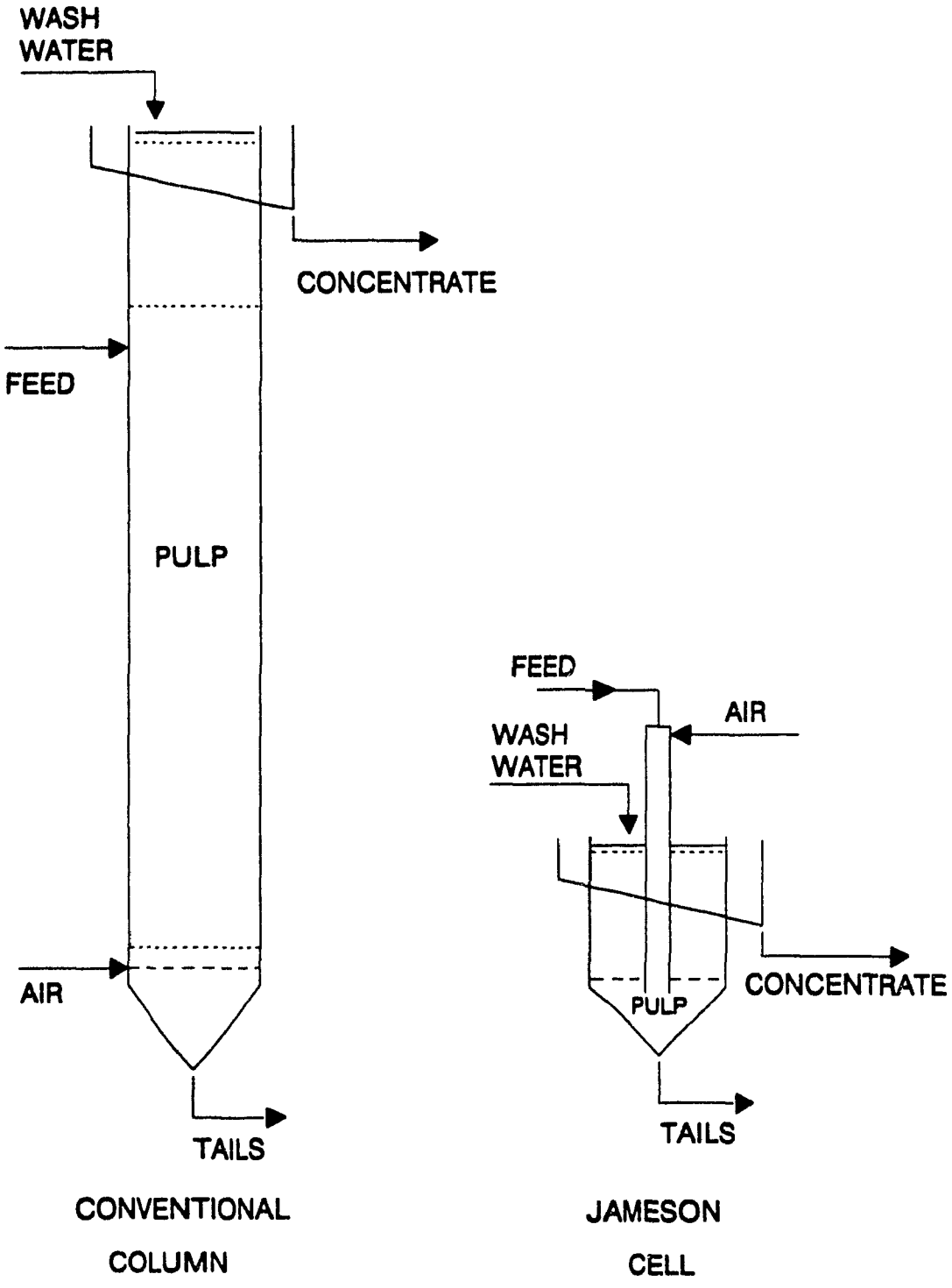

Figure 1.13 Size comparison between the conventional flotation column and the Jameson cell

nozzle. At this point air can be admitted; providing the rate of inflow does not exceed the rate at which air is being entrained by the jet, the liquid (or pool) level inside the downcomer will remain at or near the point of entry of the liquid jet. Under these conditions, the whole downcomer remains filled with a downward moving foam bed.

1.6.- The Free Jet Type Flotation System.-

Similar to the Jameson cell, the free jet type flotation cell (Güney et al., 1991) was developed at the Berlin Technical University in 1985. Using the principle of the liquid jet plunging in a pool to entrain air, the free jet type machine, shown in Figure 1.14, consists of two zones:

i. The zone of high turbulence inside the "encasing tube", where occurs generation of air-bubbles and their loading with some solid particles near the point where the jet hits the pool.

ii. The zone of quiescent-laminar flow, (or separation compartment), where loaded bubbles rise up to the surface of the pulp, forming a froth layer .

One difference with the Jameson cell described in (1.5) is the use of a deflector in the separation compartment to avoid bubbles being dragged to the tailings discharge, and also considering a much shorter downcomer, with a shorter column of liquid being held.

1.7.- The Concurrent Downwards Flotation Column

The use of jets is not the only means of introducing air in a device otherwise similar to the Jameson cell. Sanchez-Pino and Moys (1991), used a gas sparger to introduce bubbles into the downward moving slurry.

The disadvantage of this method of introducing air, as reported by Sanchez-Pino and Moys, lies in the necessity of using high frother concentrations (> 100 ppm) to avoid coalescence problems at the bottom of the column. At these frother concentrations gas holdups comparable to those in the Jameson cell at much lower frother concentrations were obtained.

1.8.- The Downflow Bubble Column

The use of downward concurrent bubble columns is well known in the area of water treatment since the early '80s (Fujie et al., 1980), and in chemical reactors to chlorinate or for oxidation of organic compounds (Shah et al., 1983).

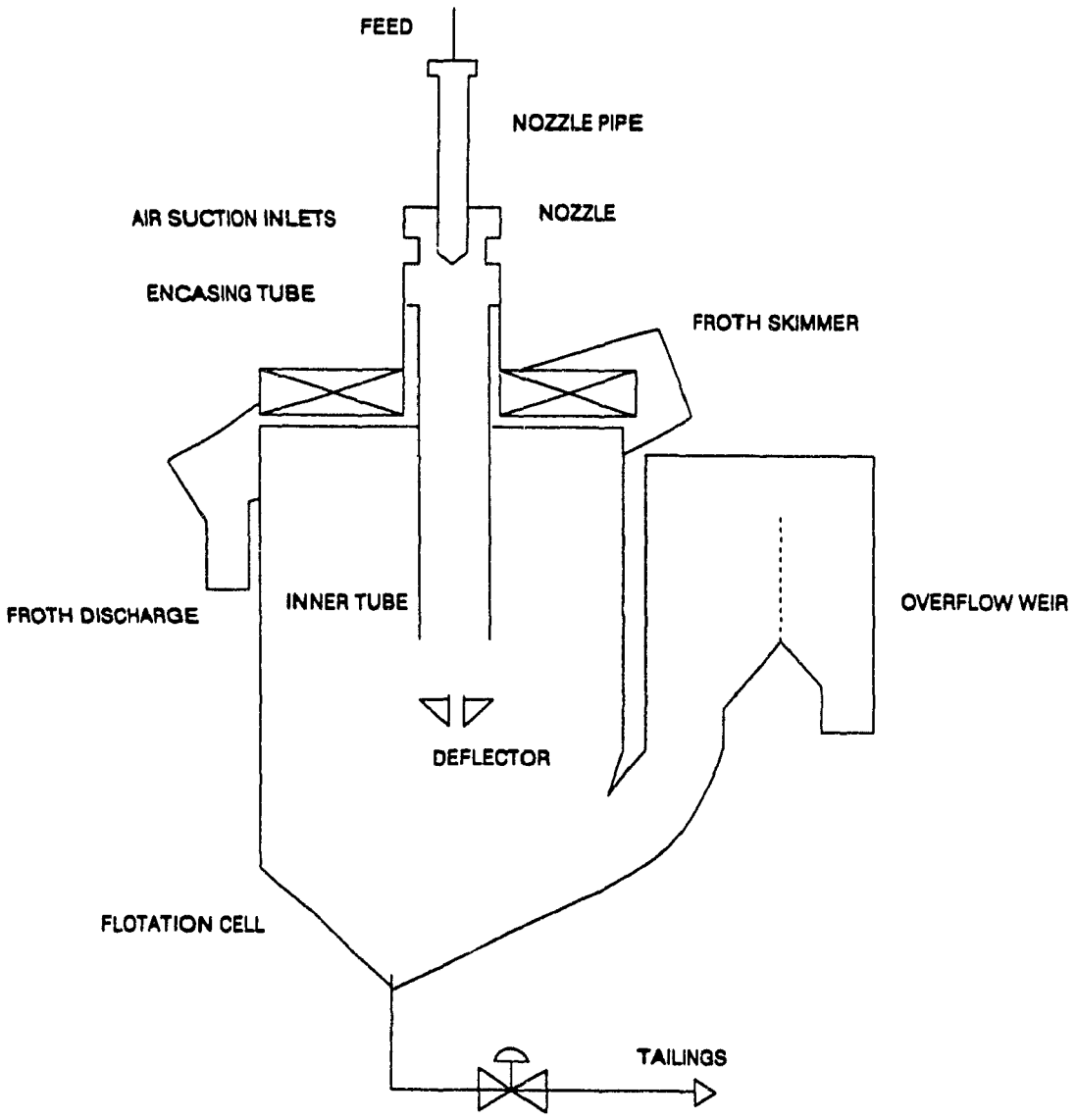

Figure 1.14 Free jet type flotation cell described by Güney et al. (1991)

The apparatus described by Fujie consisted of one downcomer, 6 m long (without separation compartment) where wastewater is fed from the top of the tube and the air is fed through a porous sparger (similar to the concurrent downwards flotation column described by Sanchez-Pino and Moys (1991)), and discharged back to the reservoir.

Shah described a similar device using a 256 cm long downcomer, with a separation compartment, that included a baffle to prevent loss of gas to the discharge (similar to the free jet type flotation cell (Güney et al., 1991)).

Kusabiraki (1990) also described a similar device, using an inclined jet, 30 cm long, enclosed inside a tube to aspirate and entrain air into the liquid.

A downflow bubble column is described by Yamagiwa (1990) where the gas is entrained by a liquid jet inside a tube and includes an isolated separation compartment to disengage air bubbles.

CHAPTER II

TWO-PHASE FLOW IN PIPES

2.-Introduction

Efficient gas-liquid or gas-liquid-solid contact is a basic requirement in many processes, not only in mineral processing. Under this premise, producing an efficient device to achieve high efficiency phase mixing becomes a general problem to be solved.

One method to produce efficient mixing of two or more fluids is the use of vertical plunging jets. Using an ejector or nozzle to create a high velocity jet of fluid, the jet momentum is utilized to drag, disperse and mix a second fluid (Choudhury et al., 1983). Because of the intense shear in the ejector throat the air is dispersed into very fine bubbles and the resulting two-phase mixture flows through the vertical contacting column towards the discharge.

When a mixture of gas and liquid flow together in a vertical tube, several flow patterns are possible, depending on whether they flow down- or upwards. It is possible to have the gas as the dispersed phase and the liquid as the continuous one,i.e. *bubbly flow*; or to have gas and liquid continuous,i.e. *annular flow*, or to have the liquid as the dispersed phase and gas as the continuous one, i.e. *mist flow* (Figure 2.1). The existence of each flow pattern depends on the flowrate of each phase per unit area (Wallis, 1969; Govier et al., 1957).

To create a jet, a restriction has to be placed in the flowing stream inside the tube, i.e. some sort of orifice is required. By means of an energy balance (Bernoulli's equation), a relationship between the velocity and the restriction orifice (nozzle) diameter can be established to estimate the velocity developed by the liquid-jet inside the tube (Shames, 1982).

The liquid jet issuing from the nozzle transfers its momentum to the surrounding fluid, thus dragging the second fluid and mixing it with the jet stream (Benatt and Eisenklam, 1969; Choudhury et al., 1983). If a liquid jet is used inside a vertical tube, filled initially with air, two situations depending on the position of the nozzle can occur: if it is placed at the bottom of the vertical pipe the air must be fed under pressure, and the mixture flows upwards (Jepsen and Ralph, 1969); if the nozzle is placed in the top

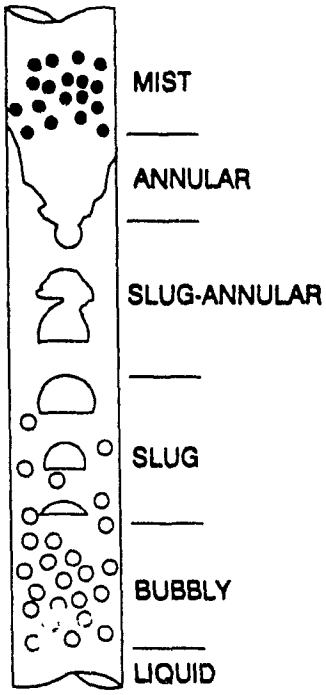

Figure 2.1 Flow pattern of Gas-Liquid mixtures in a tube

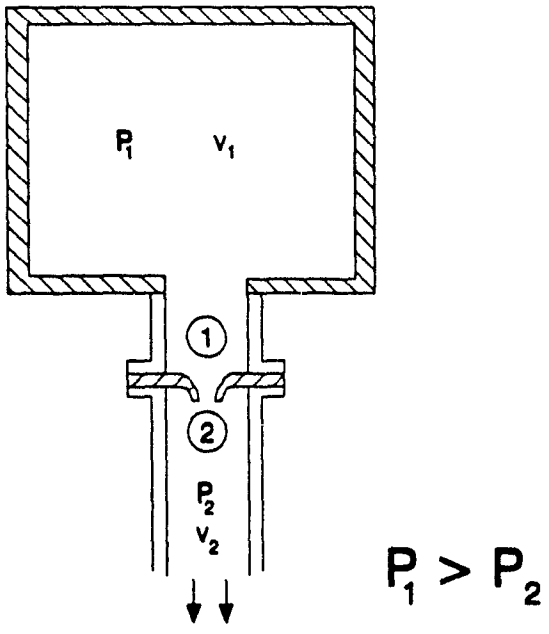

Figure 2.2 Efflux of fluid from a tank through a nozzle

of the column and both air and liquid are fed at the top, the mixture will flow downwards (Friedel et al., 1980).

The objective of this chapter is to analyze the available theory that describes the downwards concurrent multi-phase flow in tubes. The most important variable to be considered is the gas holdup, due to its effect on the performance of the downwards concurrent bubble column used as a flotation device.

2.1.- Incompressible Flow Through a Nozzle

The flow of an incompressible fluid coming out from a tank through a nozzle (Figure 2.2), produces a jet of liquid as a result of body forces (such as gravity), differences in pressure between the interior of the tank and the exterior of the nozzle, and friction. Body forces and differences in pressure exist even when the fluid is at rest; the friction forces are present only when the fluid is in motion.

To describe the flow of the jet, one of the most important relationships in hydrodynamics of ideal flow of fluids can be applied: the Bernoulli theorem, written here as a balance between two points, $i=1$ and 2.

$$\frac{P_1}{\rho} + Z_1 g + \frac{1}{2} v_1^2 = \frac{P_2}{\rho} + Z_2 g \frac{1}{2} v_2^2 \qquad (2.1)$$

where P_i is the pressure at i, Z_i the elevation at i, v_i the flow velocity of the stream at the point i, ρ the density of the fluid and g gravitational acceleration.

The case of fluid flowing through a nozzle into the downcomer is analogous to the efflux of fluid from a tank resulting from excess pressure inside.

As the liquid jet from the nozzle corresponds to a subsonic flow (the superficial velocity of the jet is less than the velocity of sound), the pressure at the exit of the nozzle is equal to that of the surrounding stream (Shih-I Pai,1954). For subsonic flow, lowering the pressure in the discharge increases the jet velocity (without reaching the critical velocity, i.e. the pressure at which the velocity of the jet equals the velocity of sound). It is possible to assume that isentropic effects (generation of heat) for this type of flow are negligible. Under these two considerations the nozzle design (i.e. its geometry) has no effect on the jet operation (Shames, 1982).

2.2.- The Downwards Concurrent Bubble Column

Pressure methods to estimate gas holdup in two- and three-phase flotation columns have been standard (Finch and Dobby, 1991). In such columns the dynamic component of pressure can be considered negligible and the problem becomes one of an hydrostatic pressure balance. In the case of downflow concurrent bubble columns where relatively high liquid throughputs are involved, dynamic terms contribute to the pressure balance, and cannot be neglected. The most evident (and the one considered here), is that arising from the sudden deceleration of the liquid jet issuing from the nozzle (See Appendix C).

Under steady operation the multi-phase column in the downcomer is maintained provided the pressure at points *A* and *B* (Figure 2.3) are balanced, that is

$$P_v + P_z + P_h - P_s + P_{atm} \qquad (2.2)$$

where P_v is the pressure inside the downcomer above the pool level ($< P_{atm}$, i.e. vacuum); P_h the hydrostatic pressure head due to the weight of the multi-phase mixture; P_z is the dynamic pressure due to the de-acceleration of the feed jet; P_s is the hydrostatic pressure head in the separation vessel at point *B*; and P_{atm} is the atmospheric pressure.

By inspection, the contribution of friction losses can be neglected due to the combination of: small friction factors (Re<7500); a short length of downcomer (H_D=1.82 m); and a smooth wall (relative roughness $\epsilon < 0.000005$) .

For the water-air and slurry-air systems studied here, the terms of equation 2.2 are listed in Table 2.1.

An earlier attempt to relate gas holdup with pressure measurements was made by Lockhart and Martinelli (1949) by using the ratio between the pressure drop in the pipe as liquid flowed alone to the pressure drop as gas flowed alone. The inapplicability of this model for the case of downcomers with self induced air comes with the fact that air cannot flow without the presence of a liquid jet. The determination of the flow-type modulus, defined by Lockhart and Martinelli in their equation, is empirical, depending on the superficial gas velocity and does not take into account the flow pattern. It has been demonstrated that the modulus is also a function of the flow rate, even when the pressure

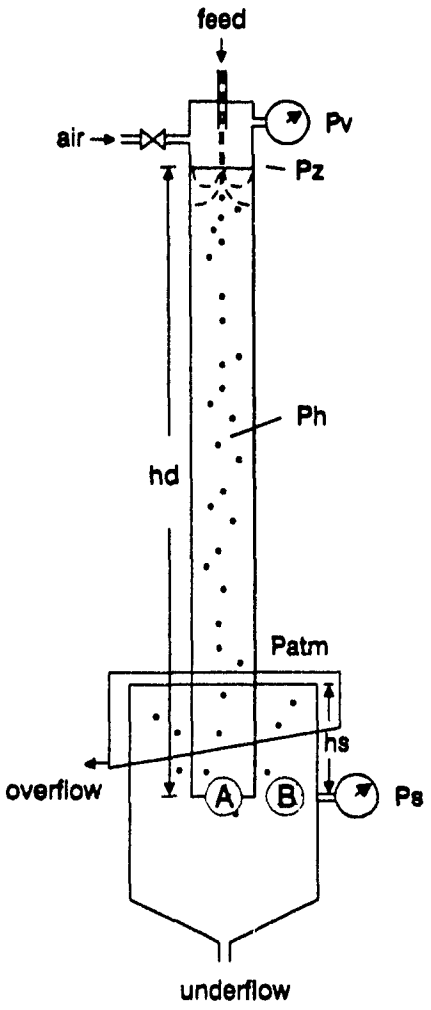

Figure 2.3 Schematic illustration of the downflow concurrent column, process variables and pressure terms involved in the calculation of gas holdup

drop ratio remains constant (Anderson and Mantzouranis, 1960).

Pressure term	Water-air system	Slurry-air system (Hydrophillic solids)
P_v	*measured*	*measured*
P_z (App. 3)	$J_f^2 \rho_l \left[\frac{D_d^2}{D_j^2} - \frac{1}{1-\varepsilon_g} \right]$	$J_f^2 \rho_{sl} \left[\frac{D_d^2}{D_j^2} - \frac{1}{1-\varepsilon_g} \right]$
P_h	$(H_D - z)\rho_l(1-\varepsilon_g)g$	$(H_D - z)\rho_{sl}(1-\varepsilon_g)g$
P_s	$measured, [-h_s \rho_l (1-\varepsilon_{g(s)})g]$	$measured, [-h_s \rho_{sl(s)} (1-\varepsilon_{g(s)})g]$

Table 2.1

Expressions for the components of pressure in the downflow column in Figure 2.3; where H_D is the height of the downcomer; D_j and D_D are the diameters of the nozzle and the downcomer respectively; h_s is the height of the liquid in the gap between the downcomer and the separation compartment; ε_g is the gas holdup; g is acceleration due to gravity; ρ_l is the density of the liquid; and ρ_{sl} is the density of the slurry The subindex *(s)* indicates that the variable is measured in the separation compartment.

2.3.- Air Entrainment

Efficient gas-liquid mixing can be achieved by using a liquid jet ejector. In such a device a high velocity liquid jet, coming out from a nozzle, is disintegrated in the throat of the ejector and the jet momentum is utilised to disperse and mix a second fluid (in this case air). Because of the intense shear stress in the ejector throat the gas is

dispersed into very fine bubbles, and the resulting two-phase mixture moves out of the throat zone (Choudhury et al., 1983).

The entrainment phenomena is also said to be produced by the effect of the action of large-scale "mixing-jets" that engulf volumes of fluid in bulk (Grant, 1958; Bradshaw, 1972).

Large-scale motions of the interface are correlated with an increase in the rate of entrainment (Gartshore, 1965), presumably by increasing the surface area of the interface and therebye controlling indirectly the rate of entrainment.

The theory of large eddies displacing the surrounding fluid was also used to explain the entrainment experimentally observed by Bevilaqua and Lykoudis (1977), who demonstrated that air entrainment is a process resembling a folding of the turbulent (liquid) and non-turbulent (air) fluids by the rotation of large eddies. These observations were made using a narrow channel (0.635 $\times$ 45 cm) where eddies artificially created by blowing air on the surface promoted the formation of waves in the direction of the air circulation, creating folding waves of liquid that entrained air. By this means only the folding action of eddies was isolated, and the theory developed can only be applied in similar situations.

In the case of turbulent jets, the entrainment of a second fluid cannot be described as a result of large eddies or waves in motion displacing and folding the fluid. Using fluid jets the entrainment is produced by the disintegration of the jet and momentum transfer to the surrounding fluid (Bennat and Eisenklam, 1969), which entrains the secondary fluid into the jet stream.

The disintegration of a free jet is influenced by the turbulence in the nozzle and the ambient pressure (Grant and Middleman, 1966). The jet spreads into a conical sheet into which gas is entrained, and a momentum exchange occurs between the surrounding gas at rest, and the moving jet. According to Benatt and Eisenklam, from then on the acquired momentum of the entrained gas itself becomes predominantly responsible for further momentum exchange.

In the case of jets impinging on a liquid surface the momentum exchange occurs mainly around the point of impact. As the cavity formed in the surface contains gas, the

submerged jet is surrounded by a gas sheet which extends the surface cavity for a short distance into the bulk liquid and momentum exchange between phases takes place, (which coincides with the proposed explanation by Benatt and Eisenklam). Inside the liquid pool, the gas sheet collapses into a multitude of very densely packed, small bubbles (Smigelschi, 1977), where interfacial areas of the order of magnitude from 500 to 1000 m^2/m^3 have been reported (Bin and Smith, 1982).

A momentum balance can give an estimation of the volumetric gas flowrate aspirated into the system. According to Bird (1960) the momentum balance in a closed system becomes:

rate of momentum accumulation = *rate of jet momentum in* + *rate of gas momentum in* + *sum of forces acting on the system* - *rate of momentum out* (2.3)

Williams et al. (1990) have reported a momentum balance for a liquid-solids dispersion which can be extended by analogy to a liquid-gas system. The momentum balance equation for the liquid phase is:

$$\frac{\partial}{\partial t}(\rho_l \varepsilon_l J_l) + \frac{\partial}{\partial z}(\rho_l \varepsilon_l J_l J_l) + \varepsilon_l \frac{\partial P}{\partial z} + \rho_l \varepsilon_l g + \sum_{i=1}^{n} f_{di}(J_l - U_{bi}) + \sum_{i=1}^{n} R_i = 0 \qquad (2.4)$$

where $\partial P/\partial z$ is the pressure gradient of the system; U_{bi} is the velocity of the ith bubble; R_i is the electric retardation force, resulting from the interaction of the *ith* bubble due to electric charges; and f_{di} is the drag coefficient of the ith bubble, defined by:

$$f_{di} = \frac{2 F_{di}}{\rho_l U_{bi}^2 A_i} \qquad (2.5)$$

where F_{di} is the drag force of the ith bubble; and A_i is the characteristic area of the ith bubble.

The momentum balance for the gas-phase, by analogy with the momentum balance presented by Williams et al. (1990) becomes:

$$\frac{\partial}{\partial t}(\rho_g \varepsilon_g U_{bi}) + \frac{\partial}{\partial z}(\rho_g \varepsilon_{bi} U_{bi} U_{bi}) + G(\varepsilon_l)\varepsilon_g \frac{\partial \varepsilon_l}{\partial z}$$

$$+ \varepsilon_g \frac{\partial P}{\partial z} + \rho_g \varepsilon_g g - f_{bi}(J_l - U_{bi}) + \sum_{k=1}^{n} C_{ik}(U_{bk} - U_{bi}) - R_i - 0 \qquad (2.6)$$

where C_{ik} is the bubble-bubble coefficient, which corrects for frictional effects resulting from bubble collisions; $G(\varepsilon_l)$ is the compressive stress between the bubble, expressed as the stress modulus (Shih et al., 1987).

Solving this equation to obtain the desired parameters that could describe the downcomer operation presents a difficult computational problem. Those terms that represent the gas momentum have to be taken into account i.e. it is no longer acceptable to let $\rho_g = 0$, which then also makes it necessary to consider those terms that represents drag forces and bubble-bubble interaction. Thus, direct measurement of some of the variables involved is required, especially U_{bi} and the local gas holdup (ε_g) in the zone for a known period of time. A suitable technique to measure these parameters is not yet available, and they are normally inferred from judicious assumptions. There are further complications as it becomes necessary to consider wall effects and secondary circulation due to non uniform distributions of flow.

Folsom (1948) also proposed a momentum balance for a jet pump with constant cross-sectional area. The equation was restricted to a straight horizontal pipe with constant flow velocity of the liquid-gas mixture, and uniform gas holdup, and was applicable only to a restricted region of the mix· · pipe. No experimental results to validate his equations were presented.

2.4.- Two-Phase Flow in Vertical Pipes

When gas and liquid flow together in a vertical tube, several flow patterns are possible. In so-called bubbly flow, the gas is dispersed throughout the continuous liquid phase as bubbles of various sizes, and as the bubbles are small compared with the diameter of the tube, their shape is not greatly influenced by the presence of the tube walls (Nicklin, 1962).

The flow of two phases in a vertical tube is described more often in the case of upwards vertical flow, which is also more frequently encountered in practice. The flow pattern cannot be described simply (as for single phase systems) as laminar, transitional or turbulent, by defining simple dimensionless parameters. In the case of two phase systems, the relative amount of each phase, their dispersion one in the other and their individual motion are all important in order to define the system.

For gas-liquid flow in a pipe the same key variables, as for single phase, are important: density, viscosity, surface tension, pressure and temperature, plus the amount of each phase in the tube, and the flowrate of phases (Govier et al., 1957). Among the geometric variables are: the tube diameter and length, and roughness of the wall.

Bubbly flow is characterized by a suspension of bubbles, as the discontinuous phase, in a continuous liquid. Bubbly flow has numerous forms, ranging from a single isolated bubble in a large container to the quasi-continuum flow of a foam, containing less than one percent of liquid by volume (Wallis, 1969). The slug flow regime can be obtained changing the gas-liquid ratio, at constant liquid flowrate, by increasing the gas flowrate until large bullet shaped slugs are produced. This slug flow pattern is characterized by alternating slugs of gas which are surrounded by a thin film of liquid, and spaced by regions of bubbly flow (Govier et al., 1957).

2.4.1.- Drift Flux Analysis

The ability to predict the volumetric concentration of a phase, i.e. the holdup, as a function of the design and operating parameters (geometry, pressure, flow rates, thermodynamic and transport properties of the phases, etc.) is of considerable importance to many processes (Zuber and Findlay, 1965), including column flotation (Finch and Dobby, 1990).

Neglecting non uniform flow and concentration profiles across the pipe, Behringer (1936) was apparently the first to consider the effect of local relative velocity between phases. From continuity considerations, an expression for the superficial velocity of a bubble in bubbly flow can be expressed as:

$$J_b = U_t - \frac{Q_l}{A} - \frac{Q_g}{A} \tag{2.7}$$

where Q_l and Q_g are the volumetric flowrate of the liquid and the gas in the downwards direction, and U_t is the terminal rise velocity of a single bubble in an infinite medium. The volumetric concentration ε from the relation between U_t and the superficial velocity of the gas can be expressed as:

$$\varepsilon = \frac{\frac{Q_g}{A}}{J_b} \tag{2.8}$$

Although the analysis of Behringer showed good agreement with his experimental data, the assumptions regarding concentration profiles and velocity distribution makes his model applicable only in some cases. Thus, further refinement became necessary.

Bankoff (1960) took into account the parameters neglected by Behringer, including the effect of the nonuniform radial flow and volumetric concentration in the bubbly two-phase flow regime. Bankoff neglected the effect of local relative velocity between phases, but included the effect of nonuniform profiles by proposing a parameter K, which is function of the pressure, quality (in the case of steam flow) and mass flow rate. This model can be applied only in systems where the relative velocity between phases can be neglected.

Following the work of Bankoff, there have been numerous publications that take into account the effect of nonuniform profiles (Griffith and Wallis, 1961; Nicklin, 1962; Neal, 1963), modifying the equation of Behringer by adding terms to correct for nonuniform distributions.

One theory that involves the relative motion of phases, rather than motion of the individual phases, is the drift-flux model (Wallis, 1969). The contribution of this theory lies in the development of a general model, using a few key parameters to determine the relative motion of each phase.

The theory states that the volumetric flux of either component relative to a surface moving at the volumetric average velocity j is represented by the drift flux j_{21} (phase 2 relative to phase 1). Thus, it can be expressed by:

$$j_{21} = v_{21}\ \varepsilon(1-\varepsilon) \tag{2.9}$$

where v_{21} is the superficial velocity of phase 2 relative to phase 1.

The drift flux is analogous to the diffusional flux in molecular diffusion of gases and provides a way of modifying the theory of homogeneous fluids to account for relative motion. Using this analysis all the properties of the flow (void fraction, mean density, etc) can be expressed as a homogeneous flow together with a correction factor which is a function of the component fluxes.

Defining the relative or slip velocity (U_s) as the velocity of one phase relative to the other (Wallis, 1969), for downward concurrent flow of both phases it becomes:

$$U_s = \frac{J_l}{1-\varepsilon_g} - \frac{J_g}{\varepsilon_g} \tag{2.10}$$

where J_g and J_l are the superficial gas and liquid velocities respectively, defined positive in the downward direction.

For bubbly flow, Wallis (1969) proposed that the slip velocity is related to the drift flux, j_{GL}, by:

$$j_{GL} = U_s \varepsilon_g (1-\varepsilon_g) \tag{2.11}$$

Richardson and Zaki (1954) proposed that the slip velocity is related with the terminal velocity by:

$$U_s = U_t (1-\varepsilon_g)^{m-1} \tag{2.12}$$

where m depends on the Reynolds number of the bubble, Re_b:

$$m = \left(4.45 + 18\frac{d_b}{d_c}\right) Re_b^{-0.1} \qquad 1 < Re_b < 200 \tag{2.13}$$

$$m = 4.45\, Re_b^{-0.1} \qquad 200 < Re_b < 500 \tag{2.14}$$

and

$$Re_b = \frac{d_b\, U_t\, \rho_l}{\mu_l} \tag{2.15}$$

where d_b is the bubble diameter; d_c is the column diameter; ρ_l the fluid density; and μ_l the liquid viscosity.

Combining Eq. (2.10), (2.11) and (2.12), the drift flux becomes:

$$j_{GL} = U_t \varepsilon_g (1-\varepsilon_g)^m = J_l \varepsilon_g - J_g(1-\varepsilon_g) \tag{2.16}$$

The application of the bubbly flow model to estimate gas holdup and bubble diameter has been applied for counter-current bubble columns with good agreement between experimental and predicted values (Dobby et al., 1988; Finch and Dobby, 1990). In this thesis the application of the model to the concurrent downwards bubble column is analyzed.

The drift flux velocity defined by Eq. (2.16) has been used by Wallis (1969) to visualize the effect of changing feed and gas velocities for the particular case of small bubbles suspended in a liquid moving in a vertical pipe.

Wallis (1969) found that for fluid-particle systems $m=3$ correlates a wide variety

of data, Eq. (2.16) thus becomes:

$$\frac{J_{GL}}{U_t} = \varepsilon_g (1 - \varepsilon_g)^3 \tag{2.17}$$

Plotting the dimensionless drift flux (J_{GL}/U_t) versus gas holdup the curve represents a balance between fluid dynamic drag and buoyancy.

It has been demonstrated that for bubbles, particle-particle interaction can be neglected (Wallis, 1969) so Eq. (2.16) should be valid for high gas holdups (>50%).

CHAPTER III
ELECTRICAL CONDUCTIVITY

3.- Introduction

The electrical conductivity of a material is an intensive property, i.e. it does not depend on quantity or shape of the material. Most chemical elements and compounds have well defined conductivities; metal alloys, minerals and electrolytes have conductivities that depend on their chemical composition and physical structure.

The use of electrical conductivity to investigate multi-phase systems is a standard (Fan, 1989); its use, for example to estimate the holdup of a non conductive phase in such systems has been successfully demonstrated (Uribe-Salas, 1991). The use of the conductivity technique, however, has been tested only in counter-current systems, such as the conventional flotation column; for downflow concurrent systems with high gas fraction no similar use has been reported, and therefore its applicability in these systems was unknown. In this chapter the theory involved in the use of the conductivity to estimate holdup is reviewed with regard to its application for the purpose of this thesis.

3.1.- Basic concepts

Electrical conductivity is the proportionality constant in Ohm's law. In its general form Ohm's law states that the current flow in any part of a given system is proportional to the potential gradient, that is

$$i = -\kappa \nabla V \qquad (3.1)$$

where i is the current density [A/cm^2], ∇V is the potential gradient [Volt/cm], and κ is the electrical conductivity [S/cm]. The sign (-) indicates that the current flows in the direction of decreasing potential.

Electrical conductivity has several equivalent denominations: *conductivity* (Raleigh, 1892; Meredith and Tobias, 1962; Uribe-Salas, 1991), *specific conductance* (Condon, 1967) and *specific conductivity* (Kasper, 1940). The most used term is conductivity, denoted by the greek letter kappa, κ, in the SI system. Throughout this

thesis the term conductivity will be used.

The units of conductivity can be derived from Eq. (3.1): if the current density is given in A/cm² and the voltage gradient in Volt/cm, the conductivity has units of Ω^{-1}/cm. The unit ω^{-1} is named *Siemens* (S) in the SI system: 1 S = 1 ω^{-1}. (mho, i.e. Ohm spelled backwards, is used by some authors, although it is not part of any unit system).

3.2.- Measurement of Conductivity

The conductivity of an electrolyte cannot be reliably measured using direct current, because this causes a build-up of electrolysis products at the electrode surface which changes the resistance at the electrode/solution interface. To eliminate this effect an alternating current is used. Using the circuit depicted in Figure 3.1 the resistance of the electrolyte is computed by applying Ohm's law ($I = (V_A - V_B)/R$). Solving for R, the conductivity can then be calculated from

$$\kappa = \frac{l}{A\,R} \qquad (3.2)$$

where A and l are the area of and the distance between electrodes respectively. (A complete derivation of this equation is given in Section 3.3.1).

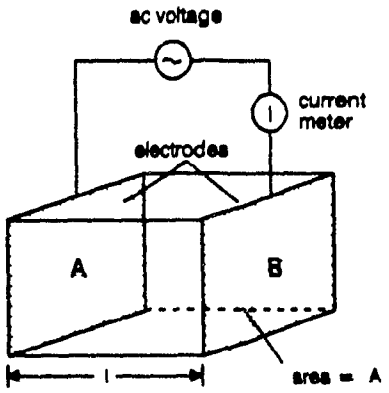

Figure 3.1 Conductivity cell and electric circuit to measure conductivity of electrolytes

When applying a voltage between electrodes immersed in a conductive liquid (liquid electrolyte) other associated phenomena are present (Braunstein and Robbins, 1971; Sawyer and Roberts, 1974):

Double-layer capacitance. A positively charged electrode will preferentially attract a layer of negative ions (as a negative electrode will preferentially attract positive ions). The double-layer, consisting of charges on the electrode and oppositely charged ions adjacent to it in solution, separated by a layer of solvent ions forms an electrical capacitor, capable of storing charge. If a low steady voltage is applied to the electrodes, sufficient to charge the double-layer, virtually no current will flow beyond the external layer due to the potential drop across the planes.

Electrolysis. As the voltage applied to the electrodes is increased, the charge in the double-layer increases until a current flow is established when the decomposition voltage is exceeded (analogous to the break-down voltage of a capacitor). The flowing current across the electrode-solution interface is accompanied by oxidation at the positive electrode and reduction at the negative electrode. This electrolytic process (following Faraday's law) partially short circuits the double layer, behaving electrically like a resistor shunting a capacitor.

Ohmic resistance. The current is carried through the bulk liquid electrolyte by cations moving towards the cathode and anions towards the anode. Current flow is accompanied by energy dissipation, since ions must overcome frictional forces in their motion through the medium.

Concentration polarization. By further increases of voltage, Faradaic removal of electroactive ions (i.e. ions that can be reduced or oxidized in the range of applied voltage to the electrodes) near the electrode may occur faster than mass diffusion from the bulk electrolyte can replenish their supply. The possibility of a concentration gradient created between the bulk electrolyte and the electrode surface can lead to a diffusion-limited value of current.

By using alternating current these effects of the processes associated with the electrodes can be overcome. By increasing the frequency, concentration polarization can be reduced or eliminated. The Faradaic effect can be eliminated by reducing the applied

voltage. Frequencies of 1 KHz and voltages less than 1 V are recommended for general applications (Cole and Coles, 1964).

3.3.- Cell Constant and Geometrical Factors.

3.3.1.- The theory of the potential

This refers to the distribution of potential energy between spatial configurations, such as plates. In electricity, these spatial configurations are represented by the electrodes at different potentials (anode and cathode), where one electrode (single configuration) is considered to be entirely at one level of potential energy, i.e. is an equipotential surface. The variation of potential from the anode to the cathode, or vice versa, can be conveniently considered in terms of equipotential surfaces; determining form and position of equipotential surfaces in conductive mediums, some restrictions are observed (Kasper, 1940):

(1).- the medium is such that the rate of energy dissipation is linearly dependent on the difference in potential level, so a linear law of conduction must be obeyed. In electricity this is known as Ohm's law, which generally holds for electrolytes (Gilmont and Walton, 1956), and states that the current flowing in any part of the system should be a linear function of the potential gradient, i.e. Eq. (3.1) with

$$\nabla V = \frac{\partial V}{\partial x} + \frac{\partial V}{\partial y} + \frac{\partial V}{\partial z} \quad (\textit{rectangular coordinates}) \qquad (3.3)$$

Additionally, it is known that a constant current enters the system at the anode, flows through it, and leaves through the cathode. If the electrodes are specified in terms of their geometry, in accordance with the law of conservation of current, if any volume of the conducting medium is selected the net resultant current entering and leaving the system will be zero. In formal mathematical language this is equivalent to saying that the divergence of the current is zero, thus

$$\nabla i = 0 \qquad (3.4)$$

Since $i = -\kappa \nabla V$, if the medium is homogeneous electrically (κ is constant), the divergence of the gradient of the potential is zero, i.e.

$$\nabla \cdot \nabla V = \nabla^2 V = 0 \qquad (3.5)$$

which is known as Laplace's equation and implies the laws of electrical flow (although it can be applied to any phenomena which may be treated by the theory of the potential).

(2).- the medium is homogenous and isotropic electrically. Since heat dissipation is associated with the electric current flow, and conductivity is a function of the system temperature, electrolytes cannot be said to satisfy this condition in a strict sense; however, as the current which is used can be made sufficiently small the influence of this effect can be neglected.

(3).- the flow of energy through the electrode does not alter the condition that the surface of the electrode. That is, the electrode must be equipotential, a condition known as the "resistance of the electrode (or terminal effect)". If the electrode size is large with respect to the point of contact, where the current enters or leaves the system (connection wire), and the electrode conductivity is high enough as compared with that of the medium, this effect will tend to vanish. Since in most practical applications the ratio of conductivity of the electrode (i.e. of the metal) to that of the electrolyte (i.e. of the medium) ranges from a hundred thousand to a million, this effect can be neglected.

(4).- the flow of energy in any direction, from the electrode to the electrolyte or vice versa, may introduce a discontinuity in potential at the electrode surface. Hence it is necessary that the magnitude of the discontinuity must be uniform over the surface. This condition applies to electrode polarization and can be avoided by selecting an appropriate frequency and using alternating current (Cole and Coles, 1964). Further reductions of this effect can be obtained by platinizing the electrode which increases the surface area and reduces the current density (Braunstein and Robbins, 1971).

3.3.2.- Geometrical factor.

Having established the conditions to be satisfied, it is necessary that a uniform current flow exists between the electrodes in the system. The simplest case is that of infinite parallel planes (Kasper, 1940).

Considering the anode and cathode surfaces as two parallel infinite planes, each being equipotential, the distribution of potential between the planes may be represented by planes to the two initial planes (electrode surfaces). The lines of current flow must leave the anode normally, intersect every equipotential surface normally and arrive, finally, to the cathode normally. In an electrically isotropic and homogeneous medium the equipotential surfaces per unit potential difference must be equally spaced; hence a constant current flows from the anode to the cathode. The current density over the electrodes and over each equipotential surface is uniform, indicated graphically by uniform spacing of lines representing current flow.

As infinitely large planes for cathode and anode are impractical, systems must be devised in an equivalent form. By applying the sectioning method, it is possible to consider the replacement of any equipotential surface by a perfect conductor (electrode), having the same shape and position. It is implicit that with real electrodes the terminal effect can be neglected. A second method of sectioning assumes that sectioning surfaces are everywhere coincident with lines (surfaces) of current flow and, accordingly, no current crosses such a surface. The process of sectioning does not alter the flow within created boundaries.

In the arrangement illustrated in Figure 3.1, (which is a section of the infinite, parallel plate system) the resistance between electrodes A and B is given by

$$R = \frac{drop\ of\ potential}{current} = \frac{V_A - V_B}{I} \qquad (3.6)$$

For a linear conductor the current density on any equipotential plane is constant, hence

$$i = -\kappa \frac{\partial V}{\partial x} = \frac{I}{A} \qquad (3.7)$$

where i is the current density, κ is the conductivity, I is the total current and A is the cross-sectional area.

By integration of Eq. (3.8) it is possible to obtain

$$K = \kappa \frac{A}{l} \qquad (3.8)$$

where K is the conductance (= 1/R), and l is the distance between electrodes.

3.4.- Electrical Conductivity of Two- and Three-Phase Systems.

The electrical conductivity of two- or three-phase dispersions (one continuous phase plus one or two dispersed phases) has been termed *effective conductivity* (De la Rue and Tobias, 1959; Fan, 1989, Uribe-Salas, 1991), *apparent conductivity* (Turner, 1976) or simply conductivity. In the present work the term *effective conductivity* -to distinguish conductivity measurements in multiphase systems from those measurements in single phase systems- will be used with the Greek letter kappa, κ, and corresponding subindices indicating the nature of the system, e.g. $\kappa_{l\text{-}s\text{-}g}$ refers to conductivity of liquid-solid-gas system.

3.4.1.- The models.

(a).- Electrical conductivity of two-phase dispersions.

In general terms, the electrical conductivity of a liquid-gas, $\kappa_{l\text{-}g}$, or liquid-solid, $\kappa_{l\text{-}s}$, system depends on the electrical conductivities of the two phases and their relative amounts. However, the conductivity of dispersions does not follow the additive rule (Maxwell, 1892), i.e. the relation between the conductivity of the dispersion and the concentration of the dispersed phase is not linear.

Maxwell (1892) apparently was the first one to investigate the phenomena, considering a sphere of different conductivity from the material around it, and studying the effect of this sphere on the current and potential field in the surrounding material. Considering many such spheres contained within a larger sphere of continuous medium of conductivity κ_l - at distances one from another large enough so their influence on the course of the current may be taken as independent of each other - the effective conductivity, $\kappa_{l\text{-}d}$, of the large sphere for a volumetric fraction ε_d of the dispersed phase

of conductivity κ_d is given by

$$\kappa_{l-d} = \kappa_l \left(\frac{1+2\beta\varepsilon_d}{1-\beta\varepsilon_d} \right) \qquad (3.9)$$

where

$$\beta = \frac{\alpha-1}{\alpha+2} \quad ; \quad \alpha = \frac{\kappa_d}{\kappa_l} \qquad (3.10)$$

This model has been successfully used by Turner (1976) for measuring holdup in liquid-fluidized beds of spheres. A range of solid particle diameters (0.15 - 1.0 mm) and conductivities (0 ~ 0.03 Scm^{-1}) was used. Although Maxwell's model considers dilute dispersions solid volumetric fractions up to 60% were adequately fitted by Maxwell's equation.

Bruggeman (1935), as reported by Nasr-El-Din et al. (1987), extended Maxwell's work to the case of spheres of various sizes and random distributions, making his equation, therefore, valid for a mixture of a wide size distribution at any concentration. For a mixture of solids of conductivity κ_s, liquid of conductivity κ_l, and a solid volumetric fraction ε_s, Bruggeman's equation is

$$(\kappa_{l-s}-\kappa_s)\left(\frac{\kappa_{l-s}}{\kappa_l}\right) = (1-\varepsilon_s)\ (\kappa_l-\kappa_s) \qquad (3.11)$$

For a mixture of nonconducting solids in a conducting liquid, Bruggeman's expression reduces to

$$\frac{\kappa_{l-s}}{\kappa_l} = (1-\varepsilon_s)^{\frac{3}{2}} \qquad (3.12)$$

Following Maxwell's work, for the case of nonconducting particles of uniform size, several models have been proposed. Hashin (1968) studied the electrical and thermal conductivity properties of solid heterogeneous media (polycrystalline aggregates and bimetallic composites for example) and proposed an expression for electrical and thermal conduction equivalent to Maxwell's equation (See Table 3.1)

Neale and Nader (1973), based on a model for an homogeneous and isotropic swarm of dielectric spherical particles and through the analogy between the problem of electrical conduction and diffusion, reported an expression equivalent to Maxwell's equation for a non conducting dispersed phase.

Yianatos et al. (1985) developed a geometrical model based on the concept of tortuosity to estimate local gas holdup from the measured ratio (γ) between the conductance of the liquid-gas dispersion and the conductance of the aqueous phase. This model differentiated between bubbling and froth zones, by considering the geometrical differences between the two zones (spherical bubbles in a homogeneous regime were assumed for the bubbling zone and a cellular bubble shape for the froth zone).

Using different particle sizes (first considered by Bruggeman (1935)), other models have been proposed. De la Rue and Tobias (1959) measured conductivities of suspensions of random-sized glass spheres, polystyrene cylinders and sand particles (ranging from 0.175 to 0.210 mm) in aqueous solutions of zinc bromide of approximately the same density as the particles. Solids holdups up to 40%w/w were tested; the finding was that the suspension conductivity is a function of the exponent m in their expression (see Table 3.1), which is a function of the particle shape and size distribution with values from 1.35 to 1.56.

Lord Raleigh (1892) studied a different geometry, considering parallel cylinders in a square array and spheres of uniform size in cubical array. In each case, the effect of a large number of "shells" of cylinders (and spheres) surrounding a central one was considered. For the cubical array of spheres where the field is perpendicular to a side of the cube, using the principle of superposition for potentials Lord Raleigh derived an expression that has an implicit upper limit for ε_d due to the geometry considered in the model (it loses physical significance at $\varepsilon_d > 52\%$, which corresponds to the limiting case of the maximum packing of spheres centred on the faces of a cube).

Maxwell (1892) General Eq.	$\kappa_{l-d} = \kappa_l \left(\frac{1+2\beta\varepsilon_d}{1-\beta\varepsilon_d} \right)$
Hashin (1968)	$\frac{\kappa_{c-d}}{\kappa_c} = \frac{k_{c-d}}{k_c} = \left(\frac{1+2\beta\varepsilon_d}{1-\beta\varepsilon_d} \right)$
Neale and Nader (1973)	$\frac{\kappa_{l-d}}{\kappa_l} = \frac{1-\varepsilon_d}{1+0.5\varepsilon_d}$
Bruggeman (1935)	$\frac{\kappa_{l-s}}{\kappa_l} = (1-\varepsilon_s)^{\frac{3}{2}}$
De la Rue and Tobias (1959)	$\kappa_{l-s} = \kappa\ (1-\varepsilon_s)^m$

TABLE 3.1
TWO-PHASE MODELS RELATING CONDUCTIVITY AND HOLDUP OF NONCONDUCTIVE PHASE

table 3.1 cont'

Lord Raleigh (1892)	$\frac{\kappa_{l-d}}{\kappa_l} = 1 + \frac{3\beta\varepsilon_d}{1-\beta\varepsilon_d - 0.525\left[\frac{\kappa_d-\kappa_l}{\kappa_d+\frac{4}{3}\kappa_l}\right]\beta\varepsilon^{\frac{10}{3}}}$
Yianatos et al. Bubbling Zone (1985)	$\frac{\kappa_{l-s}}{\kappa_l} = \frac{1-\varepsilon_g}{1+0.55\varepsilon_g}$
Yianatos et al. Froth Zone (1985)	$\frac{\kappa_{l-g}}{\kappa_l} = \frac{1-\varepsilon_g}{2.315\ \varepsilon_g}$

(b) Electrical conductivity of three-phase dispersions.

Flotation is a three-phase system where the liquid forms the continuous phase while the gas and solids form the discontinuous or dispersed phases.

An experimental method using electrical conductivity has been reported by Achwal and Stephanek (1975,1976), to determine gas and liquid holdups in packed columns. The method assumes that the fraction of the cross-sectional area occupied by the liquid in a homogeneous multiphase system is equal to the volumetric fraction of the liquid while the length of the path between the two electrodes is the distance between the electrodes multiplied by a tortuosity factor. If this tortuosity factor does not change significantly with the volumetric fraction of gas in the ternary system then the conductivity should be proportional to the liquid holdup in the bed, which was demonstrated. There are some concerns with the application of the model as the authors did not consider explicitly the solids holdup in the three phase-system, keeping it constant

at 54.3% (relative to solids-water only).

Begovich and Watson (1978) used electrical conductivity to measure axial variation of holdups in three-phase fluidized beds, using 4.6 to 6.3 mm glass, alumina and Plexiglas beads, being fluidized by air and water in either a 7.62 or 15.2 cm diameter column. Two 1.4 cm^2 platinum electrodes, attached 180° apart on the inside of a movable Plexiglas ring, were used to measure electrical conductivity. To obtain the pressure gradient along the column, eleven liquid manometers, spaced 9 cm from each other were used. The three-phase holdups were calculated using the equations

$$\varepsilon_l + \varepsilon_g + \varepsilon_s = 1 \qquad (3.13)$$

$$\frac{dP}{dh} = g(\rho_l \varepsilon_l + \rho_g \varepsilon_g + \rho_s \varepsilon_s) \qquad (3.14)$$

$$\frac{\kappa_{l\text{-}s\text{-}g}}{\kappa_l} = \varepsilon_l \qquad (3.15)$$

where *dP/dh* is the pressure gradient along the fluidized bed, [Pa/m], g is the local acceleration due to gravity, [m/s^2], and ρ_i is the density of the phase i (i= liquid, solid or gas), [kg/m^3].

A similar equation was developed by Kato et al. (1981), using conductivity measurements to estimate the liquid holdup in a three phase fluidized bed (see Table 3.2).

Achwal and Stephanek (1975,1976)	$\frac{\kappa_{l-s-g}}{\kappa_{l-s}} = \varepsilon_l$
Bergovich and Watson (1978)	$\frac{\kappa_{l-s-g}}{\kappa_l} = \varepsilon_l$
Kato et al. (1981)	$\frac{\kappa_{l-s-g}}{\kappa_l} = \varepsilon_l^{1.2}$

TABLE 3.2
THREE-PHASE MODELS RELATING CONDUCTIVITY AND HOLDUP

CHAPTER IV
EXPERIMENTAL TECHNIQUES

4.1.-Introduction

Contacting gas-liquid-solid phases in a downflow bubble column has been claimed to give high gas holdups. In the case of counter-current flotation columns, typical values encountered range from 10 to 25% (Dobby et al., 1988). For co-current downflow bubble columns values up to 60% have been reported (Friedel, 1980; Jameson and Manlapig, 1991; Sanchez-Pino and Moys, 1991).

(The generic term gas is normally used to indicate any kind of gas; in flotation, the gas is normally air, but in some cases, for example in Cu/Mo separation, nitrogen is the flotation gas (Aravena, 1987)).

Gas holdup is an important process variable. Shah et al. (1983) defined the gas holdup as a fundamental process control variable in bubble columns, since it defines the volumetric fraction of any other phase in the system, and hence the residence time for each one. Gas holdup has been shown to affect the metallurgical results in flotation columns (Finch and Dobby, 1990).

The present experiments were conducted with the objective of measuring the effect of the operating variables on the gas holdup.

4.2.- Measuring Techniques.

The techniques to measure the gas holdup can be divided in two groups: methods which allow "overall" measurements (Figure 4.1(a) and 4.1(b)), and methods which allow "local" measurements (Figure 4.1(c)).

(a) Methods to measure overall gas holdup.

(a.1) The bed expansion method. The bed expansion method gives the overall gas holdup by measuring the length of the expanded bed (Δh) of the aerated column of liquid (or slurry) and the clear (non-aerated) liquid l:

$$\varepsilon_g = \frac{\Delta h}{\Delta h + l} \qquad (4.1)$$

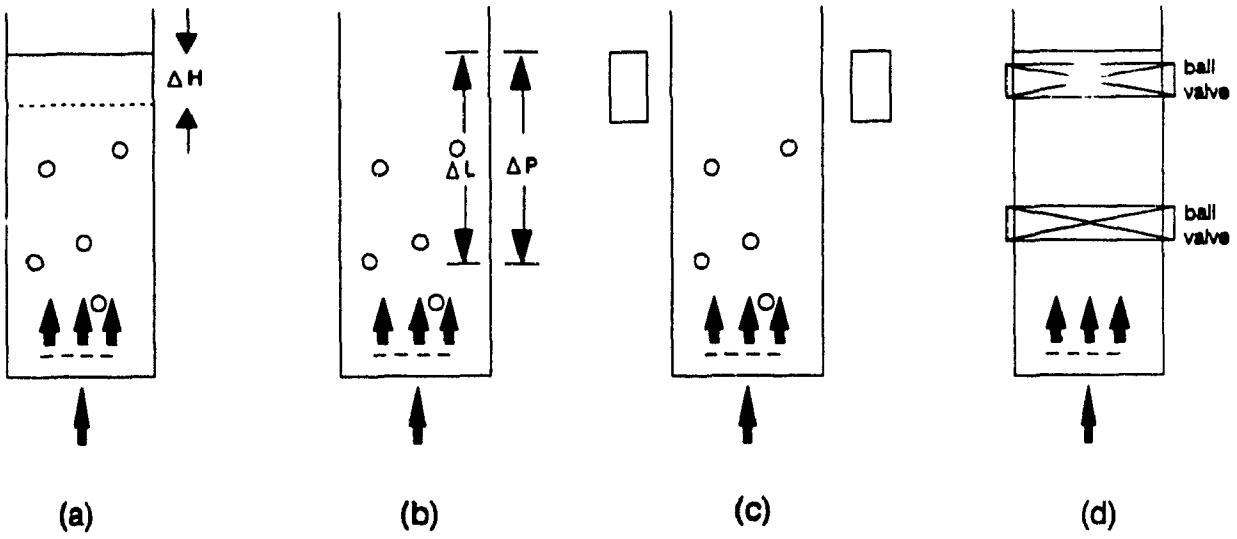

Figure 4.1 Methods to measure overall gas holdup: (a) Level rise; (b) Pressure difference (c) Sensor (e.g. X-Rays, light); (d) Isolating method

This method is difficult to use when a layer of froth (of different gas content with respect to the aerated liquid) is present because the position of the interface is also influenced by the transfer of liquid to the froth.

In case of downwards concurrent bubble columns the bed expansion method can still be applied. As described by Friedel (1980) and Ohkawa (1985), the mean gas holdup in a downflow bubble column can be evaluated by measuring the difference between the water level in the vessel where the column discharges, in the presence and absence of aeration.

(a.2) The pressure difference method. The pressure difference method gives the overall gas holdup in the section defined by the distance between the pressure tapping points. The practical case of the three-phase (slurry-gas) system is considered first. Assuming that the dynamic component of the pressure is negligible, the pressure above atmospheric at A and B (Figure (4.2)) is given by

$$P_A - \left[\rho_{sl}(1-\varepsilon_{gA}) + \rho_l \varepsilon_{gA}\right] g L_A \qquad (4.2)$$

and

$$P_B - \left[\rho_{sl}(1-\varepsilon_{gB}) + \rho_b \varepsilon_{gB}\right] g L_B \qquad (4.3)$$

where ρ_{sl} is the slurry density, ε_{gA} and ε_{gB} are the gas holdup above A and B, respectively; and ρ_b is the bubble-particle aggregate density. Eqs. (4.2) and (4.3) assumes that ρ_{sl} and ρ_b do not substantially change between A and B.

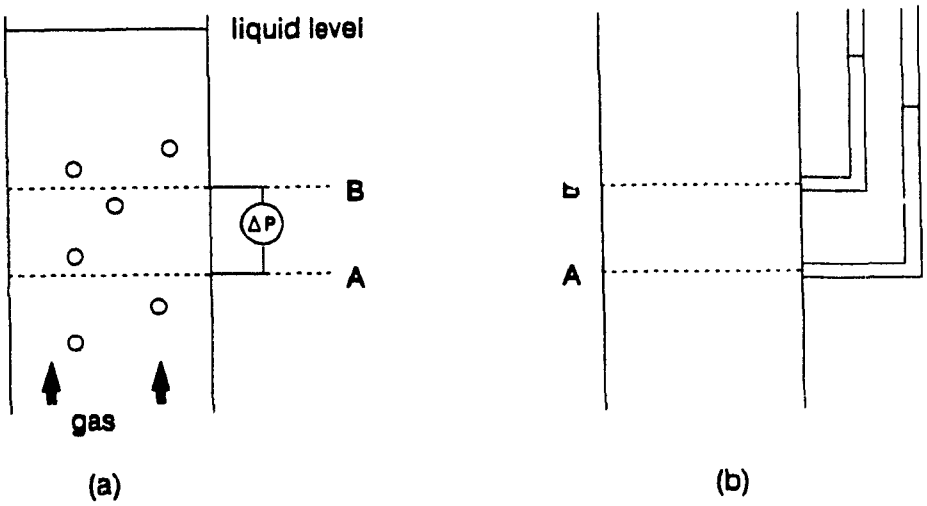

Figure 4.2 Methods to measure gas holdup by pressure difference: (a) general and (b) using water manometers

Defining $\Delta P = P_A - P_B$, and rearranging terms, the gas holdup between A and B is given by

$$\varepsilon_g = \frac{\rho_{sl} g \Delta L - \Delta P}{(\rho_{sl} - \rho_b) g \Delta L} \qquad (4.4)$$

Eq. (4.4) shows that ρ_{sl} and ρ_b are required to obtain gas holdup from pressure readings. Commonly, it is assumed that $\rho_b \simeq 0$ (i.e. lightly loaded bubbles, which may be approximately true near the bubble generator), and ρ_{sl} is the average density between feed and tails densities. Since no reliable technique exists to test these assumptions, no definitive evaluation of gas holdup in industrial flotation columns has been possible so

far (Uribe-Salas, 1991).

For the two-phase (water-gas) systems commonly tested in laboratory conditions, replacing ρ_{sl} by ρ_w and $\rho_b \simeq 0$ (no solids present) Eq. (4.4) becomes

$$\varepsilon_g = 1 - \frac{\Delta P}{\rho_w g \Delta L} \qquad (4.5)$$

If ΔP is given in meters of water (mH_2O) and ΔL in meters Eq. (4.5) can be simplified, using the appropriate units for ρ_w and g, to:

$$\varepsilon_g = 1 - \frac{\Delta P}{\Delta L} \qquad (4.6)$$

(a.3) The isolating method. The most reliable method to measure average gas holdup in any multiphase system, is by isolating a section of it and measuring directly the contents of each phase. Normally, two ball valves are synchronously closed isolating a section of the bubble column (Jepsen and Ralph, 1969; Thanh Nguyen and Spedding, 1977). Subsequently direct measurements of liquid (slurry) volume held between the valves gives the gas volume (Figure 4.1(d)).

(b) Methods to measure "local" gas holdup.

The gas holdup is measured in a section of the system defined by the signal path between probes. Methods based on electrical conductivity are among the most commonly used in two- and three-phase systems (Serizawa et al., 1975; Fan, 1989). The theory behind this method was given in Chapter 3. Punctual electrical resistivity probes are of common use in measuring local gas holdup in liquid-gas dispersions, where large bubbles are present ($d_b > 5$ mm) (Nassos, 1963; Serizawa et al., 1975; Castillejos, 1986). This technique has been attempted in flotation columns but with little success probably because of the small bubble sizes (< 1.5 mm) (Xu, 1991).

Methods based on the attenuation of β-rays (Nassos, 1963) and γ-rays (Lockett and Kirkpatrick, 1975) have been used for two-phase (liquid-gas) systems. These techniques measure the attenuation of the beam passed through the dispersion (liquid-gas), which is a function of the volumetric fraction of gas in the system (Nassos, 1963).

The use of light sources, instead of radioactive one has also been reported (Wachi et al., 1987). Phase holdup detection using light emitters is possible since the refractive index of gas and liquid differ considerably. Phase detection occurs at the surface of the probe tip, which is shaped to reflect incoming light internally if gas surrounds it and to refract light if liquid surrounds it. By this mean, the time fraction of the reflected light will then yield the local holdup (Vince et al., 1982).

The use of an isokinetic sampler to measure radial gas and liquid fluxes, and by this means local gas holdup, has been described by Jepsen and Ralph (1969) and Serizawa et al. (1975). By measuring pressure loss in the sampler at a given condition the isokinetic flowrate is obtained at the sampled point.

4.3.-Experimental Apparatus (Figure 4.3)

A downflow bubble column was designed for laboratory use with a downcomer of 190 cm length and 3.81 cm internal diameter, made of transparent Plexiglas to enable the observation of the column performance.

A cylindrical vessel was used as the separation compartment: it was 100 cm high and 10 cm internal diameter. The separation compartment had a conical bottom with a 0.127 cm opening. Usually liquid was recycled. At the top of the separation chamber were launders to collect the overflowing liquid (which was recycled).

All recycled liquids were collected in a 60 l Nalgene tank and pumped using a progressive cavity Robin-Myers pump (with a maximum capacity of 20 l/min), to a small chamber at the top of the downcomer from where liquid was forced through the brass nozzle, which was 5 cm below the top flange.

Three different nozzle diameters were used, 0.22, 0.5, and 0.7 cm, with the same geometry (Figure 4.4).

Air was admitted into the downcomer 5 cm below the top flange through a 0.635 cm diameter hole in the wall of the downcomer at the same level with the feed nozzle. Air admission was regulated using a needle valve.

Two Whitey (stainless steel) ball valves, were selected, each of internal diameter of 3.81 cm, to give a full bore opening equal to that of the inside diameter of the

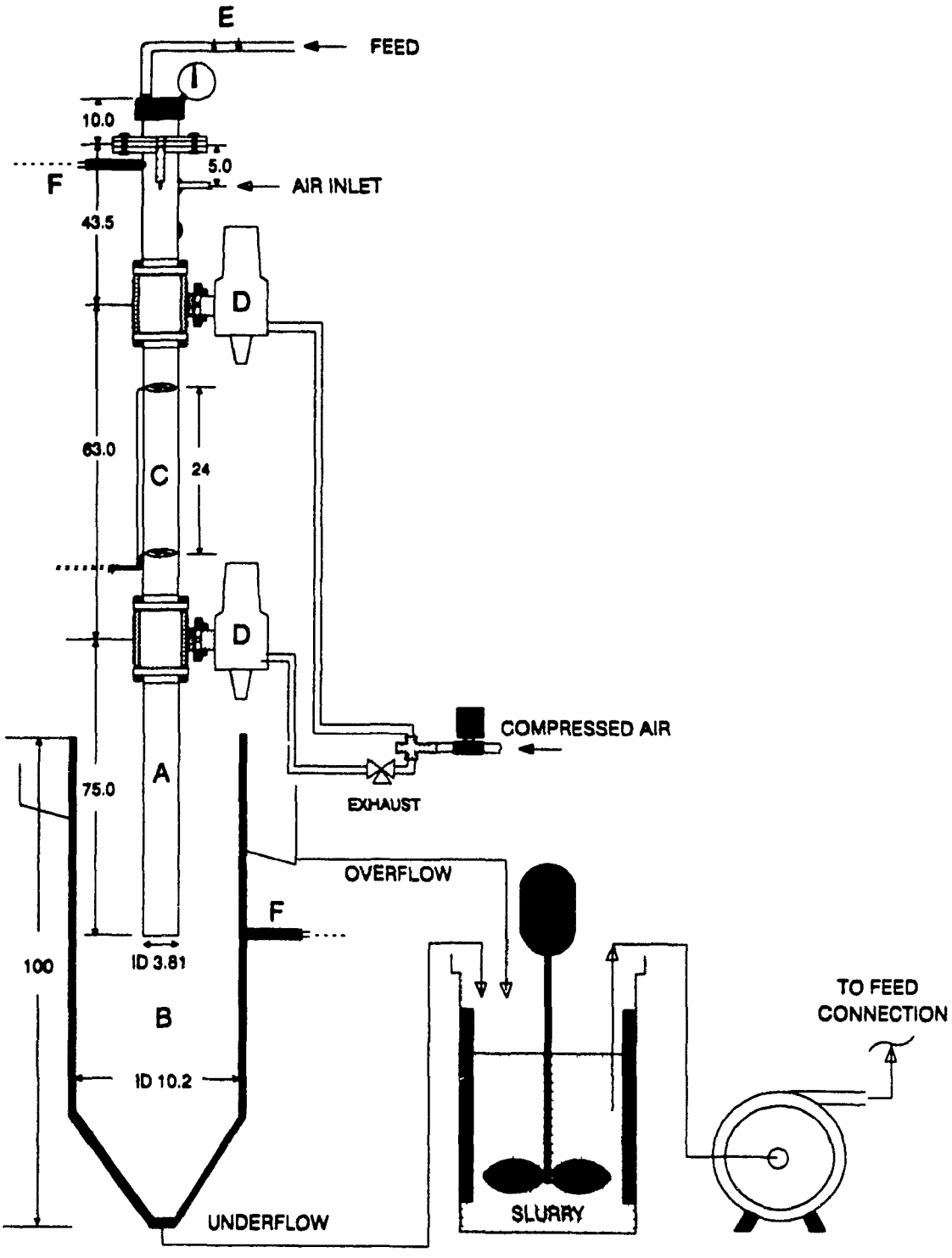

Figure 4.3 Experimental set-up showing the downflow bubble column. A: downcomer; B: Separating vessel; C: Isolating section and conductivity cell; D: Ball valves; E: Feed line conductivity cell; F: Pressure transducers

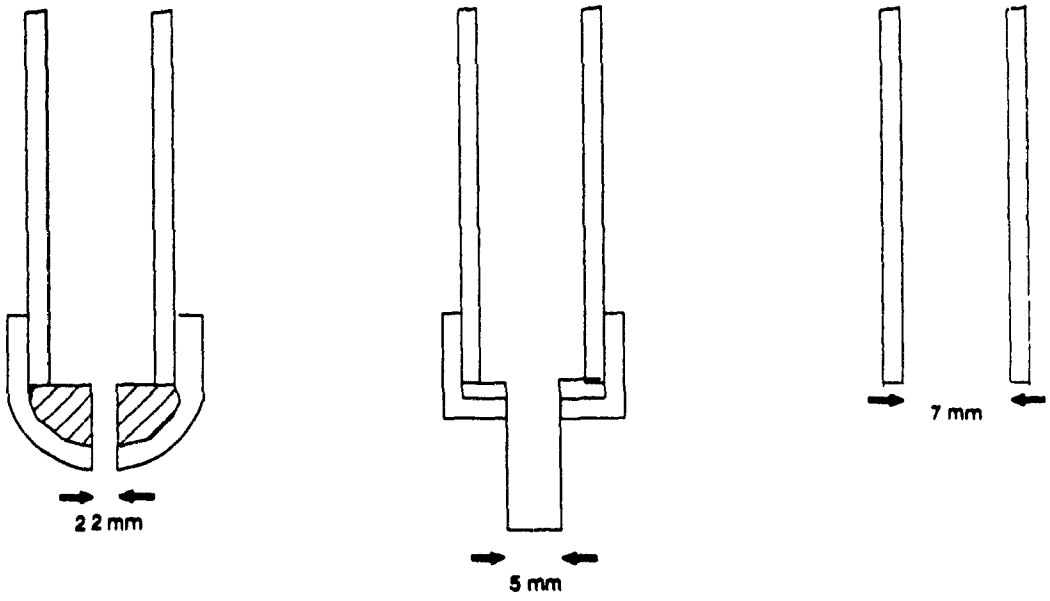

Figure 4.4 Different nozzle types used in this work for the downwards bubble column

downcomer, separated by 63 cm and connected to an air actuator (Whitey model MS-135-SR), in the middle section of the downcomer.

The distance between both valves was chosen as 35% of the total length of the downcomer to give a large sample of the air-liquid mixture inside.

A compressed-air cylinder with a pressure regulator was connected to both air actuators and an ASCO electric solenoid valve (model 8211C34) to open or close the cylinder was used to release 690 kPa (100 psi) of pressure in 5 to 10 ms, closing both valves simultaneously, with a response time of around 150 ms.

Rubber hosing (0.127 cm internal diameter), reinforced with steel wire to resist high interior pressures was used to connect the solenoid valve with the air actuators. All the fittings in the line were Swagelok type.

One pair of electrodes, to measure the conductivity of the two-phase mixture, was placed in the interior of the downcomer, separated by 23.5 cm (cell constant 0.49 cm^2/cm). Each electrode was designed accordingly to the theory described in Chapter 3. The electrodes were made using copper-tin wire, 0.1 cm in diameter (gauge 20), forming

a ring of 3.0 cm with cross-finger wires in the middle (Figure 4.5(a) and (b)). Another pair of electrodes was placed in the feed line to measure the conductivity of the incoming liquid or slurry phase (cell constant 0.98 cm^2/cm). This second pair of electrodes was made with the same copper-tin wire to form a cross perpendicular to the flow direction.

Two pressure transducers were used: one located 2 cm below the top flange of the downcomer; and the second one in the wall of the separation vessel at the same level with the end of the downcomer.

4.4.- Instrumentation.

As the objective of the experiments was the measurement of the effect of the operating variables on the gas holdup, the instrumentation of the downcomer was designed to register the appropriate information, using a computer with an analog/digital translation board to register signals from the conductimeter, the pressure transducers, and the rotameters (to measure directly the feed and gas flowrates) (Figure 4.5(c)).

Feed flowrate. The liquid (slurry) pumped from the feed tank was measured using an OMEGA rotameter (model FL-1504A), with a maximum capacity of 20 l/min. The rotameter was calibrated by adjusting different water flowrates, and measuring the collected volume in a certain period of time for each different case. The calibration curve is shown in Figure A.1, Appendix A. The intermediate values were calculated by linear interpolation from the experimental values.

Gas flowrate. To measure the gas flowrate being aspirated into the downcomer a Cole-Parmer rotameter (model N044-40), with a maximum capacity of 20 l/min of air was used. The rotameter was calibrated using as a reference an electronic flowmeter FM-380, with a controller model MIC-200 from Partlow Co. The calibration curve is given in Figure A.2, Appendix A. Intermediated values were interpolated linearly from the experimental values.

Feed pressure. To measure the feed pressure in the downcomer an ASHCROFT pressure gauge was placed in the chamber at the top, with a range between 0 and 60 psig. This value was not considered for the characterisation of the downcomer as it depends on the characteristic curve of the pump and changes with the feed flowrate; its importance, therefore, is questionable and it was taken only as a reference.

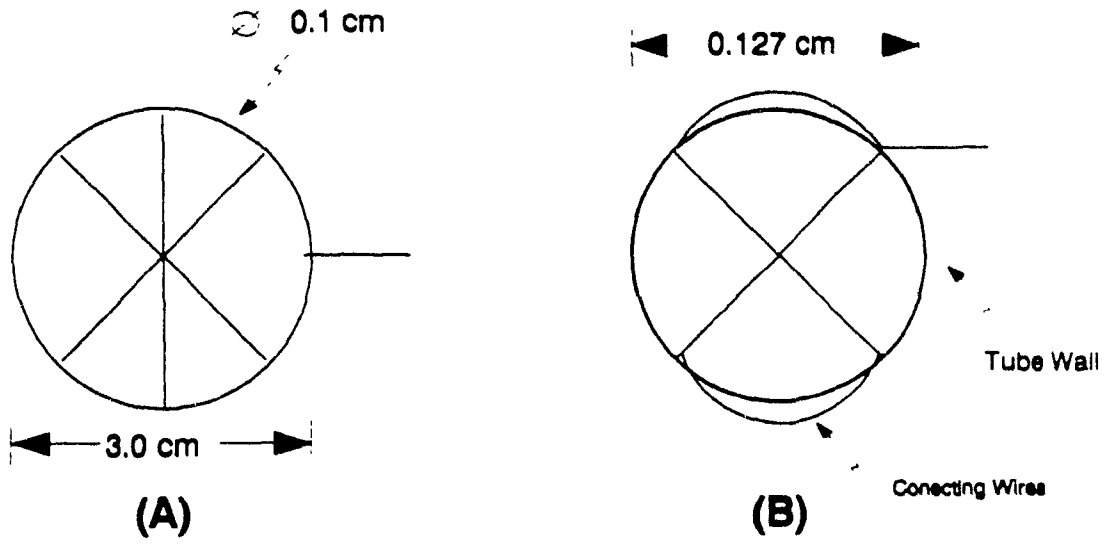

Figure 4.5(a) Electrode design in: (A) the downcomer; and (B) the feed line

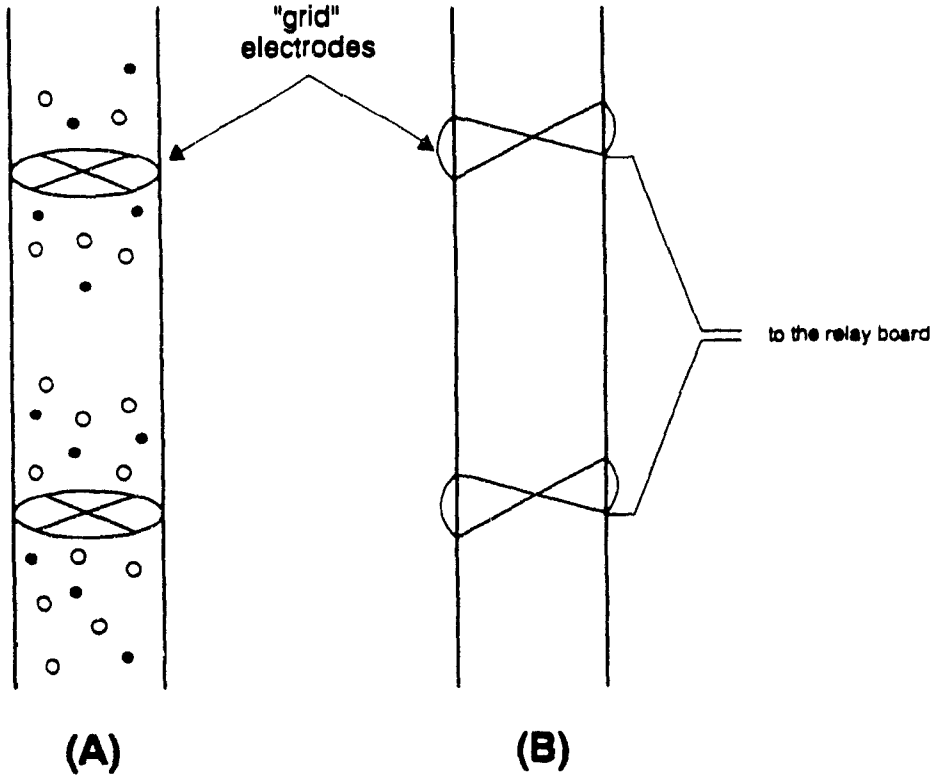

Figure 4.5(b) Cell arrangement to perform conductivity measurements in. (A) the downcomer; (B) the feed line

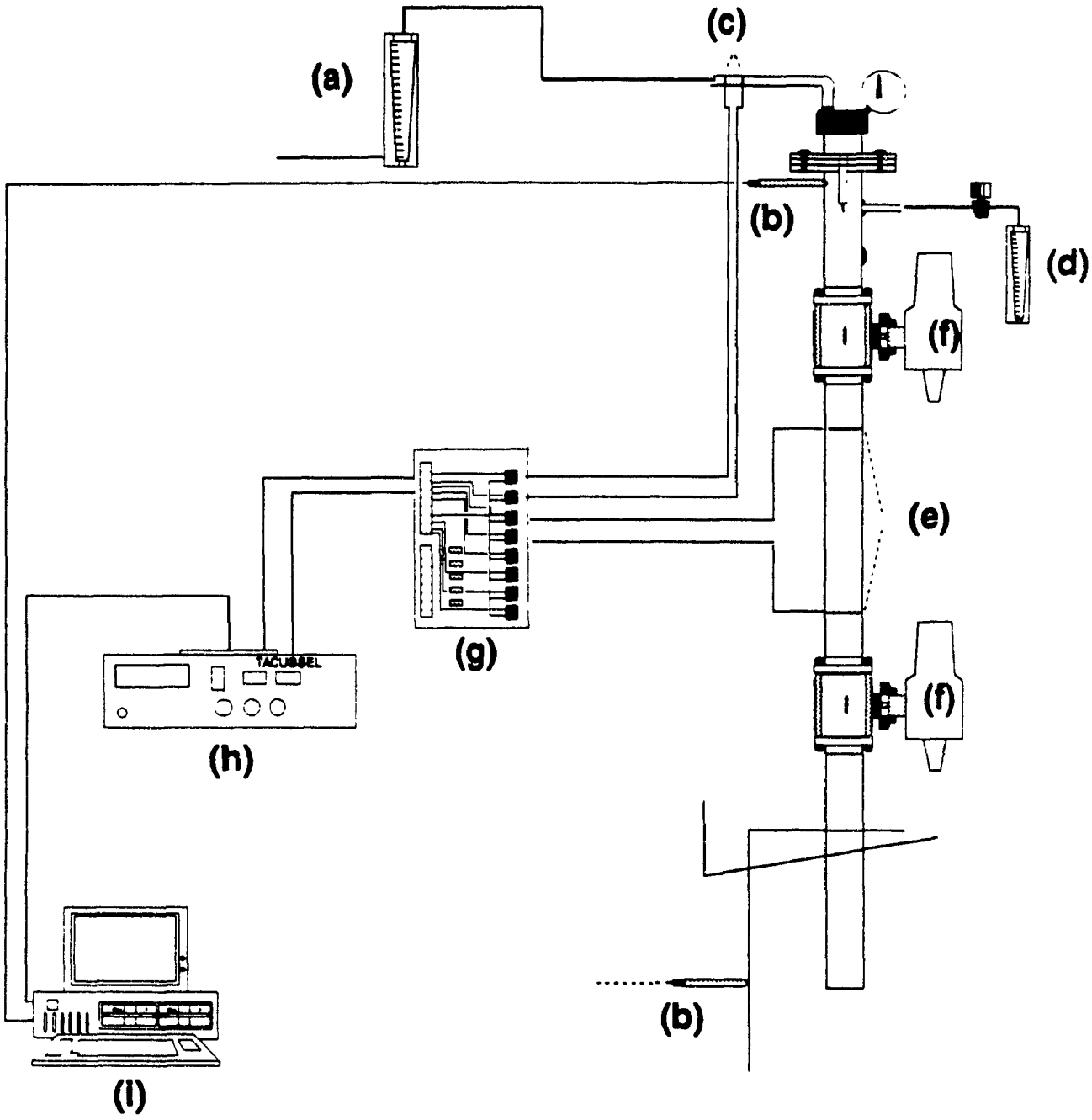

Figure 4.5(c) Instrumention of the downflow bubble column used in this work, indicating: (a) Feed rotameter; (b) Pressure transducer; (c) Feed line electrodes; (d) Air rotameter; (e) Downcomer electrodes; (f) Ball valves; (g) Relay board; (h) Conductivity meter; (i) Personal computer

Hydrostatic pressure. The pressure inside the downcomer was measured by an OMEGA pressure transducer model PX304-050A5V. The pressure transducer has an operating range from 0 to 3.4 absolute atmospheres giving a proportional electric signal between 0.5 to 5.5 volts. The calibration of the pressure transducer was made measuring the voltage response applying different water heights, assuming that the linearity is kept over the range below the atmospheric pressure. The calibration curve is shown in Figure A 3, Appendix A.

Pressure head in the separation compartment. The pressure head above the end of the downcomer, in the separation vessel, was measured by a DRUCK pressure transducer model PDCR 860. The pressure transducer has an operating range from 0 to 0 7 atmospheres giving a proportional electric signal between 0 and 10 mV. The calibration of the transducer was made in an analogous manner to that for the pressure transducer in the downcomer.

4.5.- Experimental Technique

The column, initially empty, was fed using water, containing a known concentration of surfactant (Dowfroth 250C) and with the air inlet fully closed. The water jet from the nozzle started hitting the surface of the pool at the bottom of the downcomer and, as the superficial (downwards) velocity of the liquid is higher than the rising (buoyancy) velocity of the bubbles, it begins to evacuate the air from the interior, creating a slight vacuum which lifts liquid up into the column. Once the downcomer was filled with liquid, the feed flowrate was set to the desired value and the air inlet opened Aspirated air, regulated by the needle valve on top of the rotameter to keep the pool level inside the downcomer near the nozzle, produced a stable, downwardly moving bubble-liquid (slurry) mixture.

To measure the effect of feed, gas flowrate and surfactant concentration on the gas holdup the one-variable-at-a-time procedure was taken.

The conductivity technique, as described in Chapter 3, was used to measure the gas holdup in the downcomer. Conductivity measurements were taken in the feed line and in the section between the ball valves inside the downcomer for each set of conditions. A minimum of twenty values were taken at intervals of 6 seconds to check

for steady operation. The cell constant was tested and remained invariant over the full range of encountered conductivities.

The electrodes were connected to a Tacussel conductivity meter (with a reproducibility of measurement better than $\pm 0.03\%$) using an Omega ERA-1 electromechanical relay board controlled by a computer signal to close the circuit. The conductivity meter gave a proportional analog signal between 0 and 5 volts which was connected to an IBM computer, using a Data Translation interface, model 2801, to convert the analog signal to a digital signal that can be used by the computer. The digital values were converted to conductivity values using a correlation with conductivity and were stored on a floppy disk (Figure 4.5(a)). The correlation was:

$$\kappa = \left(\frac{DV}{4096} CR \right) 707.27 - 332.04 \qquad (4.1)$$

where DV is the digital value corresponding to the voltage from the conductivity meter, CR is the conductivity range being used.

Pressure measurements inside the downcomer were taken simultaneously with the conductivity measurements, at intervals of 6 seconds to give an average value.

The experimental gas holdup was measured directly by isolating the section. At each set of conditions these holdup measurements were made by closing the valves in the downcomer simultaneously through release of the pressure from the compressed-air cylinder through the solenoid valve. The isolated section, filled with the air-liquid mixture, was left for at least 5 minutes to allow the air and the water (slurry) to disengage. Water height was measured to calculate the gas holdup (See Appendix A).

CHAPTER 5

EXPERIMENTAL RESULTS, DISCUSSION AND CONCLUSIONS

5.- Introduction.

The hydrodynamic characterisation of a concurrent downflow bubble column in this thesis is divided into the study of two- and three-phase systems. To analyze the hydrodynamics, the effect of variables on the gas holdup was measured.

The variables studied were: gas flowrate, feed flowrate, frother concentration and solid percentage.

Gas holdup was measured directly and by a conductivity technique. A new technique to estimate gas holdup for this type of device was also developed, based on pressure measurements.

The drift flux model was used to help correlate the data.

5.1.- TWO-PHASE SYSTEMS

5.1.1.- Lifting up a liquid column.

To determine the conditions under which a water column is raised, both pressure and conductivity in the downcomer were recorded for different operating conditions for the water-air system.

The height of the water column held inside the downcomer is a function of the vacuum created -by the entrainment and evacuation of the air- by the plunging jet. To detect the rising liquid column the conductivity between the electrodes was recorded.

To start-up the column, the liquid level in the separation vessel is raised above the bottom of the downcomer, effectively sealing it. With the air inlet closed, the gas trapped inside the downcomer is compressed due to the head of liquid in the separation vessel above the bottom of the downcomer which creates a slight overpressure above atmospheric (zones **A** and **B** Figure 5.1). This overpressure starts decreasing as air is entrained into the liquid pool (zone **C**). The entrained air produces bubbles which are evacuated from the column due to the downwards velocity that is higher than the buoyancy of bubbles, this produces a slight vacuum that starts to elevate the liquid column (zone **D**). If no gas is admitted into the downcomer, the conductivity increases

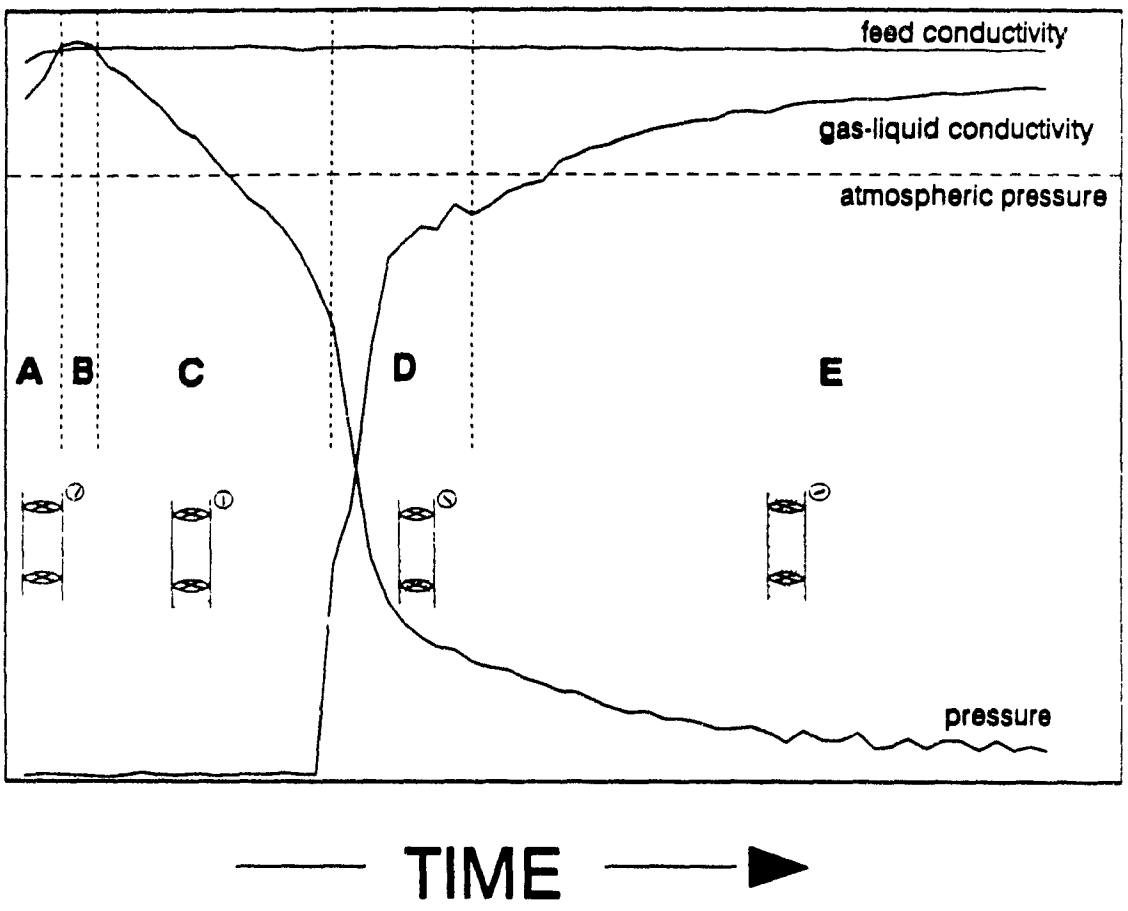

Figure 5.1 Transient stages during the start up of the downwards concurrent bubble column

to approach that of the feed (zone E): it will equal the feed conductivity when all gas bubbles have been evacuated.

The feed flowrate, which is responsible for the rate at which air is being entrained into the liquid, affects the time necessary to lift up a water column (Figure 5.2(a) and (b)); higher feed velocities entrain air faster and evacuate bubbles more rapidly thereby reducing the time necessary to create the vacuum to lift up the liquid column.

Since air is being evacuated in the form of bubbles, the presence of frother (surfactant) helps to reduce coalescence and stabilize the operation; this further reduces the time necessary to fill the downcomer with liquid (Figure 5.3(a) and (b)). The presence of frother reduces the bubble size, which decreases their buoyancy velocity, thus increasing the rate of gas evacuation. In the absence of frother (Figure 5.3(a)) bubble coalescence produces an unstable condition due to the formation of large slugs that rise to the pool surface where they are redispersed in the form of fine bubbles due to the action of the liquid jet. A new stable condition is reached at a new pool level.

5.1.2.- Pressure measurements inside the downcomer.

Superficial feed and gas (air) velocity affect the absolute pressure inside the downcomer (Figure 5.4). Variations in the superficial feed velocity affect the pressure more strongly than variations in the superficial gas velocity.

The pressure can also be used as a variable to control the air admitted into the downcomer; the difference between atmospheric pressure and the interior pressure has to be greater than 0.5 mH_2O to prevent formation of slugs or a pool level too far below the nozzle.

In certain cases pressure can be used to determine the flow regime inside the downcomer. Figure 5.5(a), line (**A**) corresponds to developed slug flow, while line (**B**) corresponds to the signal obtained under bubbly flow conditions.

Although the pressure signal can help to determine the flow regime in the downcomer under certain operating conditions bullet shaped bubbles are formed in the downcomer which remain stationary (oscillating). Under these conditions of "undeveloped" slug flow the pressure remains invariable. Conductivity measurements, however, can detect this condition. Figure 5.5(b) shows examples of pressure and

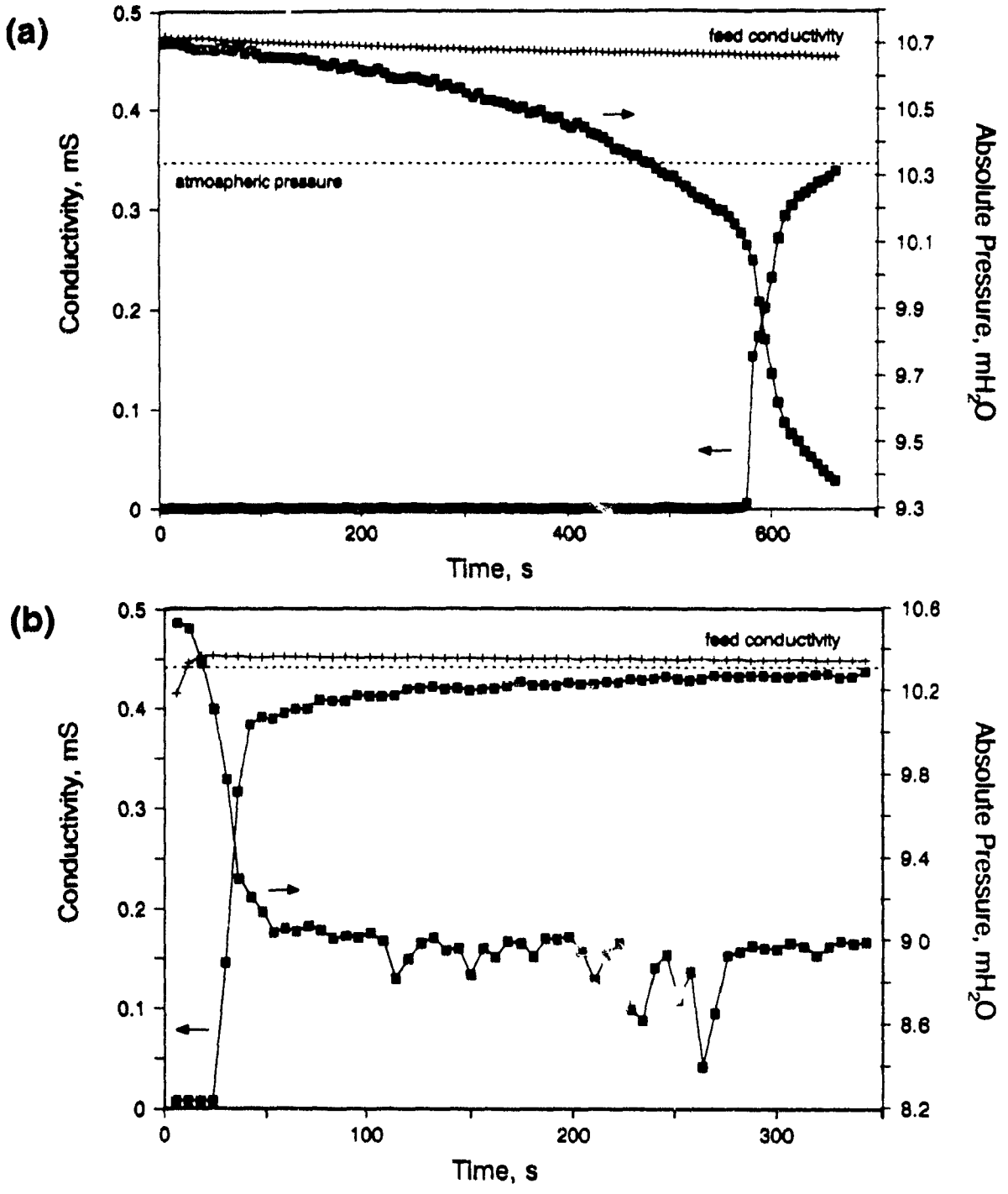

Figure 5.2 Effect of superficial feed velocity on the time to lift up a water column in the downcomer with 5 ppm of frother and JI: (a) 5.64 cm/s and (b) 16.55 cm/s

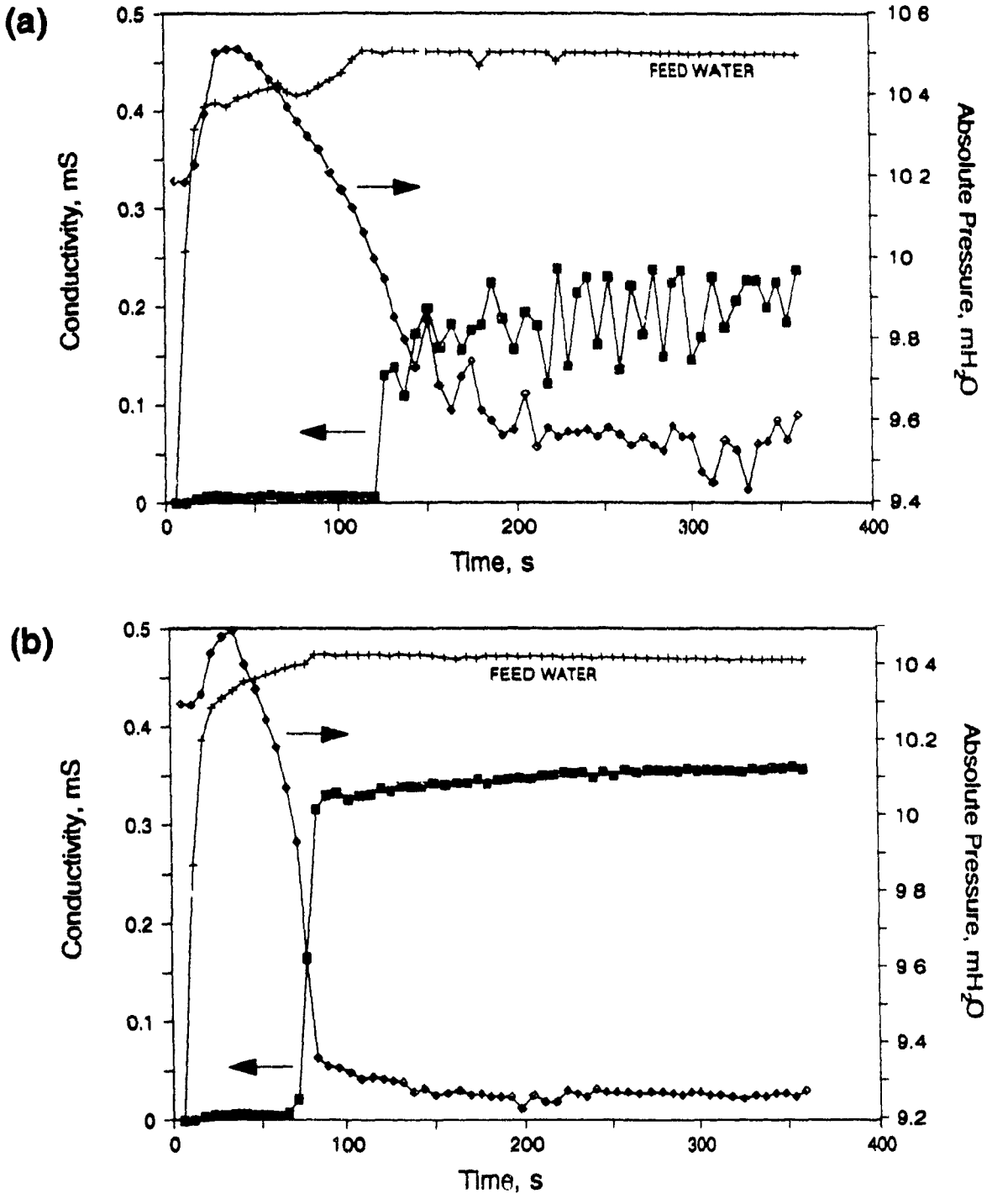

Figure 5.3 Effect of frother concentration on the time to lift up a water column in the downcomer for Jl= 15.57 cm/s, Jg= 1.08 cm/s and:(a) 0.5 ppm and (b) 5 ppm of frother

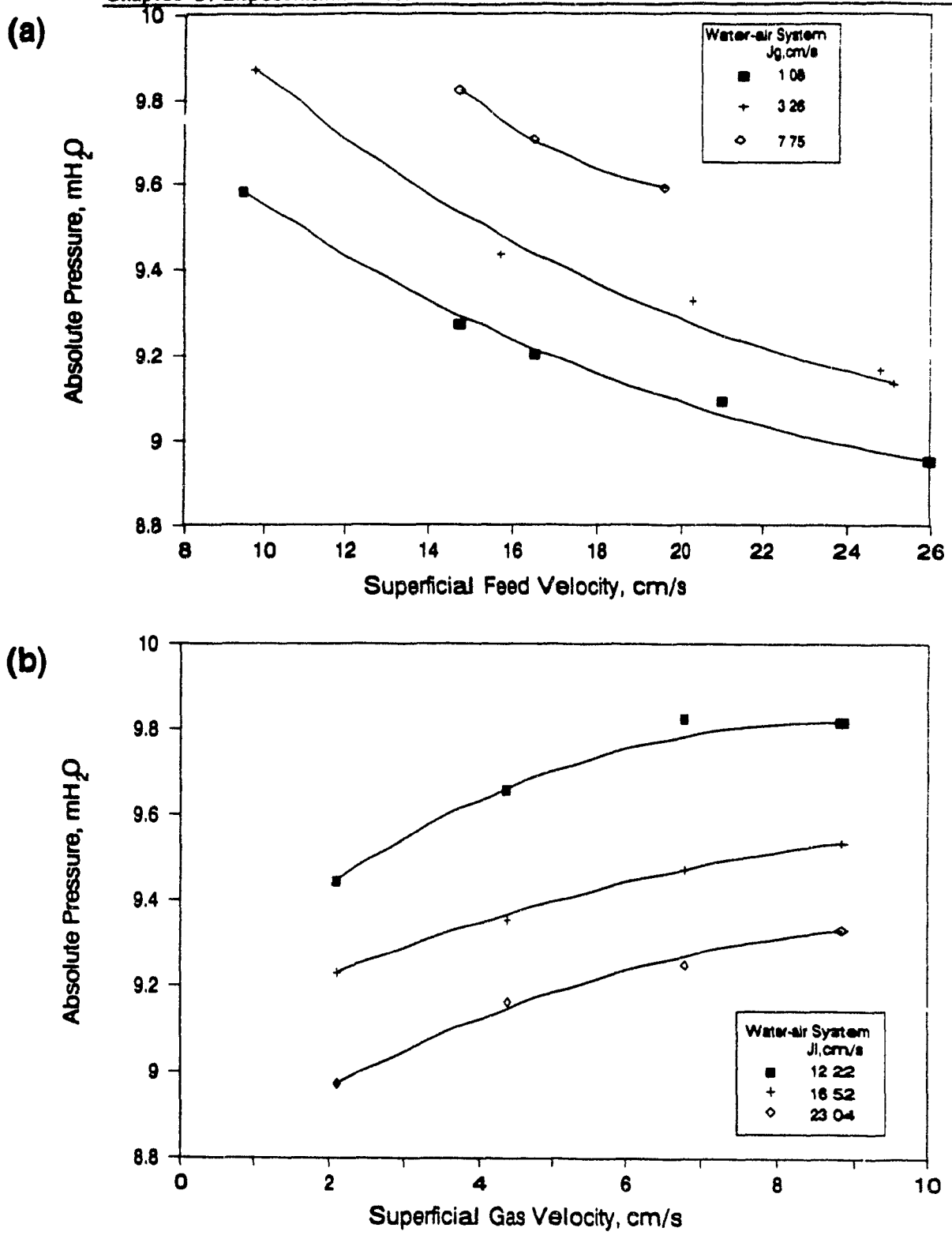

Figure 5.4 Absolute pressure variation inside the downcomer with: (a) Superficial feed velocity and (b) superficial gas velocity.

conductivity measurements in the downcomer for: bubbly flow (a), undeveloped slug flow (b), and developed slug flow (c), showing that the conductivity signal can detect undeveloped slug flow in the downcomer.

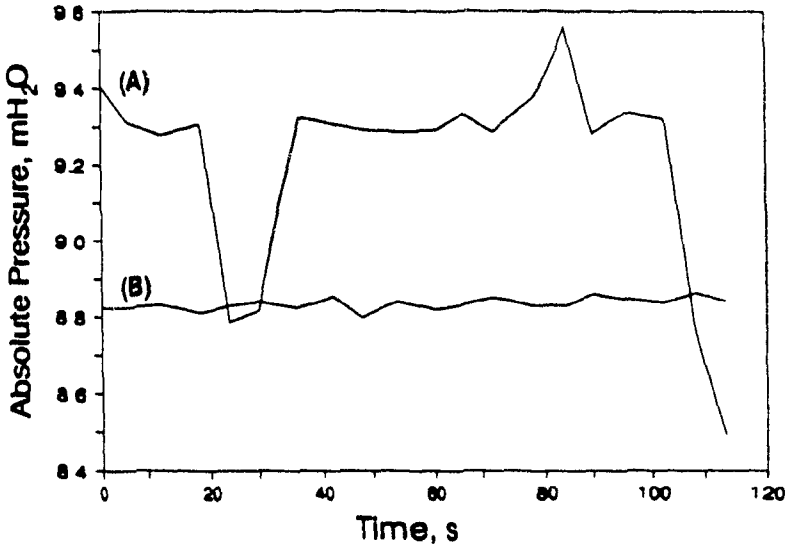

Figure 5.5(a) Pressure signal for: (A) Slug Flow; (B) Bubbly Flow

5.1.3.- Frother Concentration.

The downward movement of bubbles, opposed by their natural tendency to rise due to buoyancy, increases bubble retention time in the downcomer, thus creating high gas holdups. At the same time this crowded environment increases the probability of coalescence.

Surfactants have the property of decreasing coalescence and producing stable gas bubble dispersions. Small amounts of frother (a few ppm) can significantly increase stability.

Gas holdup indicates the relative amount of air in the system under steady state conditions. Column flotation aims to achieve high gas holdups while maintaining bubbly flow to improve metallurgical performance (Finch and Dobby, 1990). In the downcomer under similar conditions of feed flowrate, increasing the amount of frother from 5 to 25 ppm increased the maximum gas rate that could be aspirated under bubbly flow

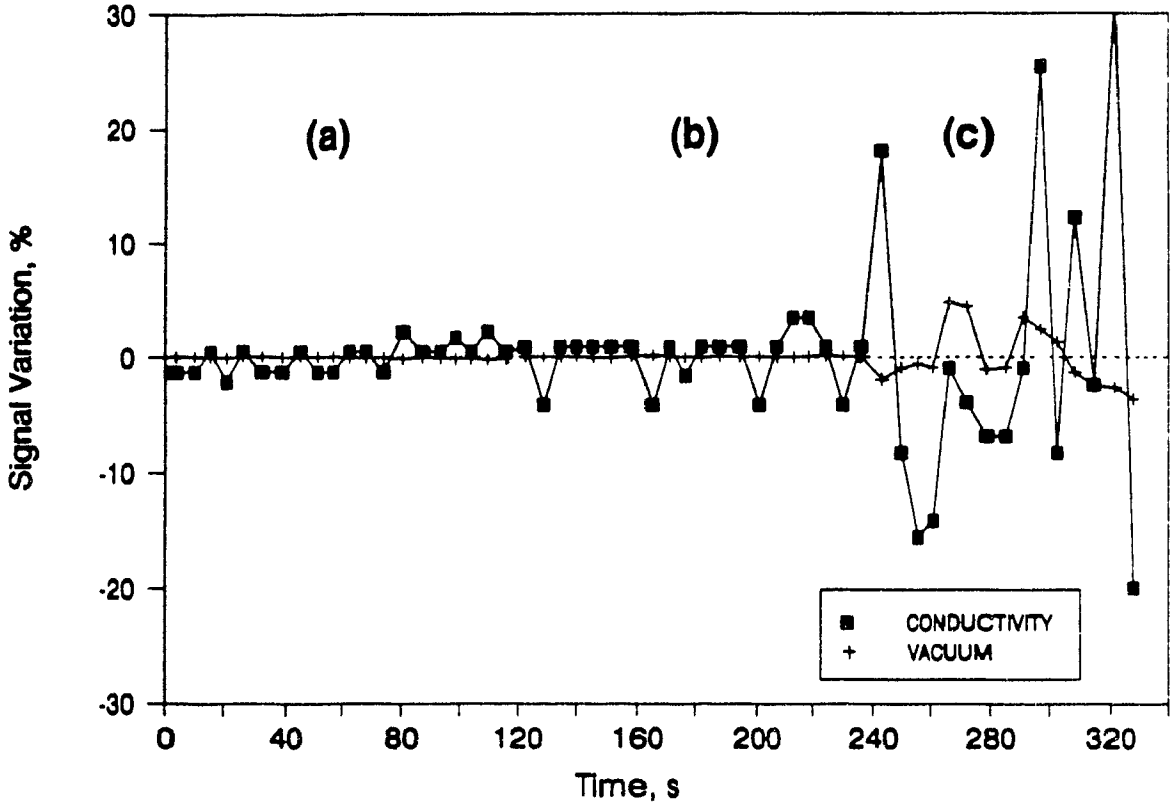

Figure 5.5(b) Use of pressure and conductivity measurements to determine the flow regime inside the downcomer (a) bubbly flow; (b) undeveloped slug flow and (c) developed slug flow.

conditions from 5.5 to 6.8 cm/s due to the greater stability of the bubbles (Figures 5.6 and 5.7). The higher concentration of surfactant in the system however, produces finer bubbles, which means a lower buoyancy velocity. As a result the smaller bubbles are carried downwards through the column faster, lowering the gas holdup Eissa and Schügerl (1975) and Shah et al. (1983) have reported similar observations using different alcohol solutions where an increment of the chain length decreased the bubble size and also decreased the gas holdup.

5.1.4.- Pool Level (i.e. liquid level in the downcomer)

The pool level, relative to the end of the nozzle (Figures 5.8 and 5.9) can be modified by changing the superficial feed velocity or the superficial gas velocity The level of liquid in the downcomer is particularly sensitive to changes in the gas velocity at low feed velocities, because of the reduced ability of the jet to produce a sufficient vacuum to entrain the air. As shown in Figure 5.9, at low liquid velocity (7.5 cm/s) increments in superficial gas velocity significantly affected the pool level, while at a higher velocity (18.7 cm/s) the effect of changes in the gas rate became less important

The pressure inside the downcomer is proportional to the rate of entrainment of air by the liquid jet; if no more gas is admitted to the downcomer, the pool level increases to a new point of equilibrium that balances the external pressure by increasing the weight of the liquid-gas column The opposite extreme would be when excess air is admitted and the interior pressure matches the atmospheric pressure and the pool level is located at the bottom of the downcomer.

5.1.5.- Nozzle Diameter

To normalize, the ratio between the nozzle diameter and the diameter of the downcomer is used. Three different ratios were studied: (a) 0.06 (nozzle of 2.2 mm diameter); (b) 0.13 (nozzle of 5 mm) and (c) 0.18 (nozzle of 7 mm). Due to the design it was not possible to change the diameter of the downcomer.

The feed flowrate that can be pumped into the downcomer is restricted by the nozzle diameter. With a ratio of 0.06, the maximum volumetric flowrate was 4 3 L/min at 50 psi, while increasing the ratio to 0.18 increased the maximum volumetric feed flowrate above 20 L/min at 50 psi. Due to the pump limitations it was not possible to

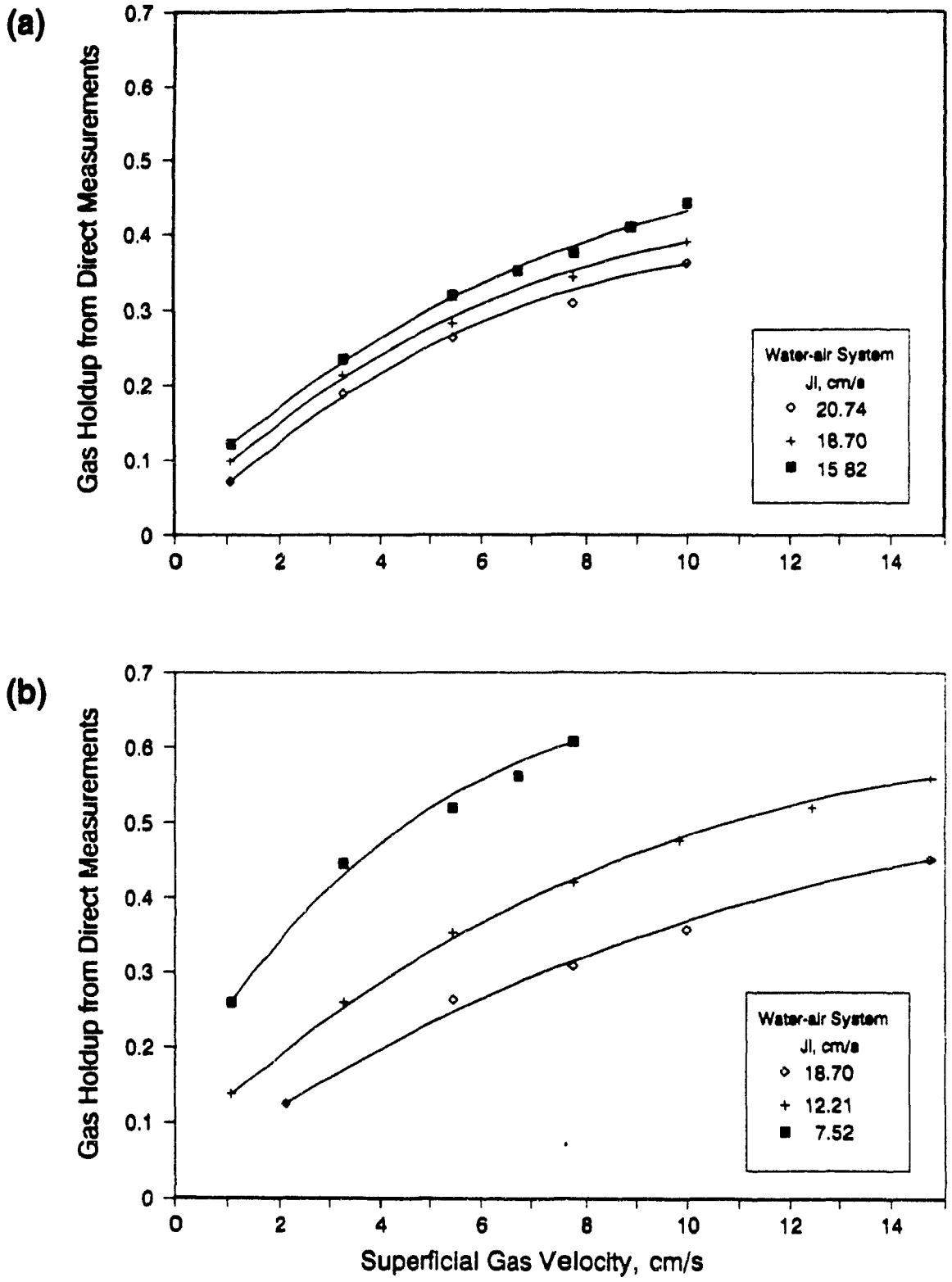

Figure 5.6 Effect of frother concentration on the gas holdup in the downcomer for the water-air system against superficial gas velocity: (a) 5 ppm and (b) 25 ppm.

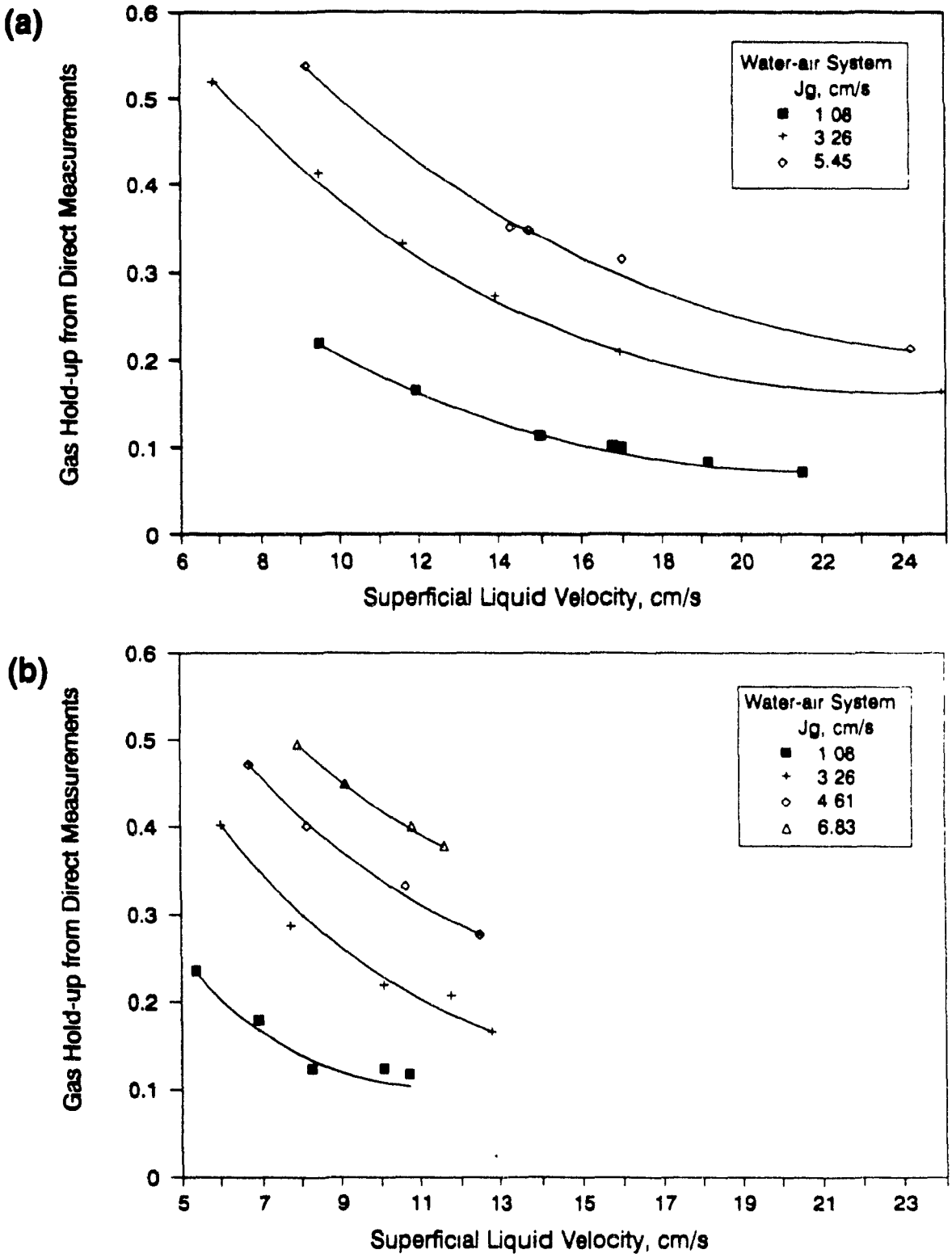

Figure 5.7 Effect of frother concentration on the gas holdup in the downcomer for the water-air system against superficial liquid velocity (a) 5 ppm and (b) 25 ppm

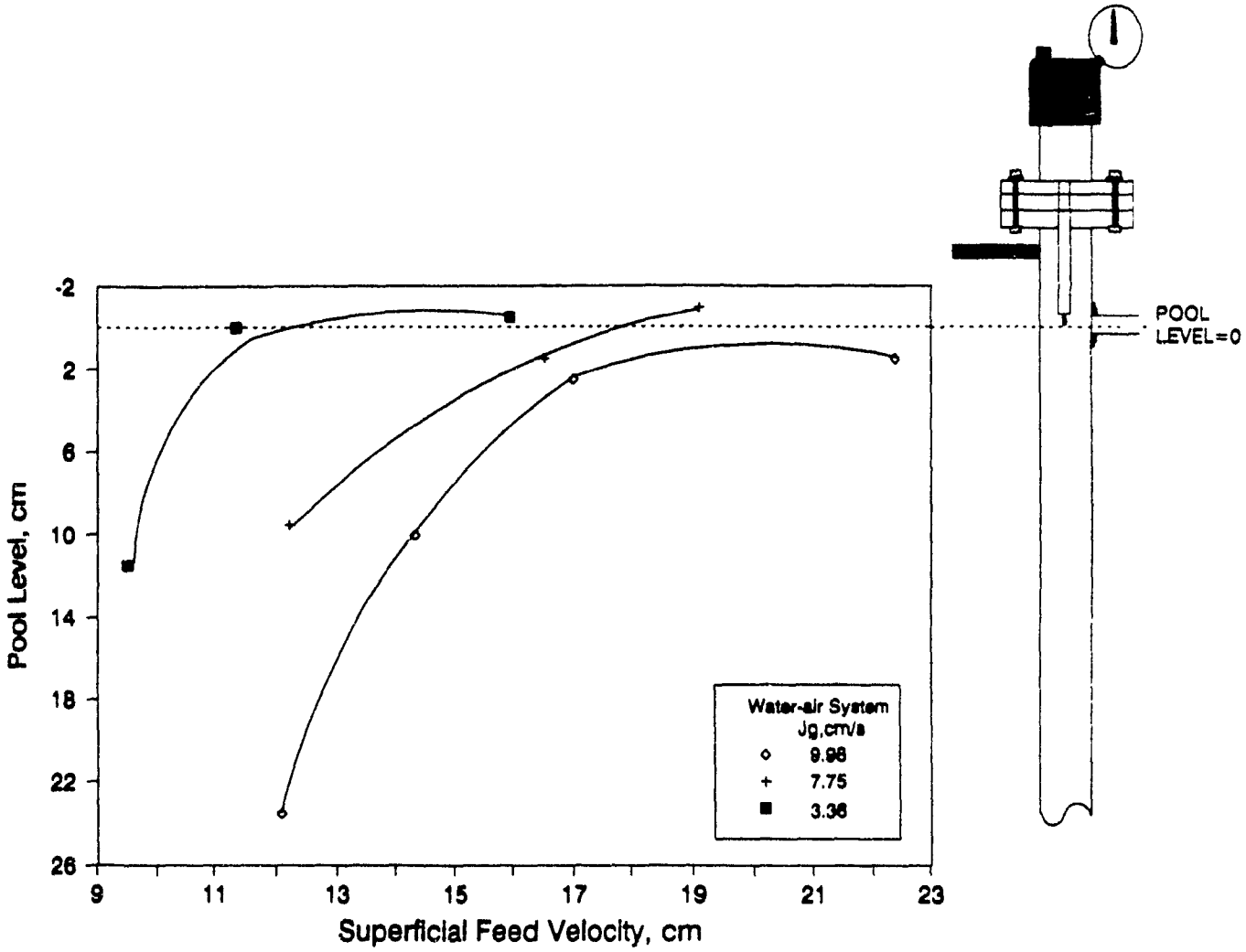

Figure 5.8 Pool level variation with the superficial feed velocity.

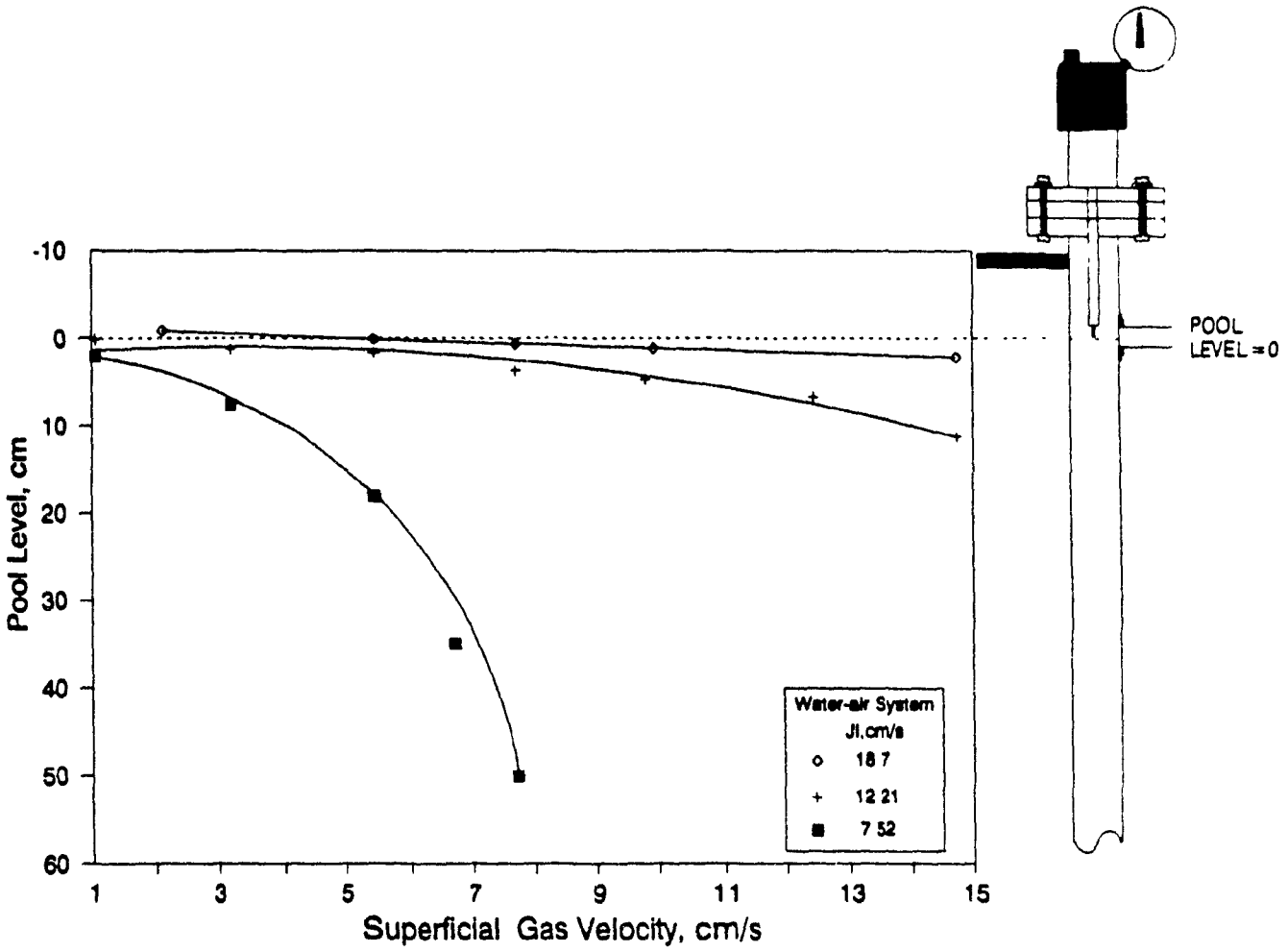

Figure 5.9 **Effect of superficial gas velocity on the pool level at constant feed velocity for the water-air system.**

reach 50 psi using a ratio $\geq$ 0.18.

The jet velocity, which is responsible for the bubble formation, is also affected by the nozzle diameter: large ratios produce a low energy jet that entrains air with less shear and consequently gives coarser bubbles.

5.2.- THREE-PHASE SYSTEMS

The effect of hydrophillic solids was studied using silica (100% -75 μm). The effect of different slurry densities on the gas holdup, absolute pressure and pool level was studied.

5.2.1.- Pressure in the downcomer.

By increasing the density of the slurry being fed to the downcomer the jet momentum is increased. Consequently, the vacuum created inside the downcomer for a water-silica-air system is greater (under the same conditions of superficial feed and gas velocities) than with a water-air system. The pressure tended asymptotically to a constant value (Figure 5.10), which corresponds to the maximum compaction of gas bubbles; further increments in the gas velocity modified the pool level (provided the frother concentration was high enough to prevent coalescence) to a new point of equilibrium in the downcomer. Figure 5.10 also shows the variation of the absolute pressure with the superficial gas velocity, at constant superficial feed velocity. In the case of water-silica-air mixtures, the increase in slurry density increased the vacuum in the downcomer, making it possible to aspirate more gas under the same conditions of feed and gas velocities.

5.2.2.- Pool Level.

Figure 5.11 shows the pool level in the downcomer as a function of absolute pressure for different concentrations of solids. As discussed previously in section 5.1.4, if the superficial gas velocity is increased, the vacuum inside the downcomer decreases, consequently decreasing the ability of the system to support the (multi-phase) column; the level thus moves to a new point of equilibrium further below the nozzle.

The effect of the pressure on the pool level becomes more significant at low feed velocities (Figure 5.11(a)) as was demonstrated in section 5.1.4 for the water-air system

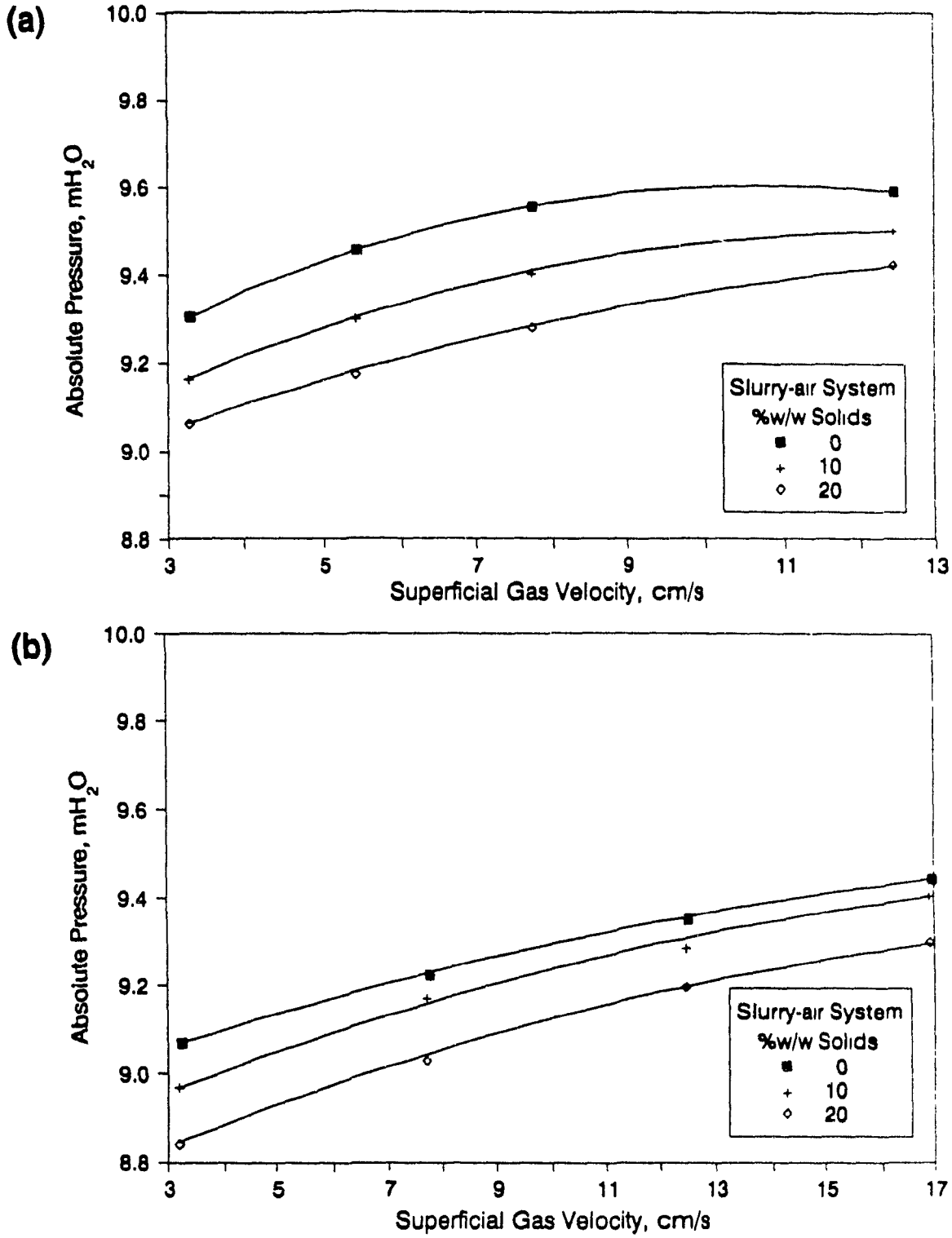

Figure 5.10 Absolute pressure variation in the downcomer against superficial gas velocity for slurry-air system: (a) Jl= 15.57 cm/s and (b) 20.36 cm/s

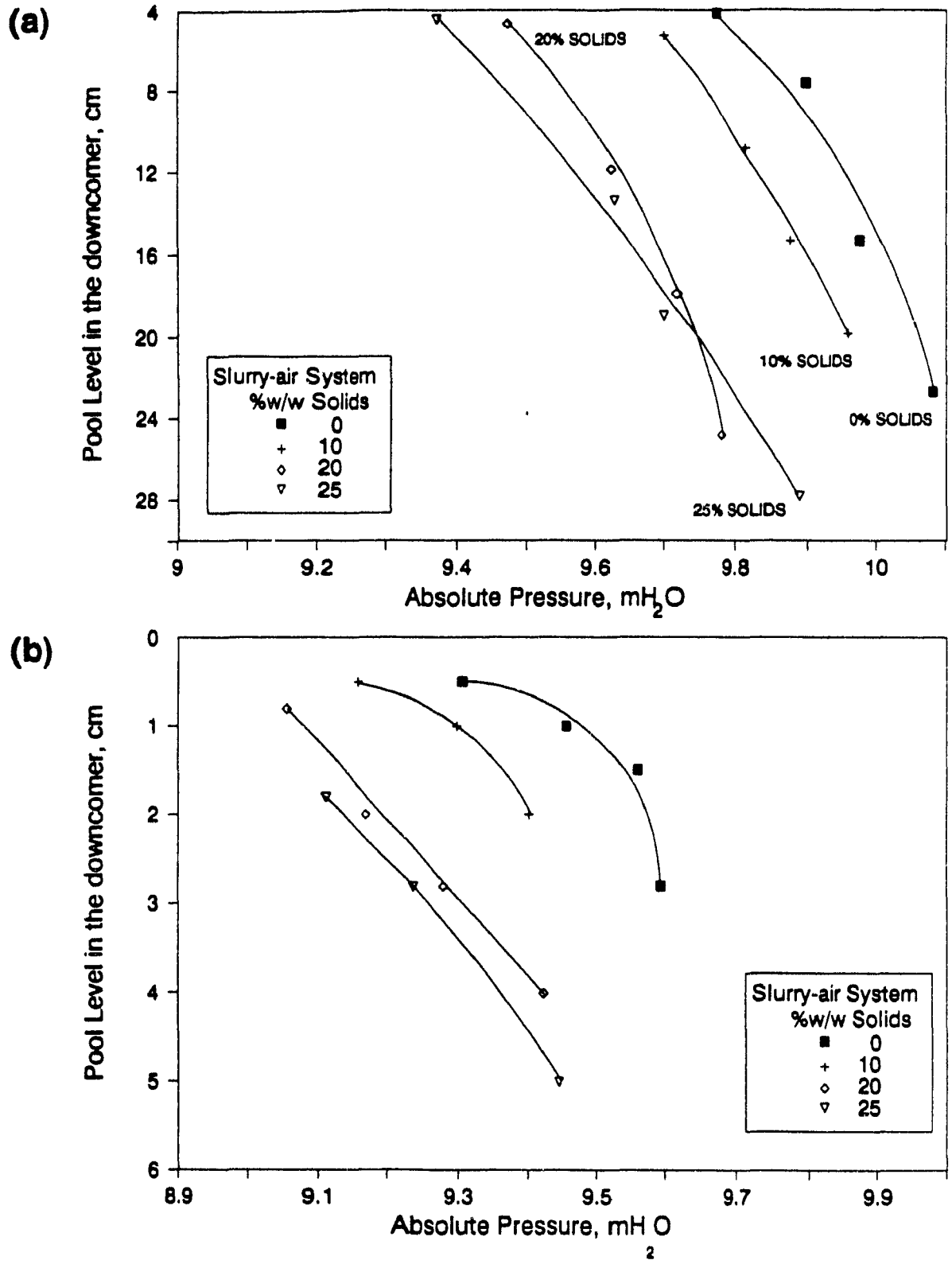

Figure 5.11 Pool level from direct measurement versus absolute pressure in the downcomer with Jl (a) 8.83 cm/s and (b) 15.57 cm/s

The effect of increasing the solid percent in the slurry at constant feed velocity was to increase the vacuum necessary to maintain a constant gas velocity; as the column contents became denser due to the higher content of solids, the pool level moved downwards from the nozzle.

5.2.3.- Gas Holdup

The gas fraction in the downcomer depends on the rate of gas entrainment by the liquid jet. As the entrainment depends on the energy (or momentum) of the liquid jet, it can be increased by using higher liquid velocities or higher densities Figure 5.12 shows the overall trend for the gas holdup (measured with the isolating method), using water-air and slurry-air mixtures, showing that the gas holdup increases by increasing the density of the liquid at constant pressure, regardless of the operating conditions. Similar results have been reported by Shah et al. (1983) and Yamagiwa et al (1990).

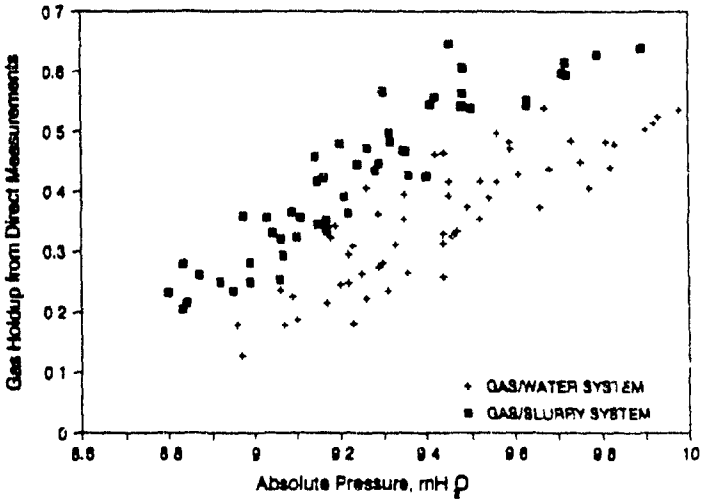

Figure 5.12 Gas holdup from direct measurements versus absolute pressure in the downcomer for the water-air system and the slurry-air system at different conditions

The capacity of a liquid jet to entrain air depends on its momentum (Choudhury et al., 1983). The momentum of a liquid jet is a function of its velocity and density an increase in momentum, at constant feed velocity, can be achieved by increasing the density of the slurry. Figure 5.13 shows the gas holdup for different superficial feed velocities using different slurry densities, while the superficial gas velocity was held

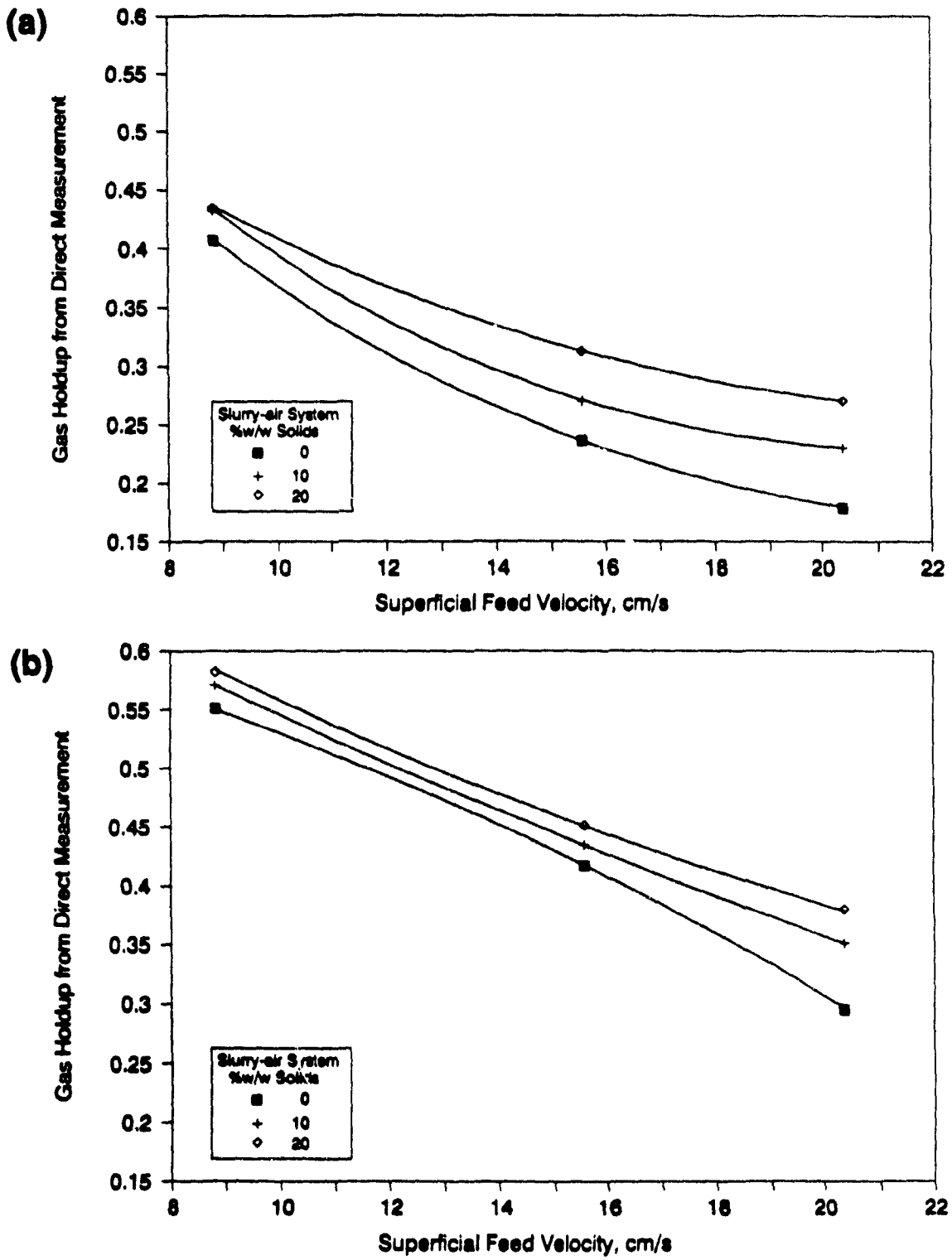

Figure 5.13 Gas holdup from direct measurement in the downcomer against superficial feed velocity for the slurry-air system and constant superficial gas velocity: (a) 3.26 cm/s and (b) 7.75 cm/s.

constant. Gas holdup increments in three-phase systems is probably related to a decrease in bubble size, due to the added momentum causing an increment in the shear stress that produces the bubbles. A smaller bubble diameter was observed compared with the water-air system.

5.3.- ESTIMATING PROCESS VARIABLES

5.3.1.- Estimation of Gas Holdup Using Pressure Measurements.

Estimation of gas holdup and interface level in conventional flotation columns using pressure has been promoted as a simple and reliable method (Kosick et al., 1991). To estimate gas holdup in a water-air system the use of pressure is well established (Finch and Dobby, 1990). The problem of using it in three-phase systems arises from the need to know the slurry density.

In the case of DCFCs the pressure balance is also a function of the slurry density, so similar problems arise.

Based on the fact that pressure can be measured in the downcomer by using a pressure transducer, the gas holdup has been related to this parameter by a simple pressure balance (Eq. (2.2)); a second pressure transducer, in the separation compartment at the level of the downcomer discharge was needed to estimate the pressure head above this point which also contributes to supporting the multi-phase column inside the downcomer. The slurry density was measured directly from the feed tank, and assumed to be uniform throughout the system (experimental measurements of the density of the slurry in the underflow from the column confirmed this assumption).

The use of transducers to measure absolute pressure overcomes the problem of recalibration for different atmospheric pressures as the calibration of the instrument shifts proportionately. The pressure balance considers the difference between the atmospheric and the interior pressure and any offset is cancelled.

From Eq. (2.2) the difference $(H_D - z)$, where H_D is the downcomer length and z is the pool level, can be measured if a transparent column is used, and included in the balance; when it is not possible to determine $(H_D - z)$ independently the gas holdup is overestimated by 1%.

The pressure method was tested in two- (water-air) and three-phase (water-silica-air) systems for different superficial feed and gas velocities, and for 15 and 30% solids w/w.

To check the pressure balance the downcomer was filled with tap water without air, and the operation was stopped to eliminate any dynamic component of the pressure from the balance. As the downcomer is sealed, the water remained inside and the interior pressure, the height of the water outside the downcomer in the separation compartment, and that inside the downcomer were measured. A balance was struck proving that there were no "hidden" factors (beside the dynamic component) present. The estimation of gas holdup in the dynamic system (Figure 5.14(b)) using pressure gave good results; to determine the accuracy of the estimation (Figure 5.15) error on the pressure measurement was taken as two times the standard deviation of the measurement (~95% confidence interval): the resulting relative error on the gas holdup was less than 5% for the water-air system, indicating the method is suited to estimate gas holdup in downflow bubble columns.

For low gas fractions (Figure 5.15), the balance tends to underestimate the gas holdup due to the increased relative error at low values of pressure. The overall estimation gave a good results, specially in the range $25 < \varepsilon_g < 50\%$ which is considered the normal range of operation for DCFCs.

In the three-phase system the pressure balance gave satisfactory estimates of gas holdup (Figure 5.14(a)).

The dynamic component of the balance contributes substantially to the balance in two- and three-phase systems; when this component is not taken into account, the gas holdup is underestimated in the order of 4% for low feed velocities and up to 17% for higher velocities ($\geq$ 20 cm/s).

5.3.2.- Estimation of Gas Holdup using Conductivity Measurements.

An alternative method to pressure for estimating gas holdup is the conductivity technique. It involves measurement of conductivity in the presence and absence of gas with appropriately designed electrodes, and the use of a model relating these conductivities to gas holdup. While the method is a standard (Fan, 1989), to the author's

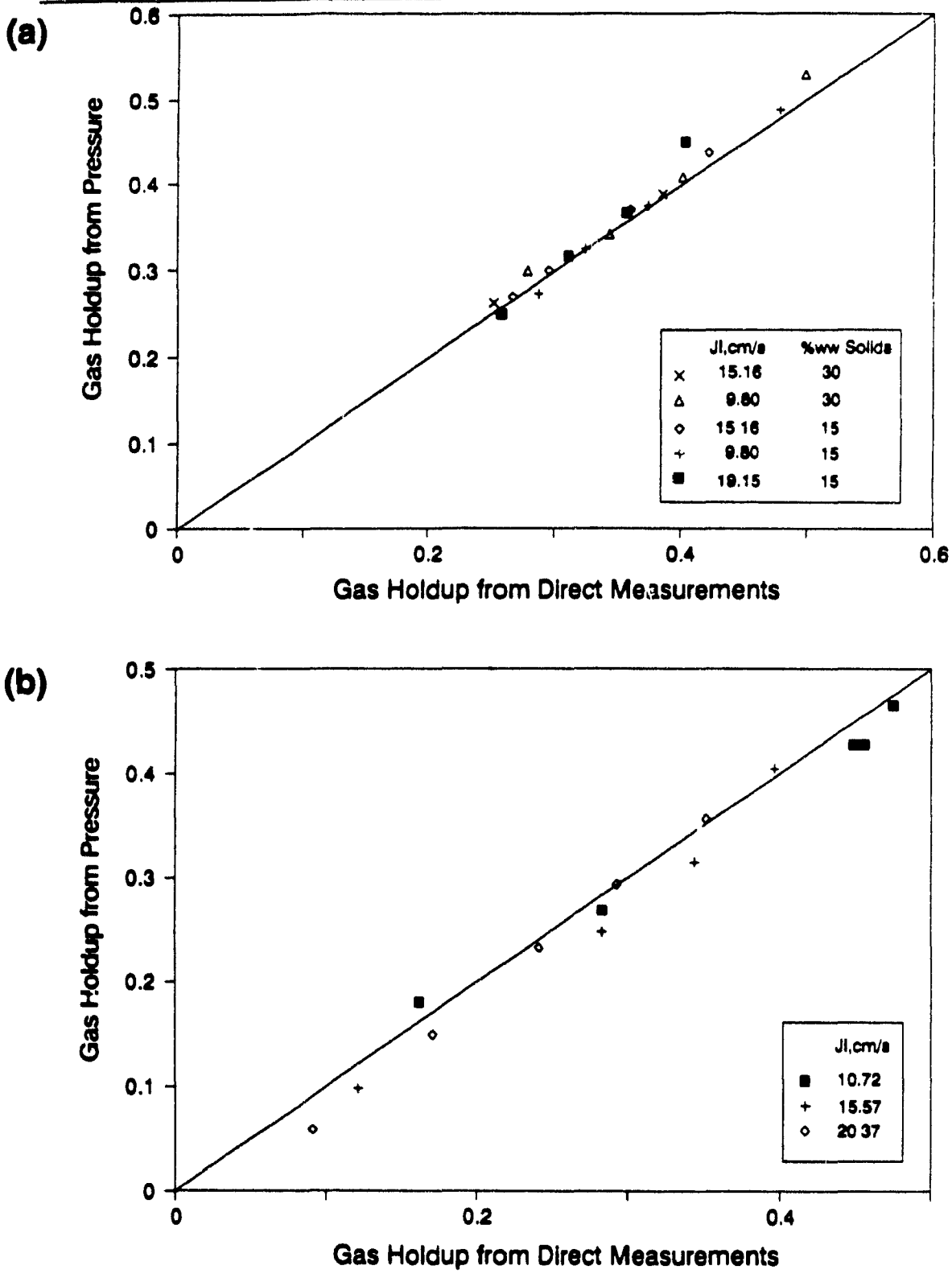

Figure 5.14 Gas holdup obtained from pressure measurements and Equation (2.2) compared to that from direct measurements: (a) Slurry-air system and (b) Water-air system

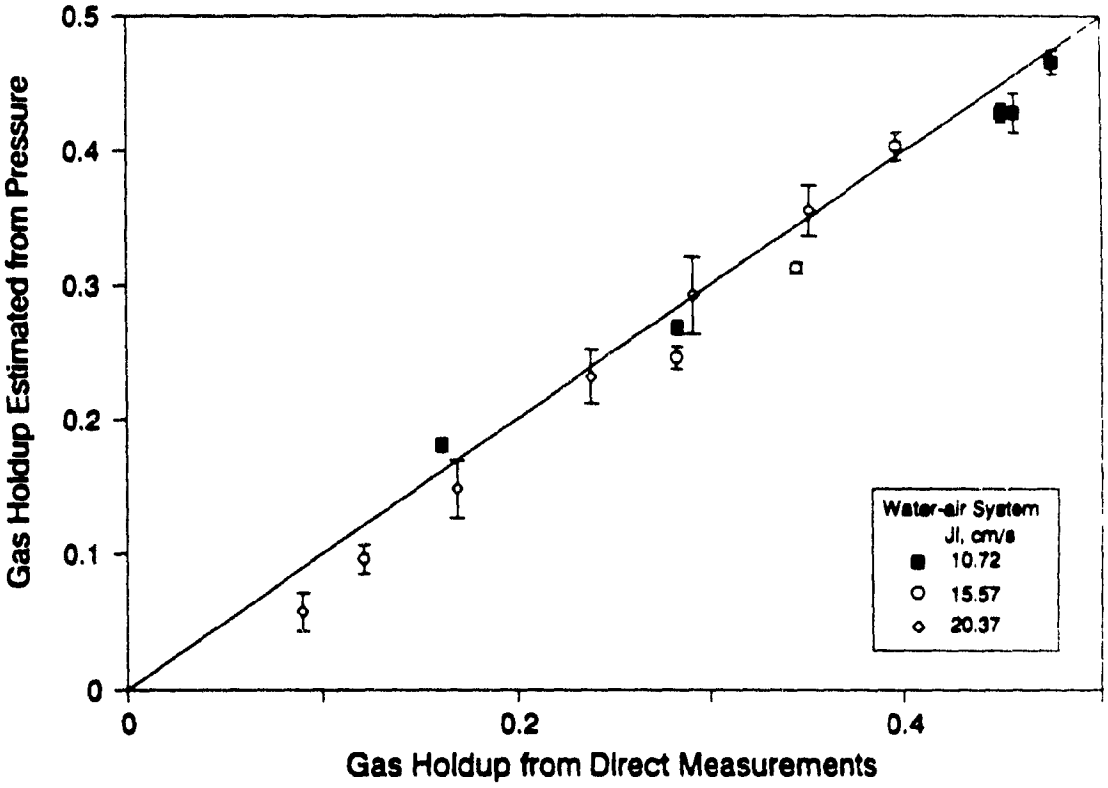

Figure 5.15 Error propagation analysis for the gas holdup estimation from pressure measurements

knowledge it has not been attempted in downflow bubble columns and for the range of gas holdup encountered in such devices (30-60%).

5.3.2.1.- Model Selection

To determine the most suitable model to be used for a downflow concurrent bubble column, four models relating conductivity and gas holdup were examined. For the case where the dispersed phase (gas in this situation) is non conducting, the models of Maxwell (1873), Bruggeman (1934), Weissberg (1963), and Yianatos et al. (1985) (for the froth zone) were tested as they offered a broad cross section of available models (See chapter 3).

As a means of discriminating among these models, the difference (experimental minus estimated gas holdup) was plotted against the experimental gas holdup. The results for three sets of experiments using a water-air system, covering a range in gas holdup from 5 to 60% (Tests 1 to 3) are shown in Figure 5.16, giving the error bars for the Maxwell model (for the other models when not shown the error bar is smaller). In tests 1 and 2 the results for the Yianatos et al. model are not given because the model estimates are off the scale.

In general, the models proposed by Maxwell, Bruggeman and Weissberg gave an adequate estimation of the gas holdup over the full range, regardless of the experimental conditions used. The estimated gas holdup from the model of Yianatos et al. approached the experimental value only for $\varepsilon_g \geq 0.4$ (Figure 5.16(c)); given that it was derived for the froth zone this is not unexpected.

Overall, the Maxwell model gave the best estimates (Figure 5.16(c)). Although the Maxwell model was derived assuming uniform geometry of the nonconductive phase, and a maximum holdup of 10% (Maxwell, 1873) this result is not surprising, as similar successful use up to high gas holdups has been reported by Turner (1976).

The underestimation of the gas holdup (except that of Yianatos et al. model), observed may indicate a small bias in the application of the technique: the electrode design did not cover the full cross-section of the downcomer and a non-uniform radial gas holdup distribution may be present with slightly higher holdups at the walls. For the purposes of this work this is not considered a significant source of error.

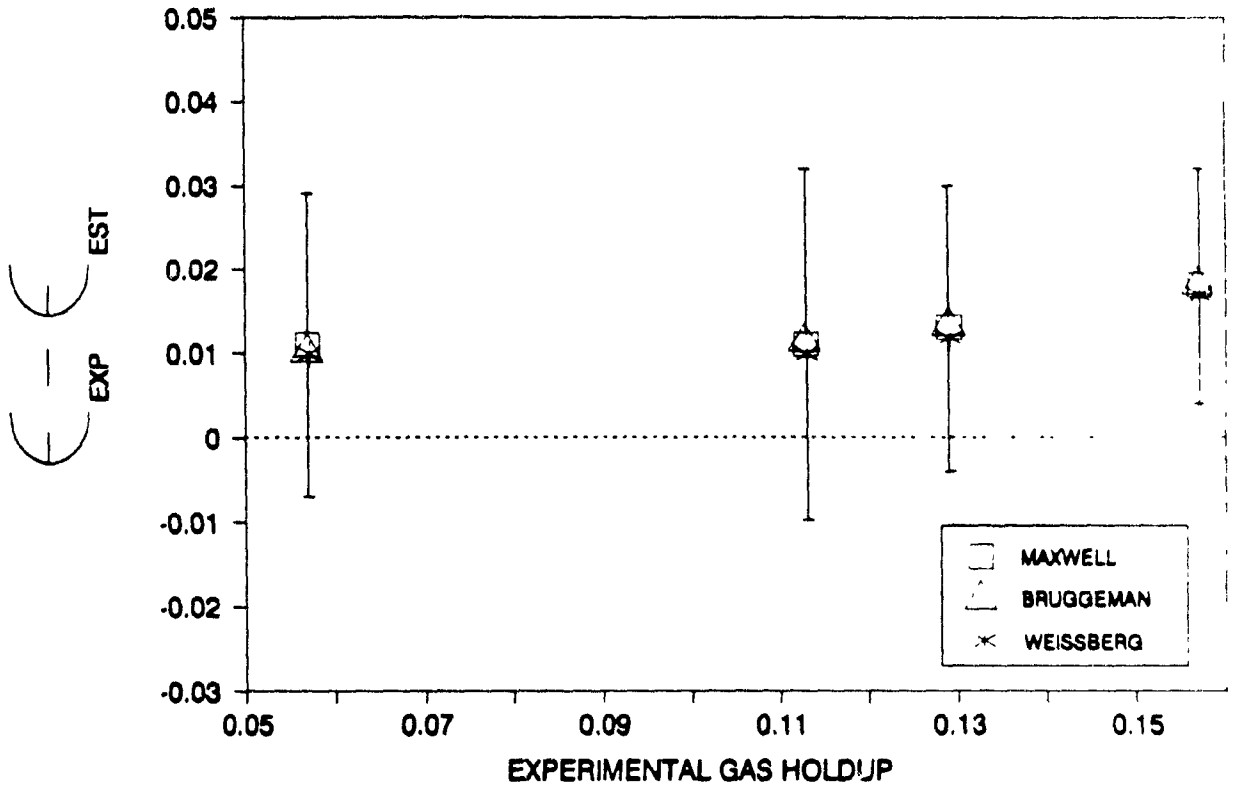

Figure 5.16(a) Difference (experimental minus estimated gas holdup) against gas holdup from direct measurements.

Test 1: superficial gas velocity, 1 08 cm/s; frother, 5 ppm, superficial liquid rates, 9.5 to 25.7 cm/s

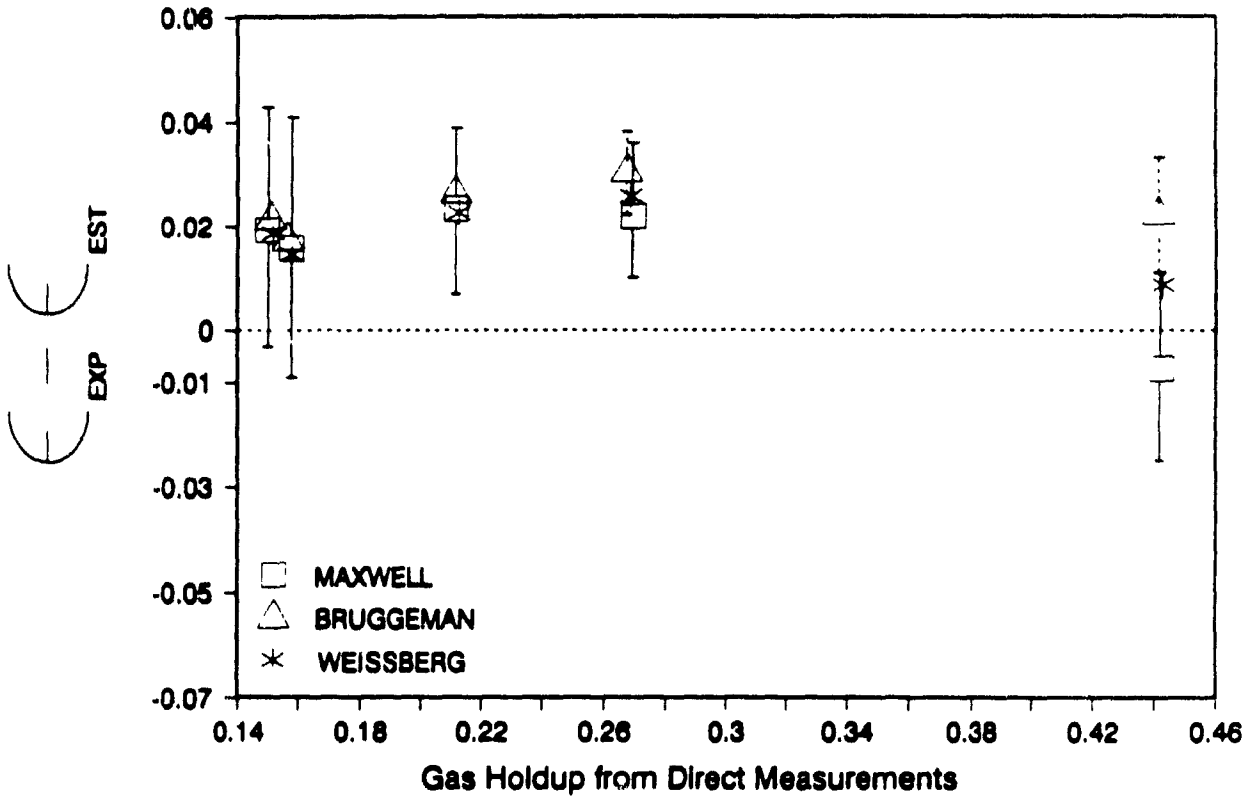

Figure 5.16(b) Difference (experimental minus estimated gas holdup) against gas holdup from direct measurements.

Test 2: superficial gas velocity, 3.26 cm/s; frother, 5 ppm; superficial liquid rates, 6.7 to 17.3 cm/s.

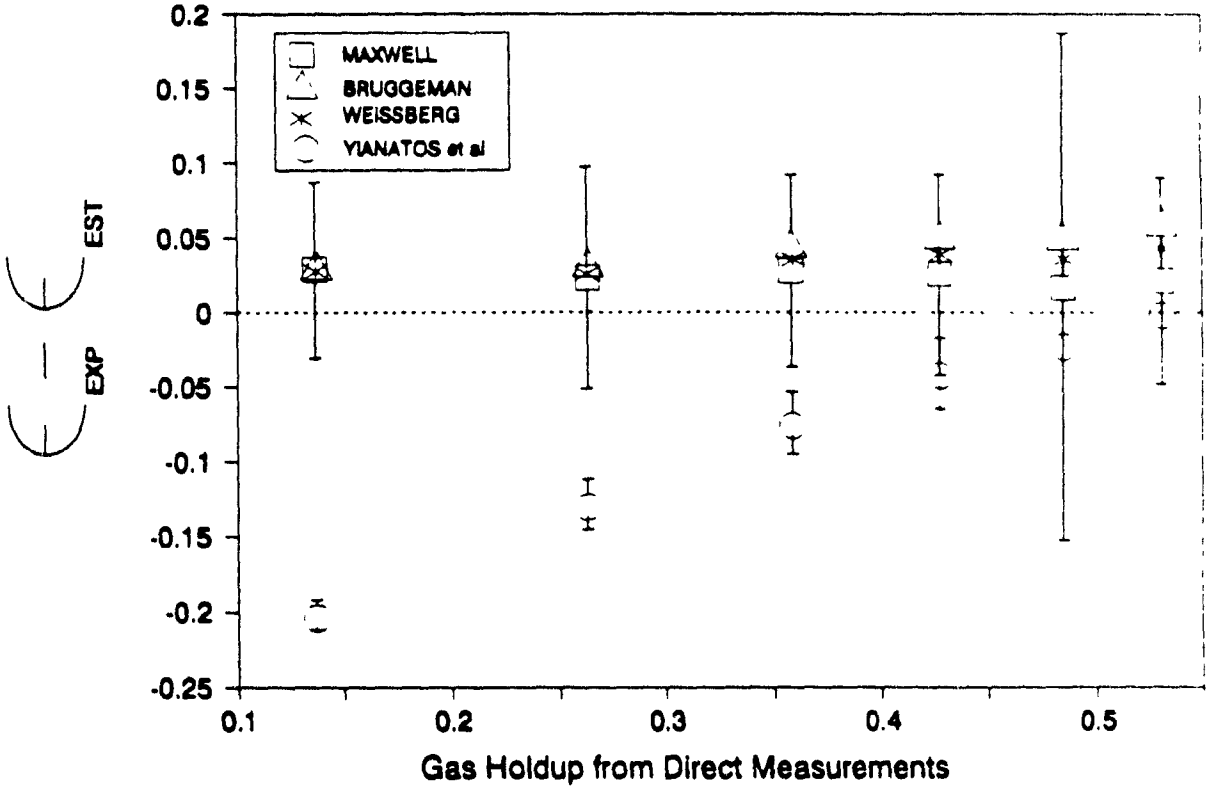

Figure 5.16(c) Difference (experimental minus estimated gas holdup) against gas holdup from direct measurements.

Test 3: superficial liquid velocity, 12 21 cm/s; frother, 25 ppm; superficial gas rates, 1.08 to 14.8 cm/s

Based on the results here, the Maxwell model was selected for subsequent work

As the experimental system was designed to measure the conductivity of the water (slurry) and water-air (slurry-air) mixtures simultaneously, the application of the Maxwell model was extended to the three-phase system, treating the water-solids mixture as one phase.

5.3.2.2.- Gas Holdup Estimation in Two-phase Systems.

The Maxwell model, used with the water-air system, to estimate the gas holdup in the downcomer gave good results for a wide range of feed velocities (Figure 5.17(a)). The model performed satisfactorily over the studied range, except for high fractions ($\varepsilon \geq 0.5$) of gas holdup, where the overestimation of the gas fraction is due to changes in the geometry of the bubble packing (Yianatos et al., 1985, Marchese et al., 1991). These results confirmed the choice of Maxwell's model.

5.3.2.3.- Gas Holdup Estimation in Three Phase Systems.

Different solids concentrations were tested using silica (100% -75 μm) as the solid phase. The apparatus permitted the measurement of the conductivity of the slurry (water-silica) in the feed line and the conductivity of the slurry-air mixture in the downcomer. Figure 5.17(b) shows the results obtained for estimated gas holdup against the experimental value (measured using the isolating technique) with different concentrations of solids, ranging from 10 to 25% w/w of solids. Three different superficial feed velocities were tested for each concentration of solids; estimated holdup against the experimental value was plotted for each concentration (Figure 5.18). There is a tendency to overestimate the gas holdup for values above 50%, which again could be due to changes in the geometry of the bubble packing. As reported by Yianatos et al. (1985), in the froth zone, where the concentration of the non-conducting phase is >50%, the effect of tortuosity becomes more important, and the consideration of a polyhedral geometry for this zone is more realistic. Hashin and Shtrikman (1962) also suggest that the Maxwell model is the lower bound for the description of the dielectric behaviour of a two phase system (which can be extended by mathematical analogy to electrical conductivity), and above this bound it is necessary to consider the spatial distribution of the phases. To analyze the effect of a different geometry in the model Figure 5.19

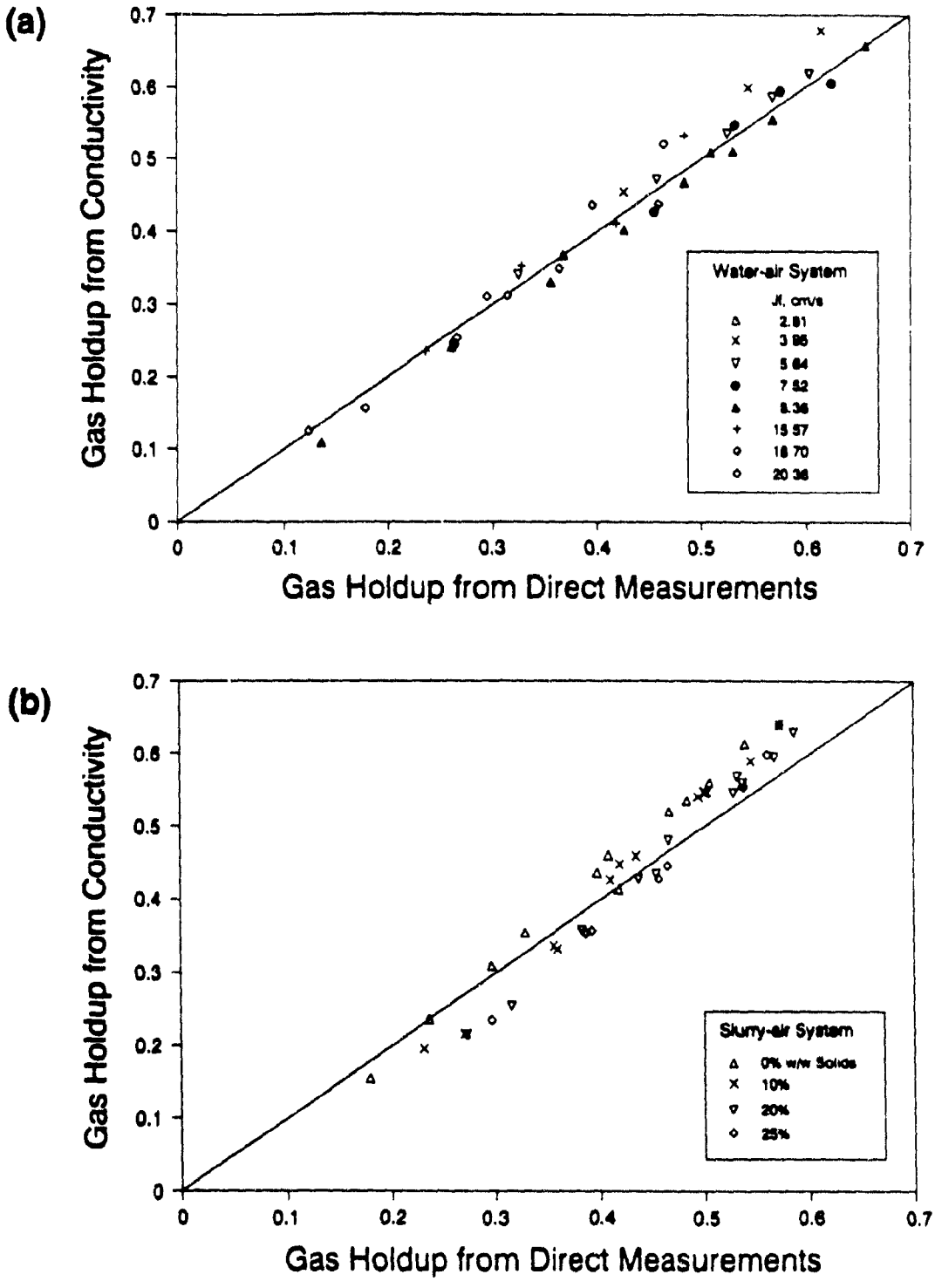

Figure 5.17 Gas holdup from conductivity measurements and Maxwell's equation against that obtained from direct measurements: (a) Water-air and (b) Slurry-air system.

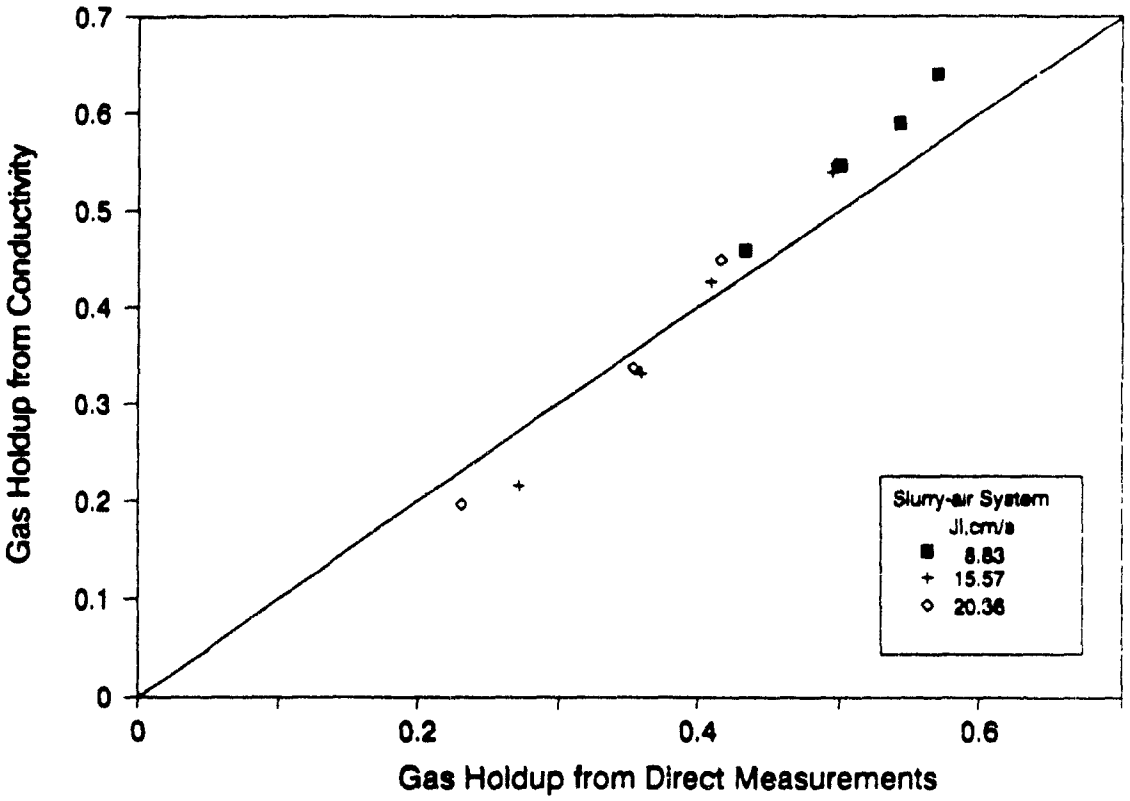

Figure 5.18(a) Gas holdup estimated from conductivity and Maxwell's equation against that from direct measurement for 10%w/w solids

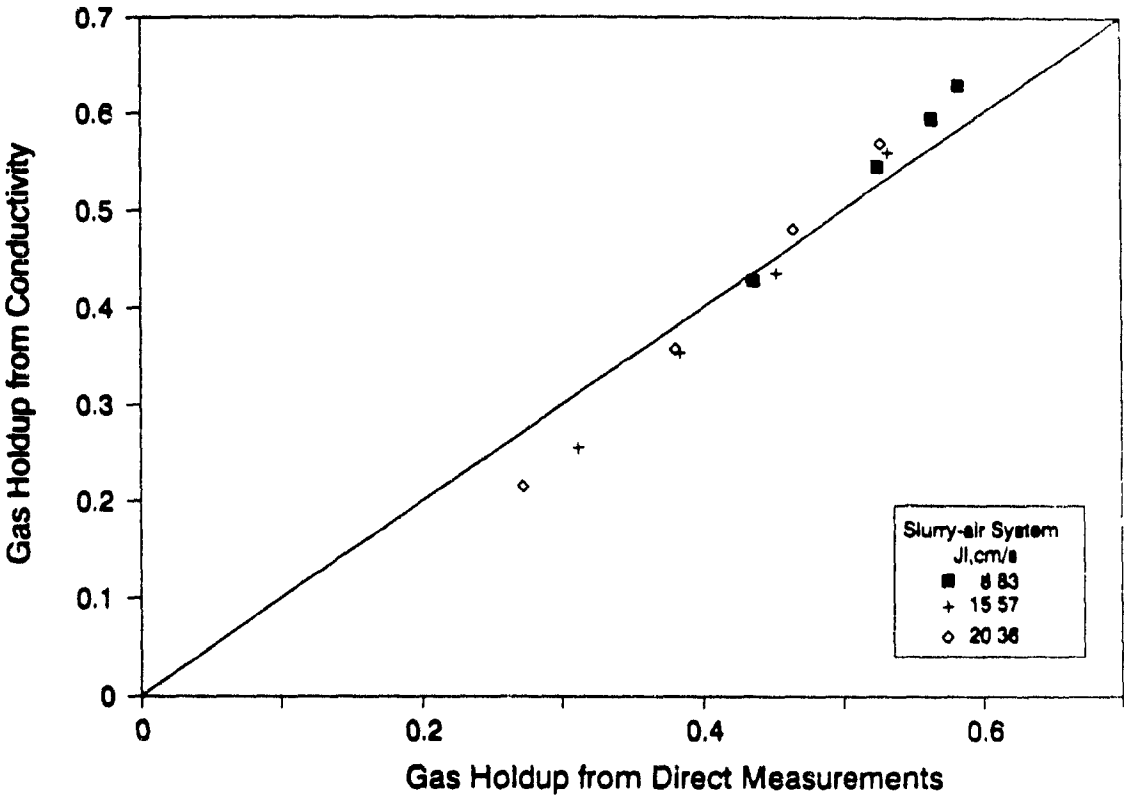

Figure 5.18(b) Gas holdup estimated from conductivity and Maxwell's equation against that from direct measurement for 20%w/w solids

considers the model proposed by Yianatos et al. (1985) for froths. The development of this "froth model" considers a polyhedral geometry of the bubbles and in this case the estimation of the gas holdup is better than the estimation given by Maxwell's model for the range above 50%. (This coincides with the analysis of the different models in section 5.3.2.1 for the water-air system).

The extension of the conductivity technique to the estimation of gas holdup in three-phase systems in a downflow concurrent bubble column has been successful: the use of the Maxwell model remains valid up to 50% of gas holdup in three-phase systems; over 50%, due to changes in the geometrical structure of the system, it is recommended to use a different model, such as the one proposed by Yianatos et al.(1985), which takes into account a more realistic geometry for high bubble packing densities.

5.4.- Drift Flux Analysis.

The drift flux model offers a means to correlate gas holdup with the various operating variables. It has been used, for example, in the estimation of bubble size in liquid-gas mixtures, provided some simple parameters are measured or known (Wallis, 1969). In this application, from the model, the terminal velocity of bubbles (U_t) is estimated and the bubble diameter is evaluated from available relationships between bubble size and terminal velocity. When no experimental measurements of bubble size are available the model is useful to estimate the bubble size in the system. This technique has been used successfully in counter-current bubble columns (Dobby et al., 1988; Dobby and Finch, 1990). It is used in this thesis to estimate U_t.

To recall, on form of the drift flux equation (Eq. (2.16)) is,

$$U_t(1-\varepsilon_g)^{n-1} = \frac{J_l}{1-\varepsilon_g} - \frac{J_g}{\varepsilon_g} \qquad \text{(Eq.(2.16))}$$

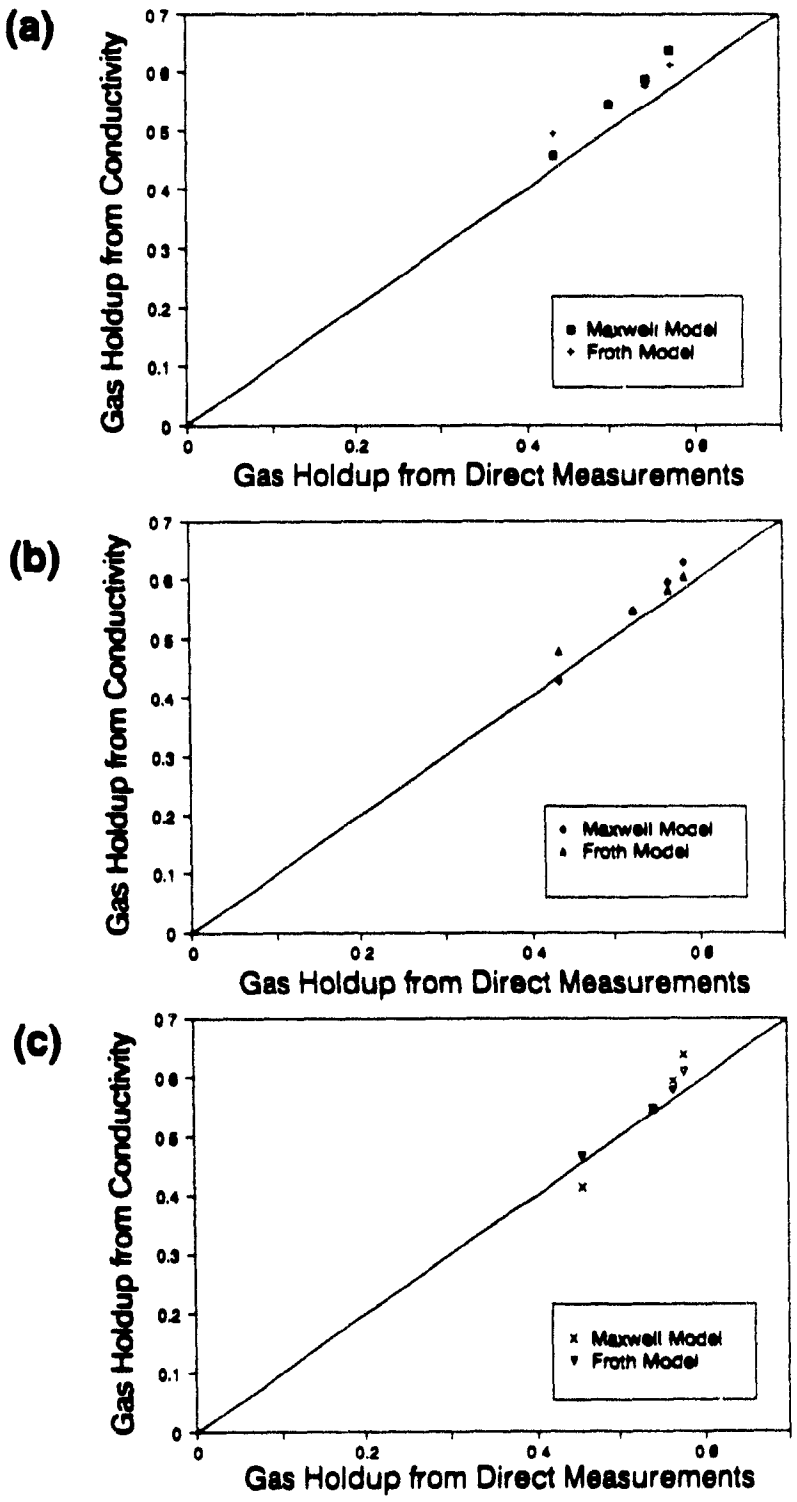

Figure 5.19 Estimated gas holdup using the "froth model" (Yianatos et al., 1985) and the Maxwell model, against the experimenatl gas holdup for (a) 10%, (b) 20%, and (c) 25% solids.

where m is a function of the Reynolds number. In the proposed use U_t will be adjusted to obtain a fit.

5.4.1.- Water-Air System.

Figure 5.20 shows the results of using the drift flux model to estimate gas holdup against the superficial gas velocity, with $m=3$ (from the average value obtained from a series of fits, see Appendix E). The experimental points show a variation in U_t: for low liquid velocity ($J_l=12.21$ *cm/s*) the points correspond to $U_t=16$ *cm/s*, while for higher liquid velocity ($J_l=18.70$ *cm/s*) the experimental points correspond to $U_t=5$ *cm/s*, suggesting that as the liquid velocity increases for constant gas velocity, the bubble size decreases, which is consistent with the observations.

Figure 5.21 summarises the results of the analysis for water-air and slurry-air systems, (using 25 ppm of frother). The calculated terminal velocity of the bubbles is shown against the gas drift flux, J_{GL}. The terminal velocity increases with the increase in gas drift flux, suggesting a larger bubble size. Using Figure 7.3 from Clift et al. (1978), for contaminated water, the range of terminal velocity (U_t) for the different tests suggests that the bubble diameter varies between 0.5 to 1.5 mm, which is reasonably consistent with the visual perception.

Figure 5.22 shows the results of plotting Eq. (2.17),

$$\frac{J_{GL}}{U_t} = \varepsilon_g (1-\varepsilon_g)^3 \qquad \text{(Eq.2.17)}$$

for the water-air system and for the slurry-air system. The use of the dimensionless drift flux (J_{GL}/U_t) appears valid for downwards concurrent flow in the water-air system.

5.4.2.- Water-Solids-Air System.

Drift flux analysis can be applied for three-phase systems provided that the particles are small relative to the bubble (Dobby et al., 1988), (in this case solids are 100% -75 μm, and therefore they qualify). Under these conditions the same equations for the water-air system can be used, substituting the value of the parameters that describe the liquid for those that describe the slurry (e.g. density, viscosity).

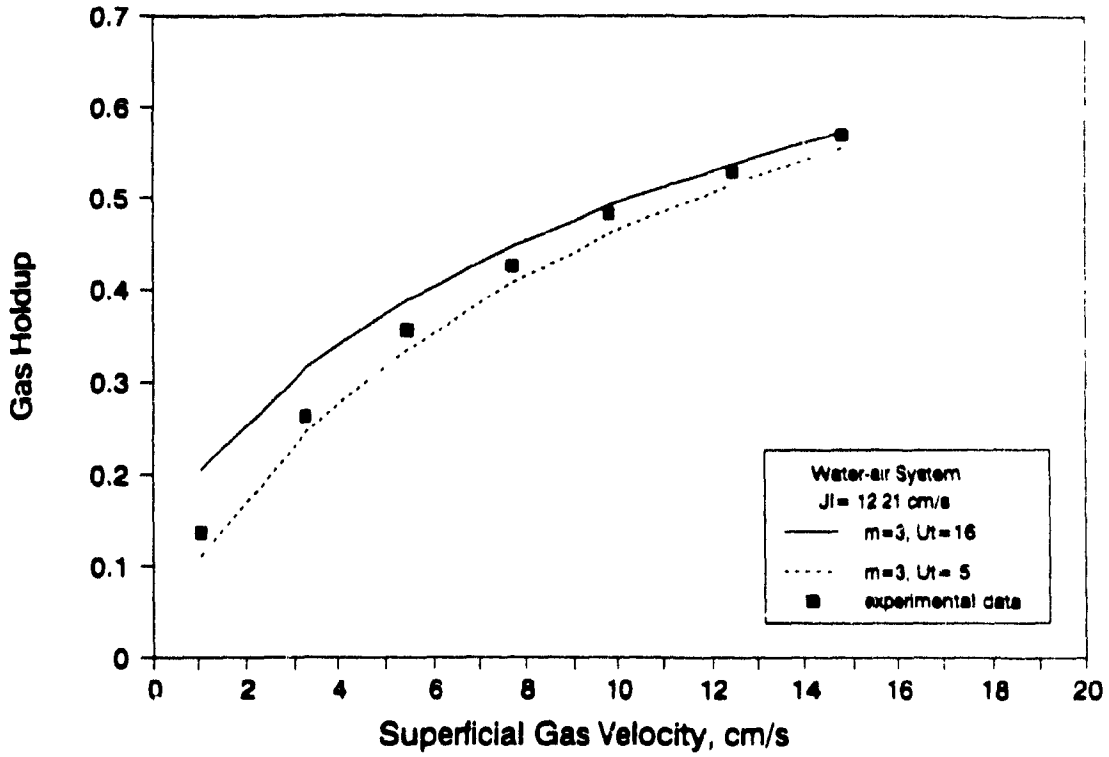

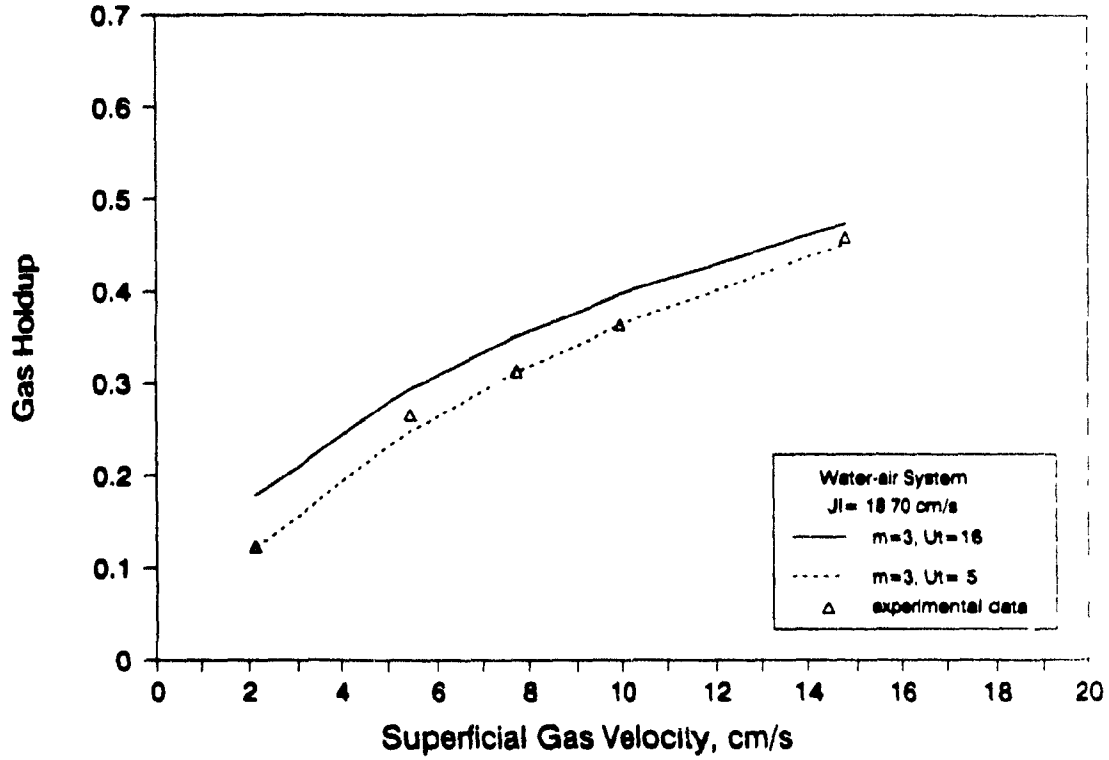

Figure 5.20 Gas holdup estimated from the drift flux model (Eq. (2.16)) against the superficial gas velocity.

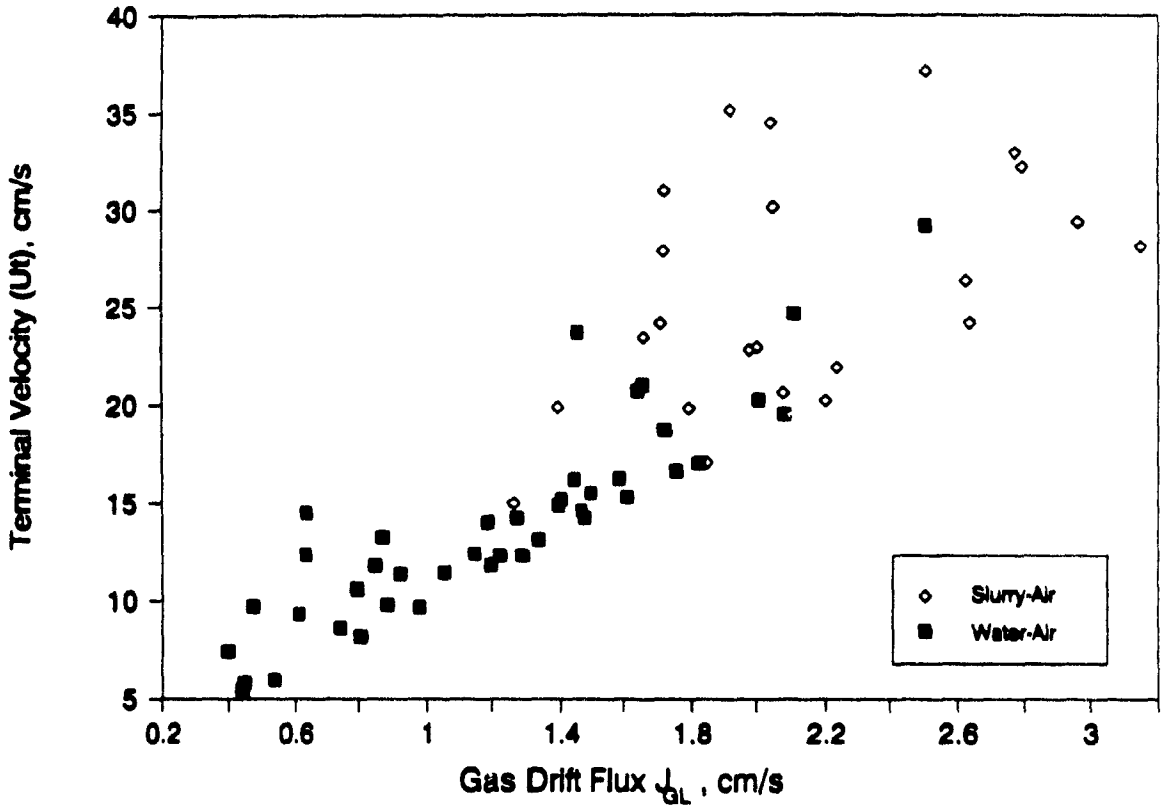

Figure 5.21 Terminal velocity of bubbles calculated from the drift flux model against the drift flux velocity from Equation (2.16) for water-air and slurry-air systems.

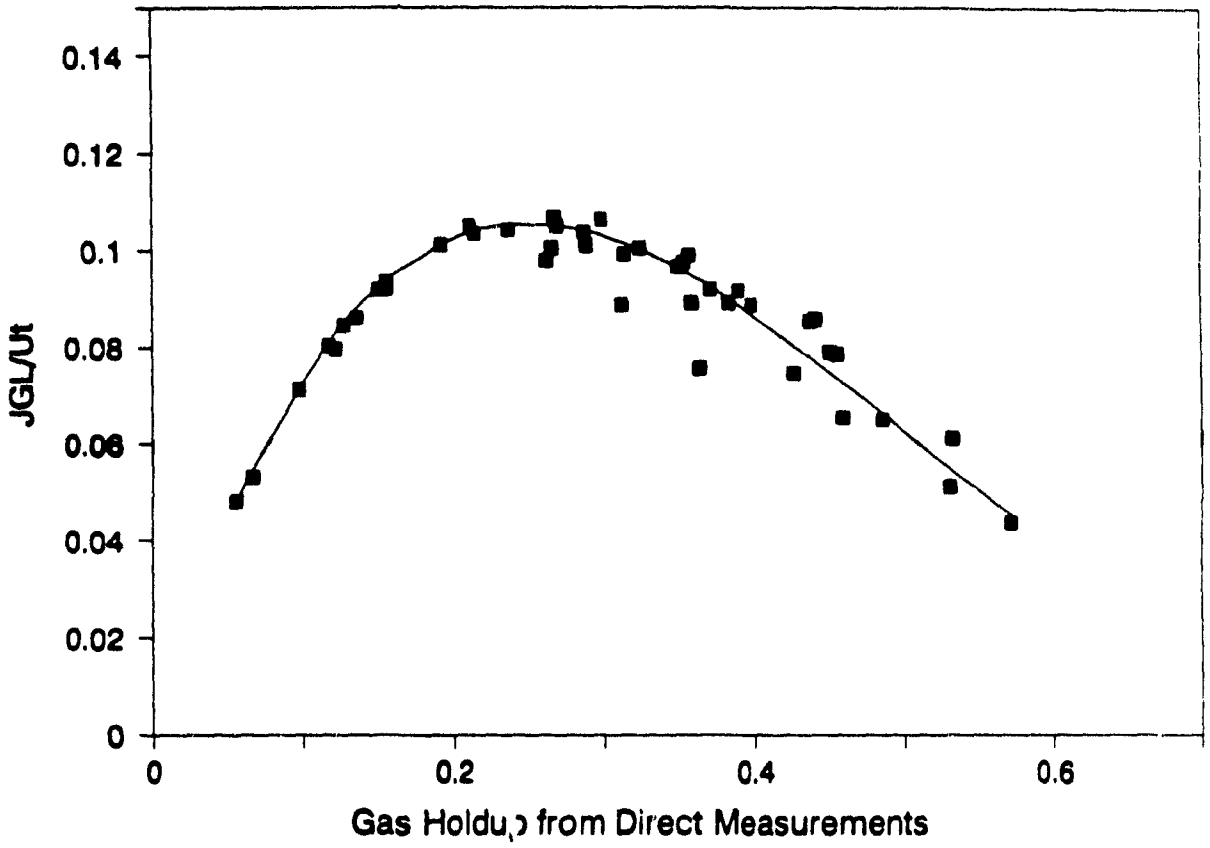

Figure 5.22 Dimensionless drift flux from eq. (2.17) against gas holdup from direct measurements, for the water-air system. The points represent the values from eqs. (2.10) and (2.13) and the experimental data.

From observation, the apparent effect of solids in the system was to decrease the bubble size; however, the drift flux model predicted an increase in terminal velocity in three-phase systems with an increase of the gas drift flux, suggesting that the bubble size increases.

Figure 5.23 shows the drift flux model fit to the ε_g *vs* J_g data. It suggests that as the percent of solids increases the bubble terminal velocity increases (compare U_t values in (a) and (b)), which implies the bubble size increases. This result is at odds with the observations. A similar inconsistency was also reported by Sanchez-Pino and Moys (1991) for the three-phase system.

In conclusion, the drift flux analysis gave reasonable results in the water-air system. In the case of the three-phase system, where the model predictions are at odds with the experimental observations, it is necessary to determine bubble size to further test the model. The presence of solids produced higher gas holdup but, from observation, apparently smaller bubbles.

Figure 5.24 shows a plot of Eq. (2.17) the dimensionless drift flux. This means that the terminal velocity in the three-phase system smaller than in the two phase system, which is coincident with the previous discussion.

The full line is the result from the water-air system (Figure 5.22). Compared to that the J_{GL}/U_t values for the three-phase system are greater for a given ε_g.

The application of the drift flux model is promising for water-air system in the downwards concurrent bubble column. This result is similar to that presented by Wallis (1969) for data obtained by Wilhelm and Kwauk (page 93, Figure 4.2 Wallis, 1969). The use of $m=2$ in Eq. (2.16) does not appear to be a suitable value to describe downwards concurrent bubble columns; $m=3$ shows a better fit to the data. From Eqs. (2.13) and (2.14) for the water-air system, using the Reynolds number of the bubbles the obtained value for m is in the range 2.9-3.1 in all cases.

However, in the case of slurry-air mixtures the bubble size estimation is meaningless, showing a variation between 1.5 and 40 mm according to Figure 7.3 from Clift et al. (1978). Similar results were reported by Sanchez-Pino and Moys (1991): they

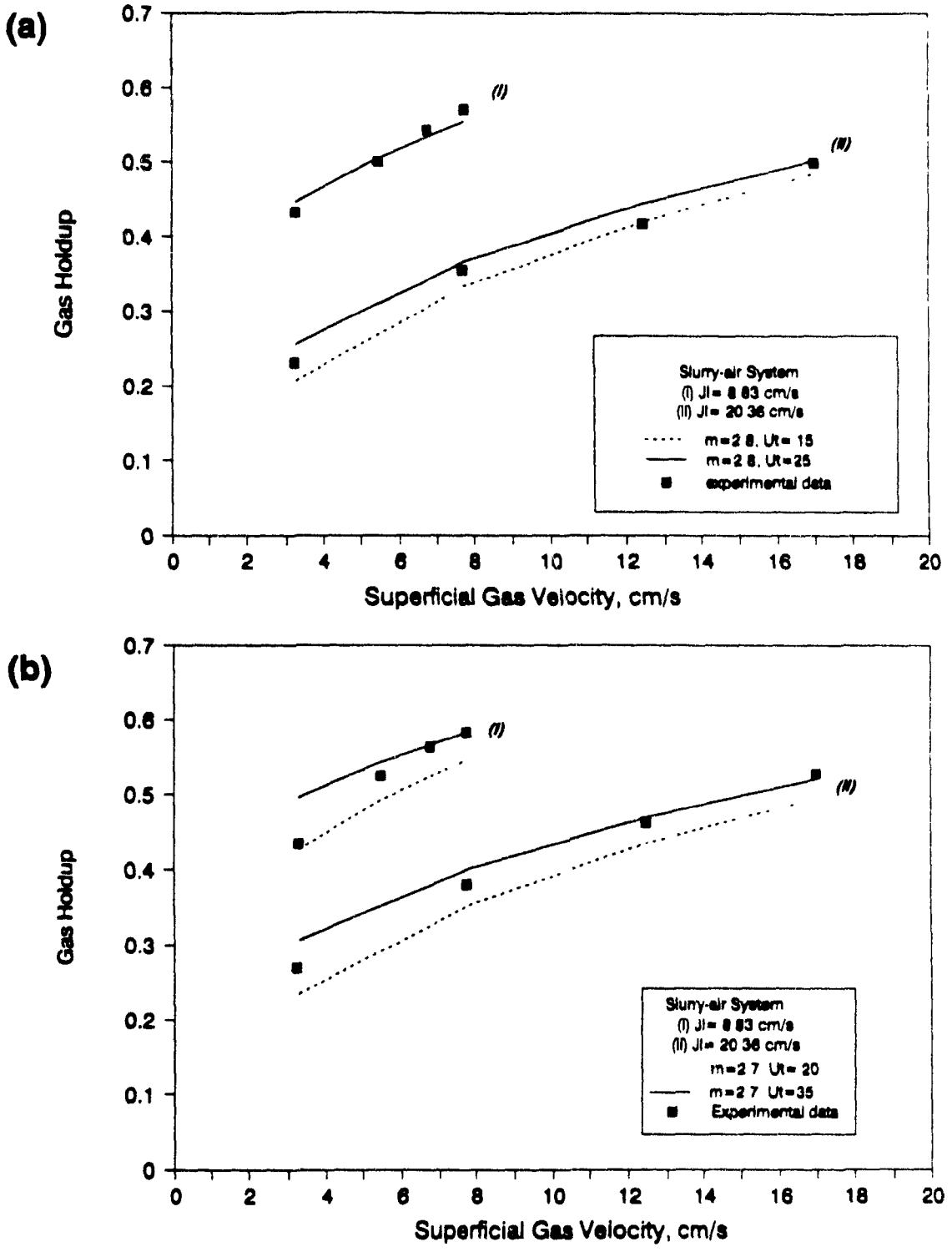

Figure 5.23 Gas holdup estimated from the drift flux model (Eq.(2.16)) against the superficial gas velocity with slurry: (a) 10% w/w and (b) 20% w/w.

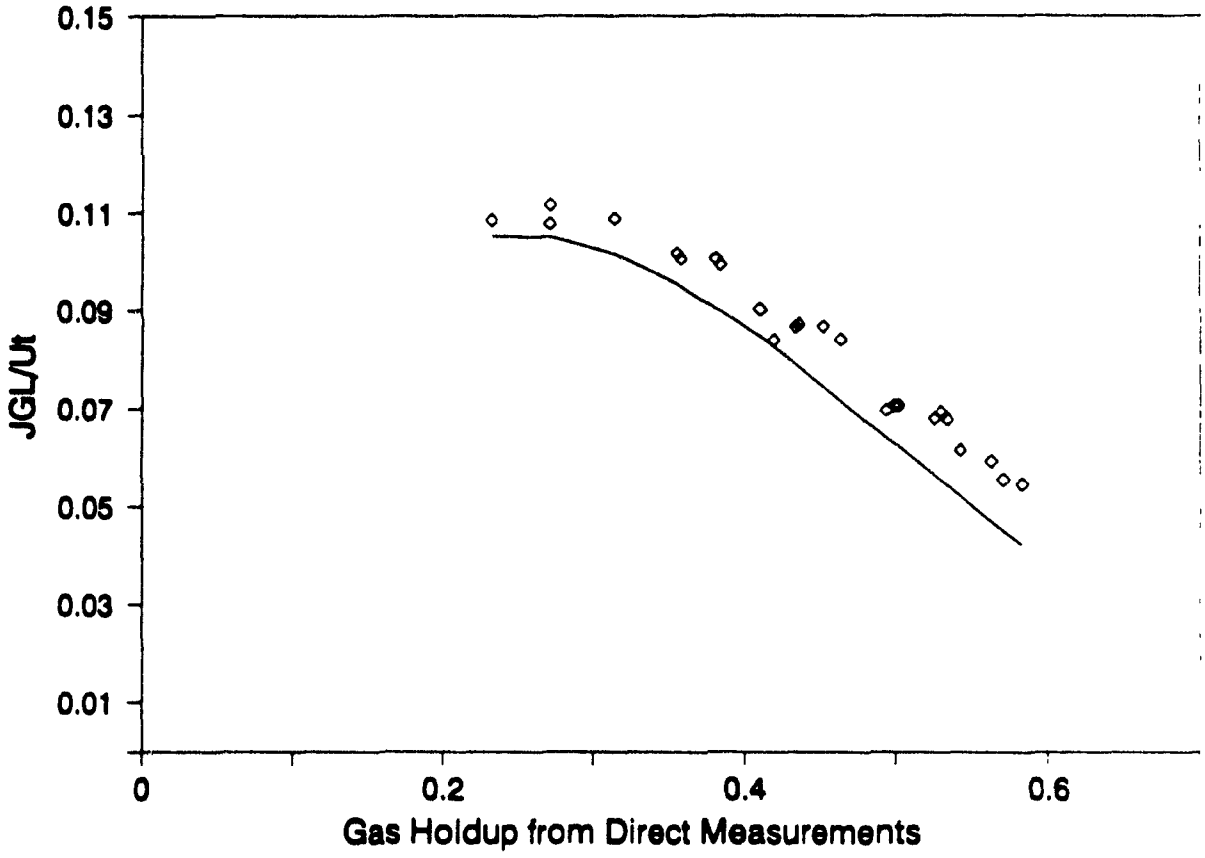

Figure 5.24 Dimensionless drift flux from eq. (2.17) against gas holdup from direct measurements, for the slurry-air system. The points represents the values from eqs. (2.10) and (2.13) and the experimental data.

concluded that the drift flux model cannot be applied in downwards concurrent columns as the estimation of bubble diameter is meaningless. Their experiments were up to superficial liquid velocities (of 42 cm/s) in a 6.8 cm diameter downcomer with similar gas holdups as those reported here.

5.5.- CONCLUSIONS.

1.- The hydrodynamic characteristics of the downflow concurrent bubble column (or downcomer of the Jameson cell) have been studied and the effect of the operating parameters on the gas holdup was determined. Studies in two- and three-phases were performed covering a wide range of conditions.

2.- The multi-phase column is supported inside the downcomer as a result of the balance of hydrostatic pressures, including a dynamic component due to jet deceleration. The jet issuing from the nozzle at the top of the downcomer hits the liquid surface and entrains the gas phase creating a slight vacuum. As bubbles are forced to move downwards against their natural buoyancy their retention time is increased producing gas holdups between 10 to 65% while maintaining a bubbly flow regime.

3.- The pressure inside the downcomer, above the pool level, is the key parameter to control the downcomer performance. It depends on the density of the feed (the presence of solids increases the momentum of the jet issuing from the nozzle thus increasing the vacuum created), and it can be used to determine the flow regime inside the downcomer, by analyzing the signal pattern it is possible to distinguish between bubbly and slug flow, for example.

4.- Pressure measurements have been related to gas holdup through a pressure balance. The dynamic component of pressure contributed substantially to the balance, underestimation of gas holdup in the order of 4 to 17% was obtained when it was not considered. The use of pressure to monitor behaviour is promising from the point of view of industrial application, since only two pressure measurements are required. The density of the slurry can be taken as that of the feed because it is unlikely to change significantly along the downcomer. The same applies in case of hydrophobic solids, provided bubbles move downwards at similar velocity with the liquid (i.e. for high liquid throughputs).

5.- The superficial feed velocity controls the amount of air that can be aspirated into the

downcomer by controlling the entrainment rate of gas into the liquid. The bubble size is also influenced by the jet velocity due to its effect on the shear stress that creates the bubbles. The pool level is slightly affected by the liquid velocity, more so at low gas rates ($J_g \leq 1$ *cm/s*). The frother concentration has an important effect on the stability of the multi-phase column: increasing frother dosage allows more gas to be aspirated under bubbly flow conditions; at the same time higher concentrations of frother decrease the gas holdup due to the formation of smaller bubbles that move downwards faster because of a their lower buoyancy. The overall effect of higher frother concentrations is to increase the maximum gas holdup obtainable due to the higher gas rate that can be aspirated at the same feed velocity. The superficial gas velocity affects the pool level at low superficial feed velocities ($J_l \leq 10$ *cm/s*), while at higher feed rates its effect is not important and the pool level varies within a narrow range (from 0 to 5 cm). The presence of solids increases the weight of the multi-phase column in the downcomer so a higher vacuum is required to hold the column at the same level; increased vacuum can be achieved by increasing the feed velocity at constant gas velocity, for example.

6.- Gas holdup estimation by using conductivity measurements has been successfully demonstrated. Fundamental models that relate gas holdup with the conductivity of the feed and the conductivity of the multi-phase mixture in the downcomer were tested to determine the best overall for the gas holdup range 5 to 60%. Maxwell's model proved to be the best, with a maximum error of 6%.

7.- Drift flux analysis was used to try to correlate the data in both two- and three-phase systems. For the water-air system the model was consistent with experimental observations -the model may even be suitable for bubble size estimation. For the three-phase system the model was at odds with experimental observations, predicting an increasing bubble size with an increase in feed velocity and percent solids, while visual observation suggested the opposite. The use of a dimensionless drift flux to study the balance of drag forces and buoyancy is valid; the use of $m=2$ in the equation of Richardson and Zaki does not appear to be valid for downwards concurrent bubble columns; $m=3$ was found to be more suitable.

Achwal, S.K., and Stephanek, J.B., 1975. "An Alternative Method of Determining Holdup in Gas-Liquid Systems", *Chem. Eng. Sci.*, **30**, 1443-1444.

Achwal, S.K., and Stephanek, J.B., 1976. "Holdup Profiles in Packed Beds", *Chem. Eng. Jour.*, **12**, 69-75.

Anderson, G.H. and Matzouranis, B.G., 1960. "Two-Phase (gas-liquid) Flow Phenomena-I", *Chemical Eng. Sci.*, vol. 12, pp. 109-126.

Anon., 1917, "The Cascade Method of Agitation for Selective Flotation of Sulphides", *Engineering and Mining Jour.*, vol. 104, No.23 December, pp.993-994.

Aravena, J., 1987. "Aplicación del Proceso de Concentración por Flotación en Columna en Planta Recuperadora de Molibdeno", Internal report CODELCO-Chile, Chuquicamata Division.

ASME,1971, *Fluid Meters*, 6th Edition, pp. 202-207.

Bankoff, S.G., 1960. "A Variable Density Single-Fluid Model for Two-Phase Flow with Particular Reference to Steam-Water Flow", *Journal of Heat Transfer, Trans ASME*, Series C, vol. 82, pp. 265-272.

Begovich, J.M., and Watson, J.S., 1978. "An Electroconductivity Technique for the Measurement of Axial Variation of Holdups in Three-Phase Fluidized Beds", *AICHE Jour.*, **24**, 2, 351-354.

Behringer, H., 1936. "The Flow of Liquid-Gas Mixtures in Vertical Tubes", *Zeit Ges. Kälte-Ind.*, vol. 43, pp. 55-58.

Benatt, F. and Eisenklam, P.,1969. "Gaseous Entrainment into Axisymmetric Liquid Sprays", *Journal of the Institute of Fuel*, pp. 309-315, August.

Bevilaqua, P.M. and Lykoudis, P.S.,1977. "Some Observations on the Mechanism of Entrainment", *AIAA Journal*, vol. 15, pp. 1194-1196, August.

BHRA Fluid Engineering, 1968, Engineering Outline: Jet Pumps, *Engineering Journal*, **123**, May.

Bin, A.K. and Smith, J.M., 1982. "Mass Transfer in a Plunging Liquid Jet Absorber", *Chemical Eng. Communications*, vol. 15, pp. 367-383.

Bonnington, S.T., King, A.L., 1976, *Jet Pump and Ejectors*, 2nd Edition, BHRA Fluid Engineering.

Bradshaw, P., 1972. "The Understanding and Prediction of Turbulent Flow", *Aeronautical Journal*, July, pp. 403-418.

Braunstein, J., and Robbins, G.D., 1971. "Electric Conductance Measurements and Capacitive Balance", *J. Chem. Ed.*, **48**, 1, 52-59.

Brewis, T., 1991, "Flotation Cells", *Mining Magazine*, June, pp. 383-393.

Bruggeman, D.A.G., 1935. "Berechnung Verschiedener Physicalischer Konstanten von Heterogenen Substanzen", *Annln Phys.*, **24**, 639.

Brzezina, R. and Sablik, J., 1991. "Pneumatic Flotation Machine FLOKOB-3 Industrial Model", *Column'91, Proceedings Intl. Conf. on Flotation Column*, Agar, Huls, and Hyma Eds., June 2-6, Sudbury, Ontario, Canada, Vol. 2, pp. 619-630.

Castillejos, A.H., 1986. "A Study of the Fluid-Dynamic Characteristics of Turbulent Gas-Liquid Plumes", Ph.D. Thesis, University of British Columbia.

Chase, S., 1971. *Downward Two-phase Flow in Vertical Tubes*, M.Eng. Thesis, Department of Chemical Engineering, McGill University.

Choudhury, S.D., Radhakrishnan, V.R. and Mita, A.K., 1982. "Gas Holdup in Vertical Concurrent Flow with Improved Gas-Liquid Mixing", *Physical Modelling of Multi-Phase Flow Conference*, Coventry, England, paper F3, April.

Cole, R.H., and Coles, J.S., 1964. *Physical Principles of Chemistry*, W.H. Freeman and Company, 795 pp.

Condon, E.U.(Ed.), 1967. *Handbook of Physics*, Chapter 9, McGraw Hill Book Co., 146-169.

Cunningham, R.G., 1957, "Jet-Pump Theory and Performance with Fluids of High Viscosity", *ASME Transactions*, v 79, pp.1807-1820.

De la Rue, R.E., and Tobias, C.W., 1959. "On the Conductivity of Dispersions", *Jour. Electrochem. Soc.*, **106**, 827-832.

Dobby, G.S., Yianatos, J.B., and Finch, J.A., 1988. "Estimation of Bubble Diameter in Flotation Columns from Drift Flux Analysis", *Canadian Metallurgical Quarterly*, Vol. 27, No. 2, pp. 85-90.

Fairchild, D.H., 1917, "Cascade Flotation Machine", *Engineering and Mining Jour.*, vol. 104, No.9 September, pp. 392-393.

Fan, L.-S., 1989. *Gas-Liquid-Solid Fluidization Engineering*. Chapter 2. Butterworth Publishers, 763 pp.

Finch, J.A. and Dobby, G.S., 1990, *Column Flotation*, Pergamon Press, 180 p.

Folsom, R.G., 1948, "Jet Pumps with Liquid Drive", *Chemical Engineering Progress*, vol. 44, No. 10, pp. 765-770.

Friedel, L., Herbrechtmeister, P. and Steiner, R., 1980. "Mean Gas Holdup in Downflow Bubble Columns", *German Chem. Engr.*, **3**, pp. 342-346.

Fujie, K., Takaine, M., Kubota, H., and Miyaji, Y., 1980. "Flow and Oxygen Transfer in Cocurrent Gas-Liquid Downflow", *Journal of Chemical Engineering of Japan*, vol. 13, No. 3, pp. 188-193.

Gartshore, I.S., 1965. "Experimental Examination of the Large Eddy Equilibrium Hypothesis", *Journal of Fluid Mechanics*, vol. 24, pp. 89-98.

Gilmont, R., and Walton, R.F., 1956. "New Design of an Electrolytic Cell for the Study of Electroplating Phenomena", *Jour. Electrochem. Soc.*, **103**, 10, 549-552.

Grant, H.L., 1958. "The Large Eddies of Turbulent Motion", *Journal of Fluid Mechanics*, vol. 4, pp.149-190.

Grant, R.P and Middleman, S., 1966. "Newtonian Jet Stability", *AICHE Journal*, vol. 12, No. 4, pp. 669-678, July.

Griffith, P. and Wallis, G.B., 1961. "Two-Phase Slug Flow", *Journal of Heat Transfer, Trans. ASME*, Series C, vol. 84, pp. 29-39.

Govier, G.W., Radford, B.A. and Dunn, J.S.C., 1957. "The Upwards Vertical Flow of Air-Water Mixtures", *The Canadian Journal of Chem. Eng.*, August, pp. 58-70.

Güney, A., Önal, G. and Dogan, M.Z., 1991, "Beneficiation of Üçköprü Chromite Gravity Tailings by Free Jet Type Flotation System". *Column '91, Proceedings International Conf. on Column Flotation*, Agar, Huls and Hyma Eds.,June 2-6, Sudbury, Ontario, Canada, Vol. 2, pp. 609-617.

Hall, S., 1991, "Developing Flotation Technologies", *Mining Magazine*, June, pp. 379-381.

Harvey, R.J., 1918. "The Development of Galena Flotation at the Central Mine, Broken Hill", *Transactions Inst. of Mining and Metallurgy*, vol. 28, pp. 5-21.

Hashin, Z. and Shtrikman, S., 1962. "A Variational Approach to the Theory of the Effective Magnetic Permeability of Multiphase Materials", **33**, October, pp. 3125-3131.

Hashin, Z., 1968. "Assessment of the Self Consistent Scheme Approximation: Conductivity of Particulate Composite", *J. Composite Mater.*, **2**, 284-300.

Hetsroni, 1982. *Handbook of Multiphase Systems*. McGraw Hill Book Co.

Hoefer, K., 1922, "Experiments on Vacuum Pumps for Condensers", *VDI Forschung Geb. Ing. Weseng*, No. 253.

Hongqi, L., 1983, "Liquid Gas Two Phase Flow Theory of Jet Pump", *International Conference on the Physical Modelling of Multiphase Flow*, England, paper K2.

Jameson, G.J., 1988, "A New Concept in Flotation Column Design", *Column Flotation '88 Proceedings* (K.V.S. Sastry Ed.), Phoenix, Arizona, U.S.A., pp. 281-285.

Jameson, G.J., 1990. "Column Flotation Method and Apparatus", *U.S. Patent No. 4,938,865*, July 3.

Jameson, G.J. and Manlapig, E.V., 1991, "Applications of the Jameson Flotation Cell", *COLUMN '91, Proceedings International Conf. on Column Flotation*, (Agar, Huls, Hyma Eds.) Sudbury, Ont., June 2-6. Vol. 2, pp. 673-687.

Jepsen, J.C. and Ralph, J.L., 1969. "Hydrodynamic Studies of Two-Phase Upflow in Vertical Pipelines", *Proceedings Instn. Mech. Engrs.*, vol. 184, Pt 3C, pp. 154-165.

Kasper, C., 1940. "The Theory of the Potential and the Technical Practice of Electrodeposition", *Trans. Electrochem. Soc.*, **77**, 353-384; **78**, 131-161.

Kato, Y., Uchida, K., Kago, T., and Morooka, S., 1981. "Liquid Holdup and Heat Transfer Coefficient between Bed and Wall in Liquid-Solid and Gas-Liquid Fluidized Beds", *Powder Tech.*, **28**, 173-179.

Kennedy, A., 1990, "The Jameson Flotation Cell", *Mining Magazine*, October, pp. 282-288.

Kusabiraki, D., Murota, M., Ohno, S., Yamagiwa, K., Yasuda, M., and Ohkawa, A., 1990. "Gas Entrainment Rate and Flow Pattern in a Plunging Liquid Jet Aeration System Using Inclined Nozzles", *Journal of Chemical Engineering of Japan*, vol. 23, No. 6, pp. 704-710.

LeBlanc, M., in Duyoner, L., 1962. *Vacuum Practice*, trans. by J.H. Smith (D. Van Nostrand Company, Inc., New York) pp 41-42.

Lockett, M.J., and Kirkpatrick, R.D., 1975. "Ideal Bubbly Flow and Actual Flow in Bubble Columns", *Trans. Instn. Chem. Engrs.*, **53**, pp. 267-273.

Lockhart, R.W. and Martinelli, R.C., 1949. "Proposed Correlation of Data for Isothermal Two-Phase Two-Component Flow in Pipes", *Chemical Engineering Progress*, vol.45, No. 1, pp. 39-48.

Marchese, M.M., 1991. *Processing of Copper and Molybdenum Sulphides in Chuquicamata Concentrator Plant, Chile*, Departamental Graduate Seminars, McGill University.

Marchese, M.M., Uribe-Salas, A., and Finch, J.A., 1991. "Estimating Gas Holdup from Conductivity in Downflow Bubble Columns", Technical Note. Submitted for Publication in *Chem. Eng. Sci.*

Maxwell, J.C., 1892. *A Treatise of Electricity and Magnetism*, 3rd Edn., Vol. 1, Part II, Chapter IX, 435-449. Oxford University Press, London.

Meredith, R.E., and Tobias, C.W., 1960. "Resistance to Potential Flow through a Cubical Array of Spheres", *J. Appl. Phys.*, **31**, 7, 1270-1273.

Mote, R.G., in Bathia, M.V. and Cheremisinoff, P.N., 1981. *Air Movement and Vacuum Devices*, Technomic Publishing Company Inc.

Nasr-El-Din, H., Shook, C.A., and Colwell, J. 1987. "A Conductivity Probe for Measuring Local Concentrations in Slurry Systems", *Int. J. Multiphase Flow*, **13**, 3, 365-378.

Nassos, P.G., 1963. "Development of an Electrical Resistivity Probe for Void Fraction Measurements in Air-Water Flow", Argon National Laboratory, Report ANL-8738.

Neal, L.G., 1963. *"An Analysis of Slip in Gas-Liquid Flow Applicable to the Bubble and Slug Flow Regimes"*, Report KR-62, Kjeller Research Establishment, Kjeller, Norway.

Neale, G.H., and Nader, W.K., 1973. "Prediction of Transport Processes within Porous Media: Diffusive Flow Processes within an Homogeneous Swarm of Spherical Particles", *AICHE Journal*, **19**, 1, 112-119.

Nicklin, D.J., 1962. "Two-Phase Bubble Flow", *Chemical Eng. Sci.*, vol.17, pp. 693-702.

Nicklin, D.J., Wilkies, J.C. and Davidson, J.F., 1962. "Two-Phase Flow in Vertical Tubes", *Trans. Inst. of Chem. Engrs.*, vol. 40, p. 61.

Palmer, T.H., 1917. "The Cascade Method of Agitation", *Mining and Engineering Review*, vol IX, August, No. 107, pp. 296-298.

Peele, R., 1941. *Mining Engineers Handbook*, John Wiley & Sons, Inc., 3rd Edition, vol. 2, pp 15-22 - 15-23.

Perry, R.H.; 1984. *Perry's Chemical Engineer's Handbook*, McGraw-Hill Book Co., pp. 18-64/18-65, 5th Ed.

Pitt, D.L., Asselstine, W.J. and Coulter, D.L., 1933. "Milling Methods and Costs at the Concentrator of the Premier Gold Mining Co., Ltd", Premier, B.C., Canada, *United States Bureau of Mines*, Information Circular No. 6742, August.

Raleigh, 1892. "On the Influence of Obstacles Arranged in Rectangular Order Upon the Properties of a Medium", *Phil. Mag.*, **34**, 481-502.

Richardson, J.F., and Zaki, W.N., 1954. "Sedimentation and Fluidisation: Part I", *Trans. Instn. Chem. Engrs.*, Vol. 32, pp. 35-46.

Sanchez-Pino, S.E. and Moys, M.H., 1991. "Characterization of Co-Current Downwards Flotation Column", *Column '91, Proceedings International Conf. on Column Flotation*, Ontario, Canada, June 2-6, pp. 341-355.

Sawyer, D.T., and Roberts, J.L., 1974. *Experimental Electrochemistry for Chemists*. John Wiley & Sons, Inc. 435 pp.

Serizawa, A., Kataoka, I., and Michiyoshi, I., 1975. "Turbulence Structure of Air-Water Bubbly Flow - II Local Properties", *Int. J. Multiphase Flow*, **2**, 235-246.

Shah, Y.T., Kulkarni, A.A., Wieland, J.H., and Carr, N.L., 1983. "Gas Holdup in Two- and Three-Phase Downflow Bubble Columns", *The Chemical Engineering Journal*, **26**, pp. 95-104.

Shames, I.H., 1982. *Mechanics of Fluids*, 2nd Ed., McGraw-Hill Book Co., pp. A5-A7.

Shih, Y.T., Gidaspow, D., and Wasan, D.T., 1987. *Powder Technology*, **50**, p. 201.

Shih-I Pai, 1954. *Fluid Dynamics of Jets*, D. Van Nostrand Co., Inc..

Smigelshi, O. and Suciu, G.D., 1977. "Carbon Dioxide Absorption by Turbulent Plunging Jets of Water", *Chemical Eng. Sci.*, vol. 32, pp. 889-897.

Spinks, W.S., 1966. *Vacuum Technology*, Chapman & Hall Ltd.,pp.28-29.

Taggart, A.F.,1921. *A Manual of Flotation Processes*, John Wiley & Sons, Inc., pp. 133-138.

Taggart, A.F.,1927. *Handbook of Mineral Dressing*, John Wiley & Sons, Inc., pp. 12-62.

Thanh Nguyen, V., and Spedding, P.L., 1977. "Holdup in Two-Phase, Gas-Liquid Flow - II", *Chemical Engineering Science*, 32, pp. 1003-1014.

Truscott, S.J., 1923. *A Text-Book of Ore Dressing*, MacMillan & Co., Ltd., pp. 417-421.

Turner, J.C.R., 1976. "Two-Phase Conductivity. The Electrical Conductance of Liquid-Fluidized Beds of Spheres", *Chem. Eng. Sci.*, 31, 487-492.

Uribe Salas, A., 1991. *Process Measurements in Flotation Columns Using Electrical Conductivity*. Ph.D. Thesis, Mining & Metallurgical Eng. Department, McGill University.

U.S. Patent, Jameson, G.J.,1990. "Column Flotation Method and Apparatus", Patent No. 4,938,865.

Ulan, W.W., Green, D., and Kosick, G., 1991. "In-Plant Testing of the Outokumpu High Grade Flotation Cell", *Proceedings COLUMN '91 Intl. Conf. on Column Flotation*, June 2-6, Sudbury, Ontario, Canada, vol. 2, pp. 689-702.

Van Atta, C., 1965. *Vacuum Science and Engineering*, McGraw Hill, pp. 219-273.

Vince, M.A., Breed, H., Krycuk, G., and Lahey, Jr., R.T., 1982. "Optical Probe for High-Temperature Local Void Fraction Determination", *Applied Optics*, 21, 5, 886-892.

Wachi, S., Morikawa, H., and Ueyama, K., 1987. "Gas Holdup and Axial Dispersion in Gas-Liquid Concurrent Bubble Column", *Jour. Chem. Engng. Japan*, **20**, 3, 309-316.

Wilfley, C.R., 1917 (a). "The Cascade Flotation Machine", *Engineering and Mining Jour.*, vol. 103, No.20, pp.871-872.

Wilfley, C.R., 1917 (b). "The Cascade Flotation Machine", *Engineering and Mining Jour.*, vol.103, No.21 May, p. 1117.

Williams, R.A., Xie, C.G., Bragg, R. and Amarasinghe, W.P.K., 1990. "Experimental Techniques for Monitoring Sedimentation in Optically Opaque Suspensions", *Colloids and Surfaces*, **43**, pp. 1-32.

Xu, M. and Finch, J.A., 1990. "Simplification of the Approach of Bubble Size Estimation in a Bubble Swarm: Technical Note". *J. Coll. Interf. Sci.*

Xu, M., Finch, J.A., and Uribe-Salas, 1991. "Maximum gas and Bubble Surface Rates in Flotation Columns", *International Journal of Mineral Processing*, Elsevier Sci. Publishers, **32**, 233-250.

Yamagiwa, K., Kusabiraki, D., and Ohkawa, A., 1990. Gas Holdup and Gas Entrainment Rate in Downflow Bubble Column with Gas Entrainment by a Liquid Jet Operating at High Liquid Throughput, *Journal of Chemical Engineering of Japan*, Vol. 23, No. 3, pp. 343-348.

Yianatos, J.B., Laplante, A.R., and Finch, J.A., 1985. "Estimation of Local Holdup in the Bubbling and Froth Zones of a Gas-Liquid Column", *Chem. Eng. Sci.*, **40**, 1965-1968.

Zuber, N. and Findlay, J.A., 1965. "Average volumetric Concentration in Two-Phase Flow Systems", *Journal of Heat Transfer, Trans. ASME*, Section C, November, pp. 453-468.

APPENDIX A
CALIBRATION CURVES

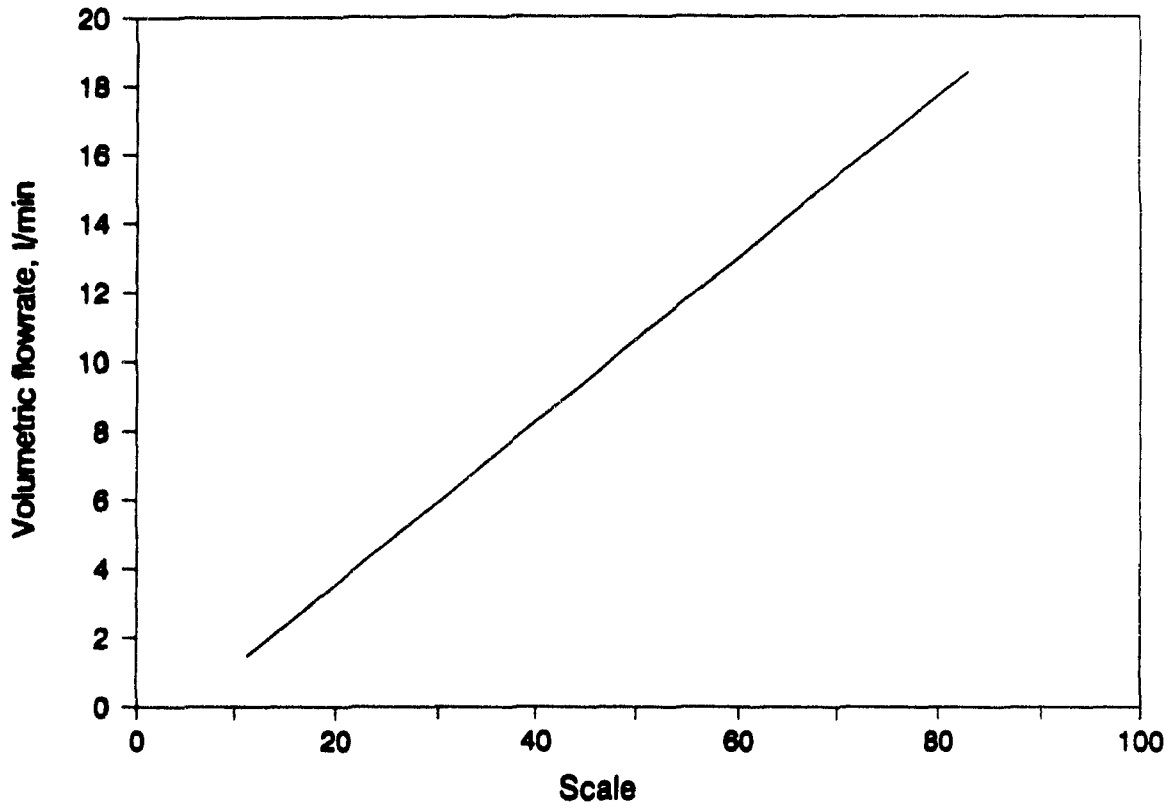

Figure A.1 Calibration curve for the feed rotameter OMEGA, model FL-1504A

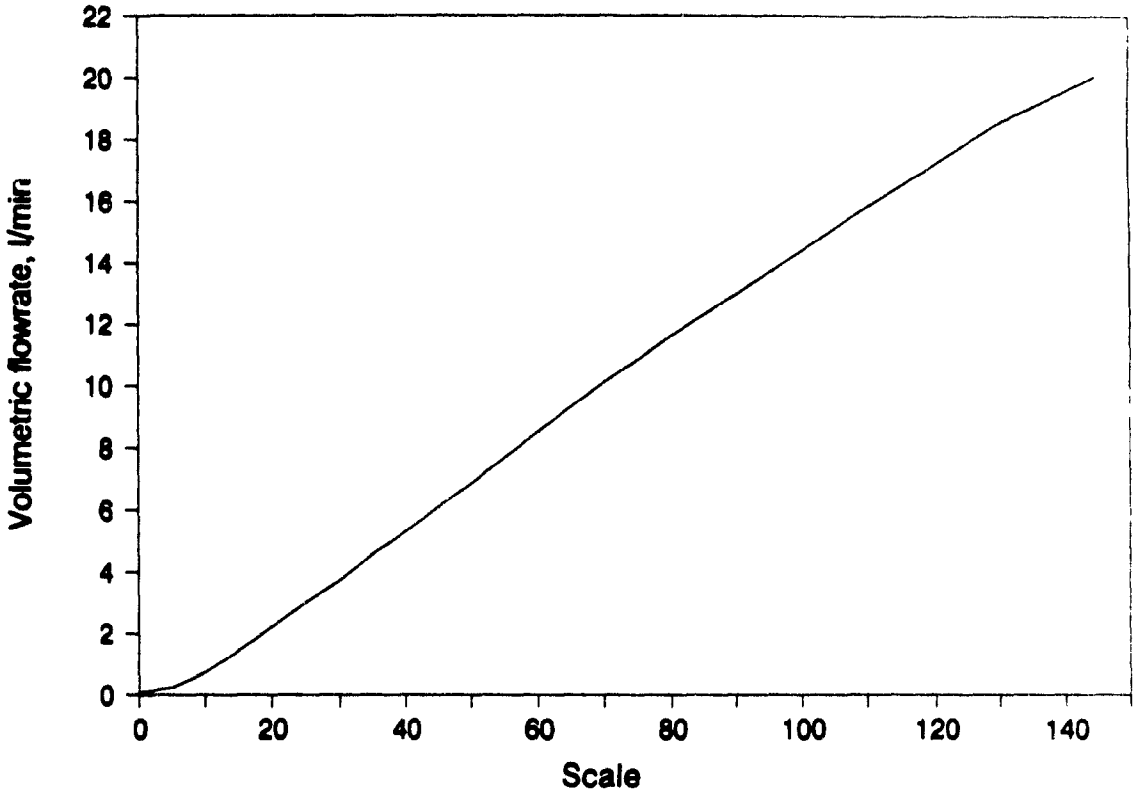

Figure A.2 Calibration curve for the gas rotameter COLE-PARMER, model N044-40

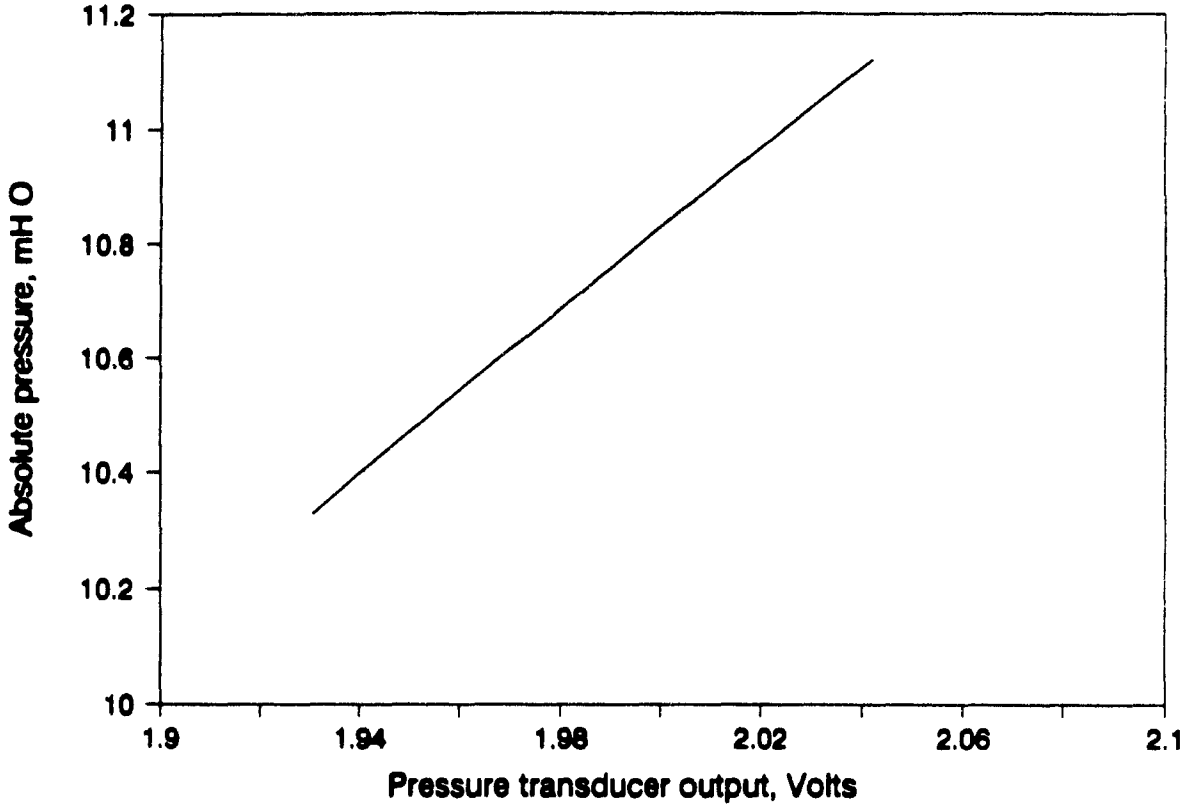

Figure A.3 Calibration curve for the pressure transducer OMEGA, model PX304-050A5V

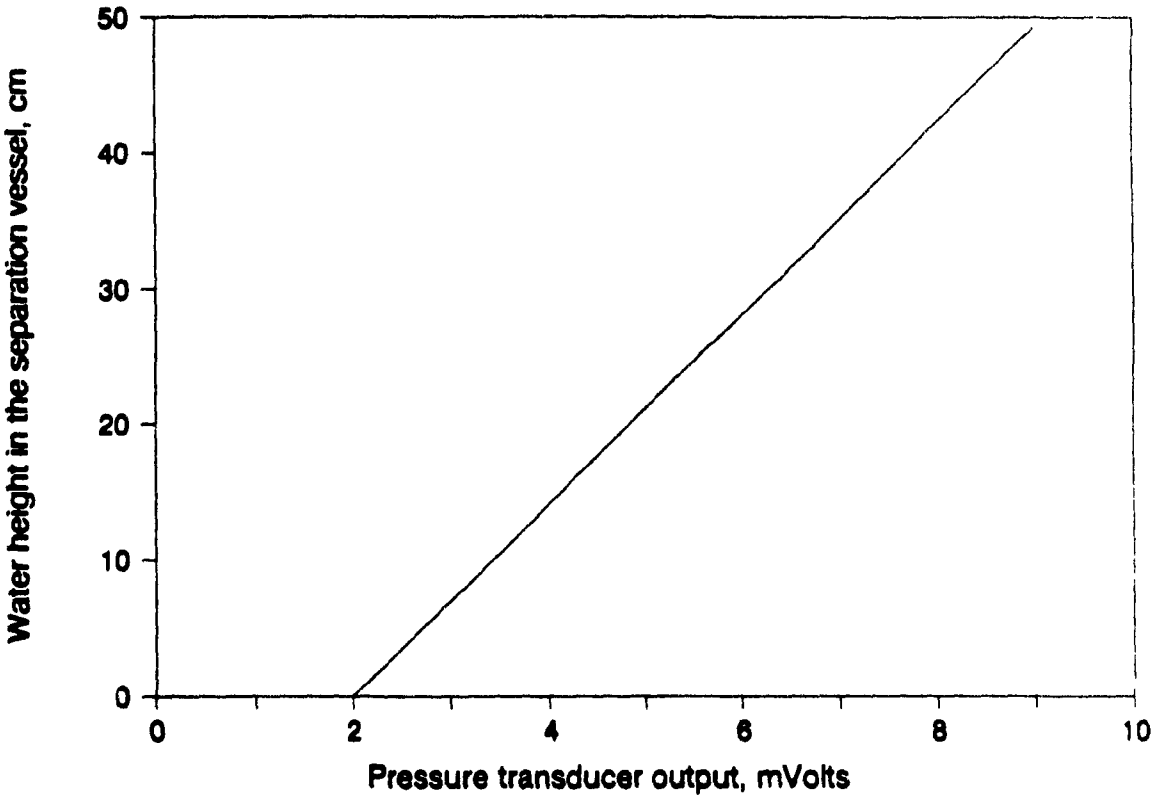

Figure A.4 Calibration curve for the pressure transducer DRUCK, model PDCR 860

The relation between gas holdup and water height was established by measuring directly the water volume at differen levels. A correlation between both values was verify by adjusting the experimental readings by linear regression ($\sigma^2 = 0.999$), giving a maximum error of 1.1% between the experimentally measured and the estimated gas holdup by using the linear regression. The correlation was:

$$\varepsilon_g = 1.0265 - 0.0174 * h \qquad (A.1)$$

where ε_g is the gas holdup, and h is the liquid height in the isolated section, cm.

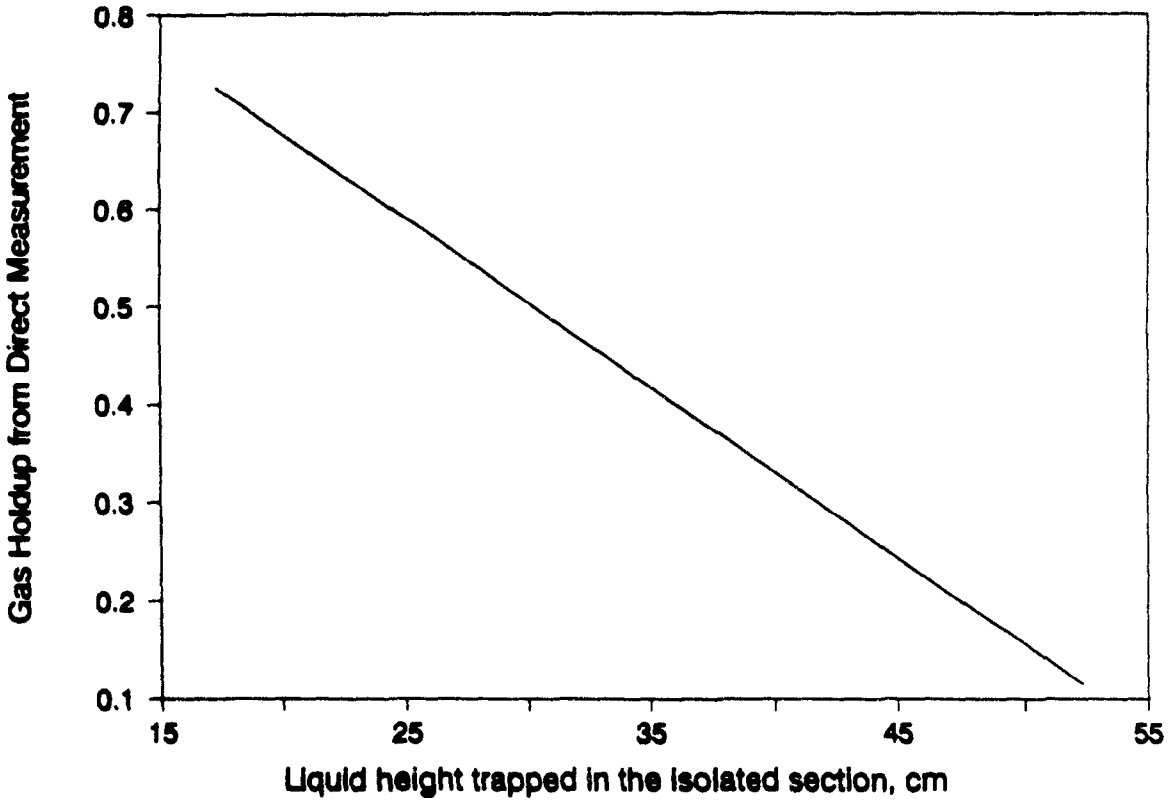

Figure A.5 Gas holdup from direct measurement against the liquid height in the isolated section of the downcomer

APPENDIX B

CASCADE MACHINES of DIFFERENT DESIGN

A.2.-The Cascade Machine

As cascade machines were presented as simple and easy to build flotation machines, it was common to find home-made units with some particular features, making them worth describing as a different machine.

A.2.1. The Cascade machine at Ray Consolidated Co. This machine, a typical cascade machine (Figure A.2.1), was about 30 ft high and was constructed in a series of steps with the sides and back boxed in a tongue-and-groove design. On each step two stave tubs were set about 3 or 4 ft in height by about 2½ ft in diameter. Each tub, on each step, were set directly in line, with those on the next step, making two lines or series from top to bottom. In the front of each tub about 8 inches below the top was an outlet, which was boxed in and the pipe carried directly downward almost to the top and just above the center of the one below. As the feed entered the top, it was equally divided between the two upper tubs, and as these two tubs filled and overflowed, the pulp falling through the perpendicular pipe to the next tub, became aerated to a certain degree, resulting in frothing in all the tubs. These froth overflowed around the edges of the tubs and felt to the floor. From step to step it progressed downward by gravity to the bottom, where the concentrate formed was removed.

A.2.2. The Court cascade machine. As depicted by Taggart (1921) (Figure A.2.2) it consisted of an iron tank with a cylindrical section, about 6 ft diameter by 1 ft high, and two conical sections of the same base diameter attached as shown. The conditioned pulp, under a head of 3 to 4 ft was discharged through the nozzle (b) within the perforated pipe (c) onto the surface of the pulp in the tank below. The froth formed overflowed the lip (e) and was carried off in the annular launder (f). Tailing was discharged through the pipe (g), where a valve (h) was used to regulate the level. To retard the flow of pulp trough the machine a dish-shaped casting (d) was used.

To increase recovery, several machines were placed in series, with sufficient vertical distance between to give from 2 to 3 ft head on the discharge nozzle and a free

fall of 1 to 2 ft from the nozzle to the surface of the pulp.

A.2.3. The Palmer cascade machine. Described by Palmer (1917) as a "cascade method of agitation", it consisted of six tubs (Figure A.2.3) placed in series, one below the other, where the pulp was delivered by an elevator to the top and passed through the pots by gravity. This machine was used for the first time in Australia in 1914 (Anon., 1917), having a capacity of 22 tpd of ore.

In this application the pots were cylindrical, 16 inches in diameter and 24 inches high. Above each pot was an aerator, consisting of an open receiving box, 12 inches square, fed through a 5 inch bend coming from a 3 inch spigot in the bottom of the pot above. The square shape of the aerator caused the pulp to swirl, and entrain a quantity of air, as it dropped into a 5 inch vertical pipe and down to a diaphragm splash plate in the center of the separating pot, where the air is churned into the pulp and formed the froth which overflowed from the periphery of the pot into the launder.

The function of the diaphragm was to intercept the falling pulp, distribute it through the pot and ensure the mixing with the entrained air.

The whole system was said to be self-operating, requiring no attention. All pots had the same-sized spigot and the height of each successive pot was reduced slightly to allow for the concentrates removed from the pot above. The pots were kept full and the froth overflowed constantly from each one.

A.2.4. The Premier cascade machine. The flotation machine devised at the Premier Gold Mine in British Columbia, Canada (Pitt, 1933), was a cascade-type machine, called the *Premier Flotation Machine* (Figure A.2.4), used to process the discharge from the grinding mill before the flotation circuit. Three cells arranged in series, where the pulp was fed to the first cell from the feed tank (a) into a cone shaped tank (d) through a feed pipe (b) that discharged to the aerating chamber (c). The froth was collected in a small cone (d) and sent to a common pipe that carried the concentrates from the other two cells. The tailings were discharged through the bottom of the second cone (e) and mixed with the overflowing fines from the cell (f) producing the feed stream to the next cell, directly below.

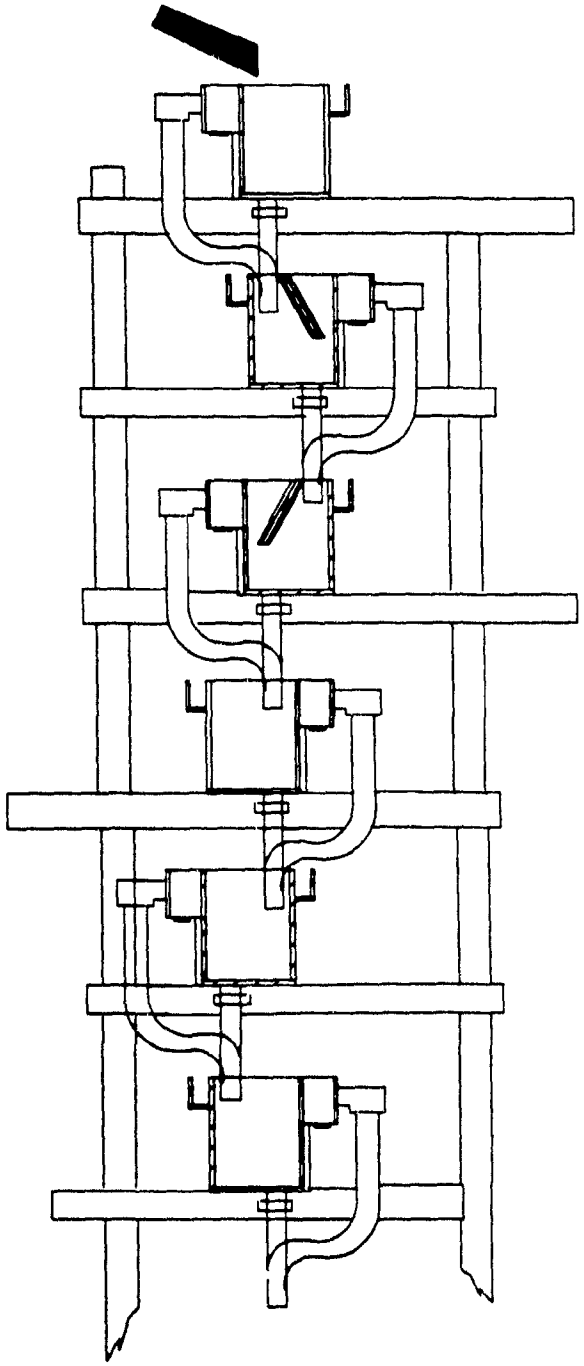

Figure B.1 The cascade machine at Ray Consolidated Co., at Broken Hill, Australia.

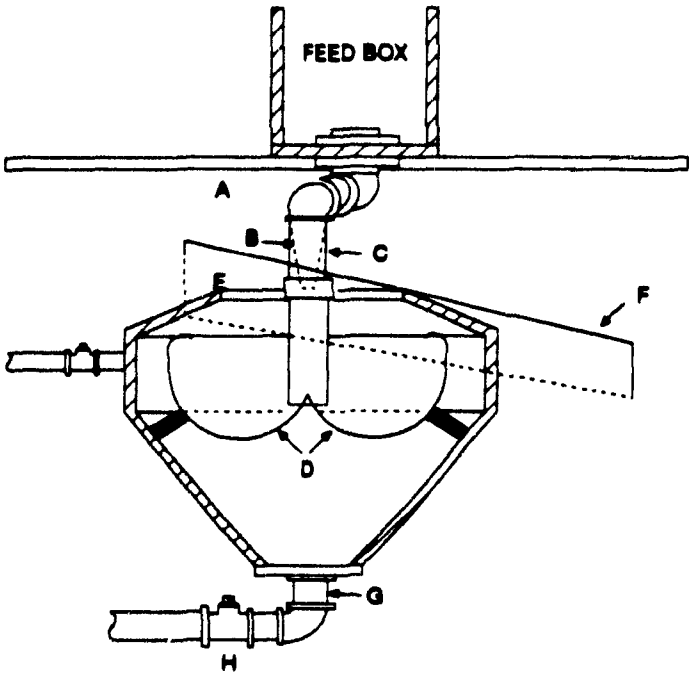

Figure B.2 Court Cascade Machine (Taggart, 1921)

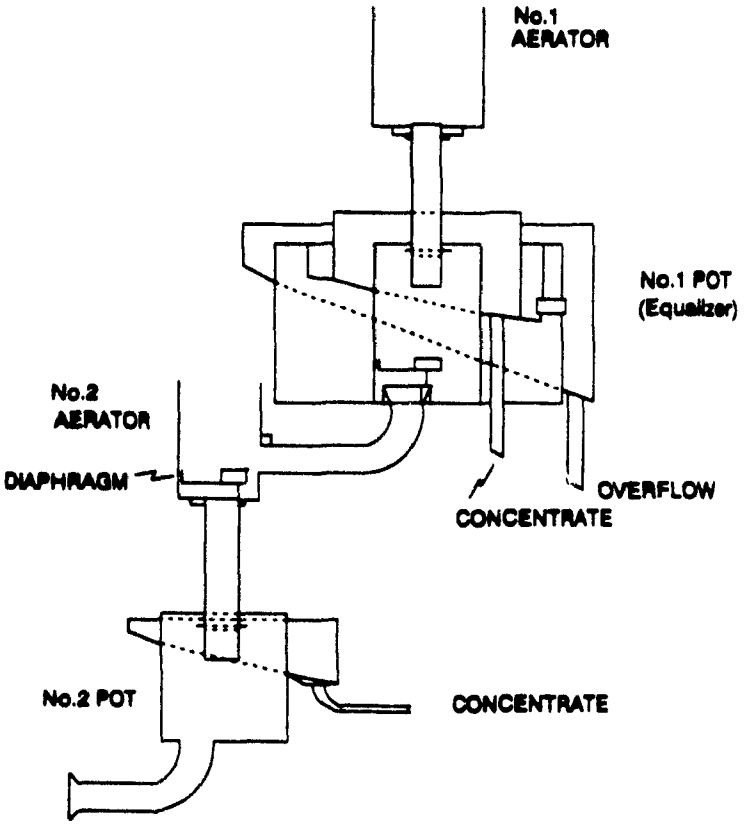

Figure B.3 The Palmer Cascade Machine (Palmer, 1917)

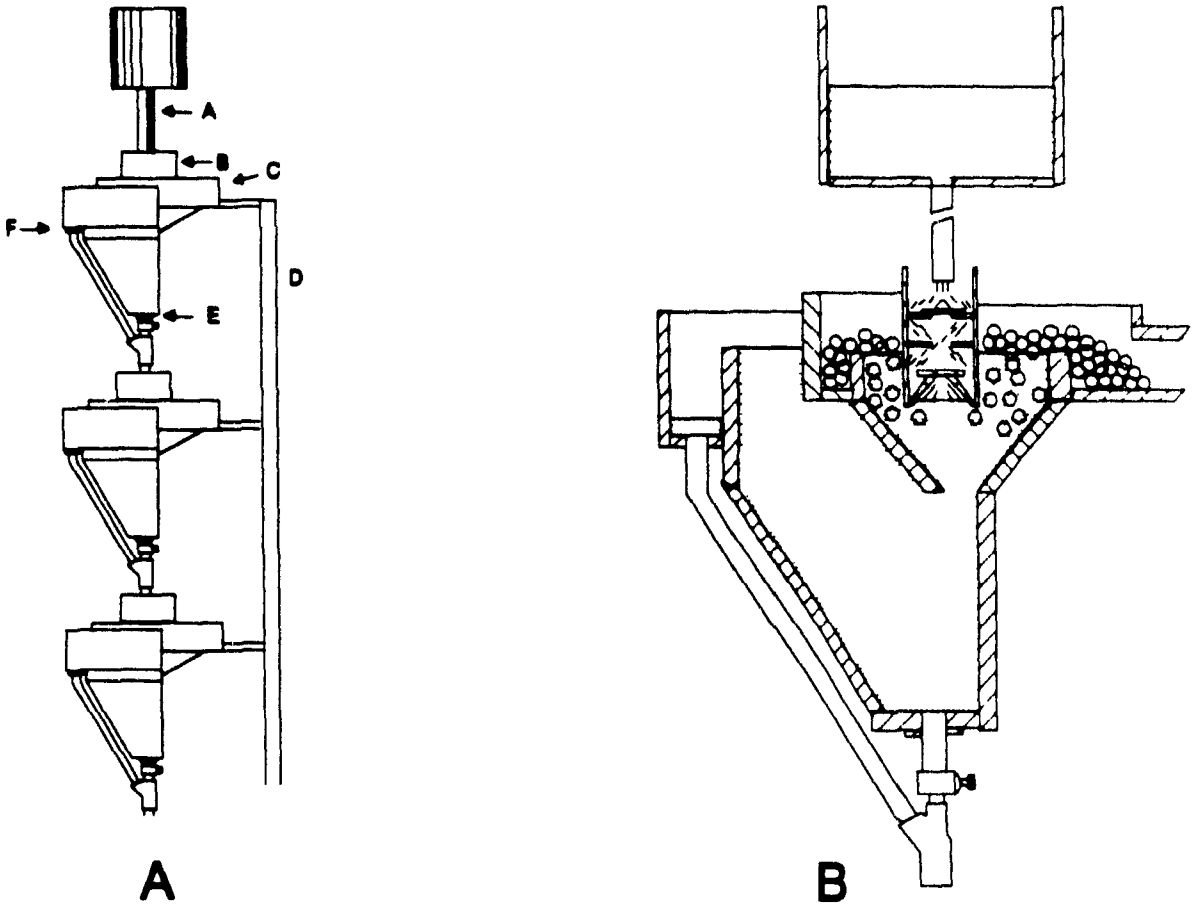

Figure B.4 The Premier Flotation Machine (Pitt, 1933)
(A) Three-cell Premier Flotation Machine
(B) Details of Premier Flotation Cell

APPENDIX C

DERIVATION OF THE EXPRESSION FOR THE DYNAMIC COMPONENT OF PRESSURE, P_z

The derivation of this term for the pressure balance is for the two-phase (liquid-gas) system. When the liquid jet issues from the nozzle the sudden expansion produces an instantaneous deceleration of the liquid which gives rise to a dynamic pressure component whose net effect is to "push" the column contents downwards. This pressure component can be expressed as follows

$$P_z = \frac{F_z}{A_d} = \frac{m a_z}{A_d} = \frac{Q_f \rho_l (J_j - J_d)}{A - d} \qquad \text{(C.1)}$$

where P_z is the dynamic component of the pressure, N/m^2, i.e. Pascals (Pa); F_z the deaceleratin force of the jet, N; a_z deceleration of the jet, m/s^2; J_j and J_d are the liquid velocity in the nozzle and in the downcomer respectively, m/s; Q_f the volumetric feed flowrate, m^3/s; ρ_l the liquid density, kg/m^3; and A_d the cross section of the downcomer, m^2.

From continuity, we can write

$$J_j A_j = J_d A_d (1 - \varepsilon_g) = J_f A_d \qquad \text{(C.2)}$$

Thus,

$$J_j = J_f \frac{D_d^2}{D_j^2} \qquad \text{and} \qquad J_d = \frac{J_f}{1 - \varepsilon} \quad \left(\text{with} J_f = \frac{Q_f}{A_d} \right) \qquad \text{(C.3)}$$

where D_d and D_j are the downcomer and nozzle diameters respectively, m.

Substituting Eq. (C.3) in Eq. (C.1) we obtain the expression for P_z in Table 2.1, namely

$$P_z = J_f^2 \rho_F \left(\frac{D_d^2}{D_j^2} - \frac{1}{1 - \varepsilon_g} \right) \qquad \text{(C.4)}$$

APPENDIX D

USE OF GAS/LIQUID RATIO AS OPERATING VARIABLE

The study of the effect of operating variables on the gas holdup was done using the one-at-a-time method to look at each variable. There is a natural tendency to think in dimensionless parameters that involve several variables at at time, such as the use of the gas/liquid ratio in this case, as they are easy and reliably measured. However it was found that to define the operating condition of the cell the use of the Gas/Liquid ratio to cannot describe all the conditions by itself (Figures D.1 and D.2).

Gas holdup and pool level versus the Gas/Liquid ratio (Figures D.1 and D.2) show the same trends as if they were plotted versus the gas velocity, and becomes necessary to define a third variable to describe the operation. The addition of solids does not change this trend (Figure D.2).

In summary, the description of gas holdup or pool level by using the gas/liquid ratio cannot be used as a single and unique parameter, is still necessary to define one more parameter, such as feed or gas velocity.

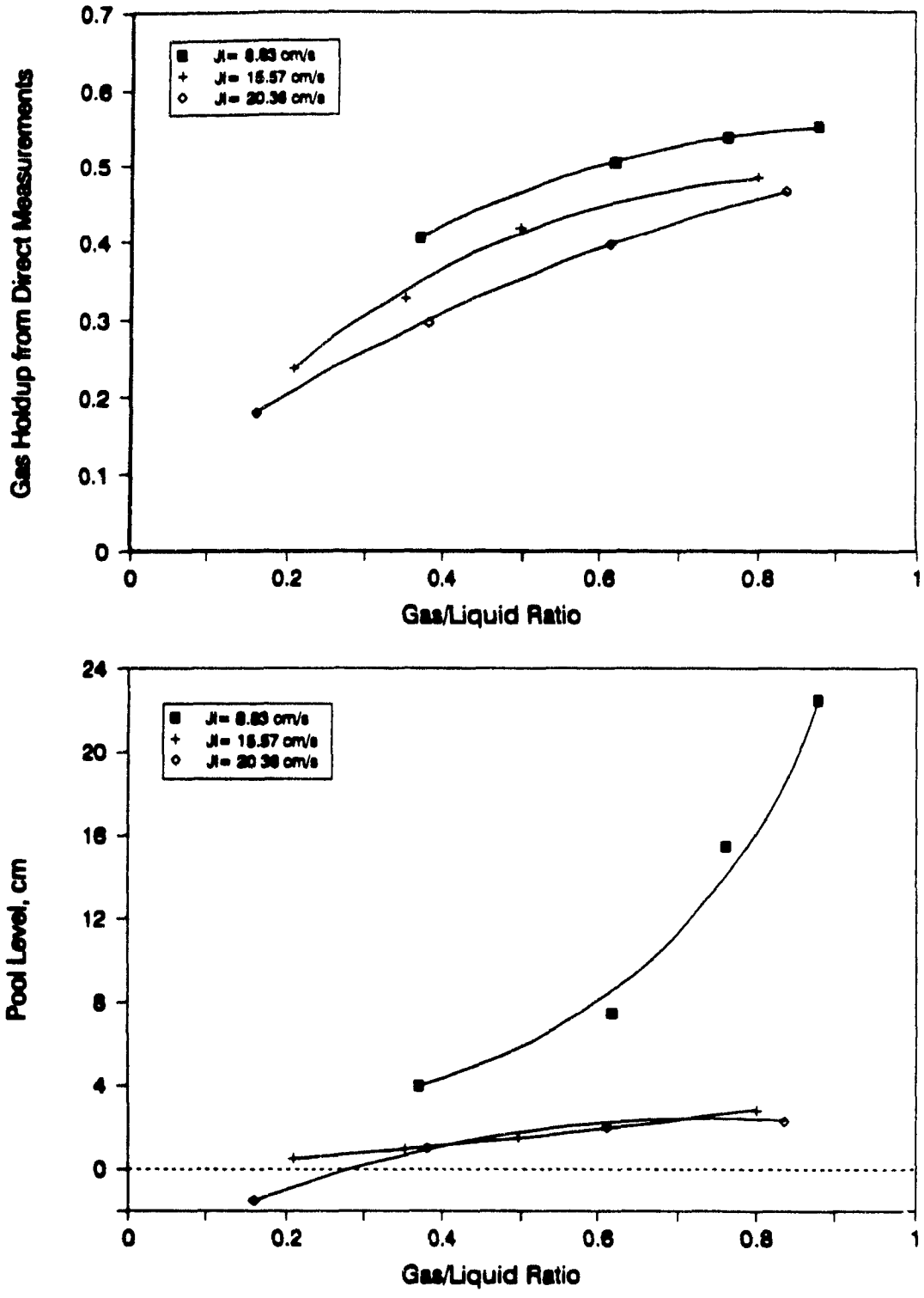

Figure D.1 Gas holdup from direct measurements and pool level against the gas/liquid ratio for the water-air system.

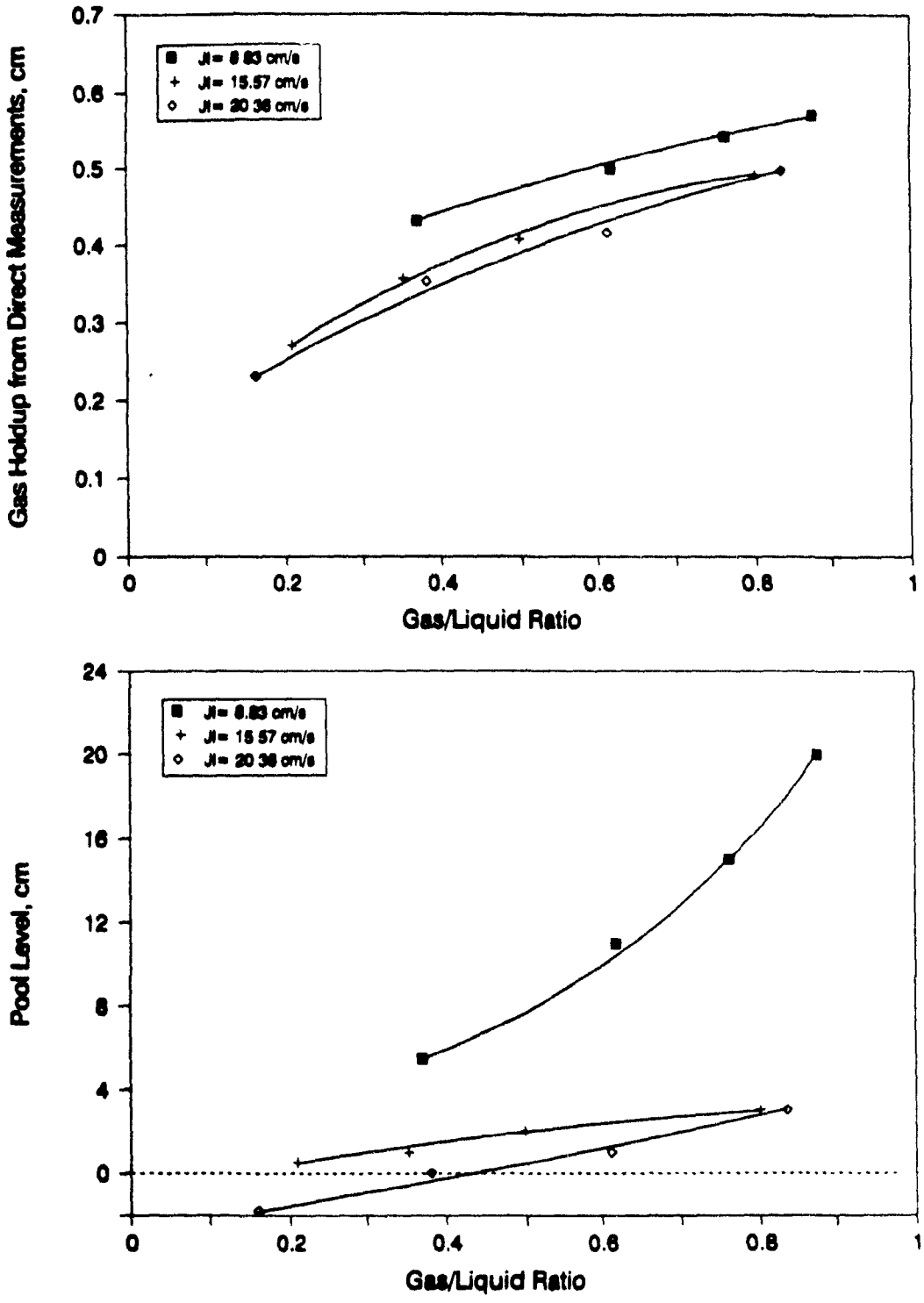

Figure D.2 Gas holdup from direct measurements and pool level against the gas/liquid ratio for the slurry-air system with 10% solids.

APPENDIX E

DRIFT FLUX ANALYSIS, AVERAGE VALUE OF m

WATER-AIR SYSTEM

J_g	J_l	ε_g	U_l	m
1.08	12.21	0.137	8.64	3.18
3.26	12.21	0.263	8.21	3.22
5.45	12.21	0.358	9.84	3.15
7.75	12.21	0.428	10.63	3.13
9.84	12.21	0.485	13.28	3.04
12.46	12.21	0.531	12.38	3.08
14.75	12.21	0.571	14.52	3.02
2.13	18.70	0.123	5.48	3.39
5.45	18.70	0.266	9.69	3.15
7.75	18.70	0.313	5.99	3.37
9.98	18.70	0.364	5.85	3.39
14.75	18.70	0.459	9.32	3.19
SLURRY-AIR SYSTEM (10% w/w Solids)				
3.26	8.83	0.433	22.84	2.84
5.45	8.83	0.501	24.19	2.82
6.74	8.83	0.543	27.92	2.78
7.75	8.83	0.571	31.00	2.76
3.26	15.57	0.271	17.12	2.92
5.45	15.57	0.358	20.66	2.87
7.75	15.57	0.409	19.86	2.88
12.46	15.57	0.494	19.95	2.88
3.26	20.36	0.231	20.27	2.88
7.75	20.36	0.355	21.95	2.85
12.46	20.36	0.418	15.03	2.97
16.97	20.36	0.499	23.49	2.83

TABLE E.1

Example of the drift flux model calculations. The value of m and U_l were obtained from iterative calculations giving an average of: 3.02.